universität wien

MASTERARBEIT

Titel der Masterarbeit

“Determination of the DNA Methylation Status of Breast Cancer-Related Genes *in Vivo* and *in Vitro* by High Resolution Melting Analysis“

verfasst von

Elisabeth Holzweber BSc

angestrebter akademischer Grad

Master of Science (MSc)

Wien, 2013

Studienkennzahl lt. Studienblatt:	A 066 862
Studienrichtung lt. Studienblatt:	Masterstudium Chemie
Betreut von:	Ao. Univ. Prof. Mag. Dr. Margit Cichna-Markl

ACKNOWLEDGEMENT

At this point, I would like to thank everyone who has supported me during my studies and without whose help this master thesis would not have been possible.

Above all, I would like to cordially thank my supervisor, Ao. Univ. Prof. Dr. Margit Cichna-Markl, who has enabled me this master thesis. Her comprehensive knowledge, the excellent support, her patience and her ability to enthuse me for this subject are especially noteworthy. In addition, I would like to thank her for the possibility to pursue my own ideas.

Special thanks go to Univ. Prof. Dr. Doris Marko for providing the equipment for cell incubation experiments, and her working group, above all Eva Attakpah, for assisting in carrying out the experiments. Many thanks go to Ass. Prof. Dr. Georg Pfeiler for providing the biopsy samples from breast cancer patients.

I am very grateful to the members of my working group for the excellent cooperation in the laboratory and the constructive discussions. Especially, I would like to thank Mag. Anna Raab for introducing to laboratory work and DI Melanie Spitzwieser for the active support during my master thesis.

The greatest thanks go to my family, who always accompanied me with humor and an open door to listen to my problems, and to my boyfriend Christoph for his personal support and his great patience at all times.

CONTENTS

LIST OF ABBREVIATIONS

°C	Degrees Celsius
%	Percent
-dF/dT	First negative derivative of fluorescence with respect to temperature
A	Adenine
ANOVA	Analysis of variance
APC	Adenomatous polyposis coli
AT	Adenine-thymine pair
ATP	Adenosine triphosphate
BRCA1	Breast cancer 1, early onset
bcDNA	Bisulfite converted DNA
bp	Base pairs
C	Cytosine
CCND2	Cyclin D2
CDKN2A	Cyclin-dependent kinase inhibitor 2A
cm	Centimeter
COMT	Catechol-O-methyltransferase
CpG	Cytosine-phosphate-guanine dinucleotide
c_T	Cycle threshold
DMSO	Dimethyl sulfoxide
DNA	Deoxyribonucleic acid
dATP	Deoxyadenosine triphosphate
dCTP	Deoxycytidine triphosphate
dGTP	Deoxyguanosine triphosphate
dNTP	Deoxynucleoside triphosphate
dTTP	Deoxythymidine triphosphate
dsDNA	Double stranded DNA
EDTA	Ethylenediaminetetraacetic acid
EtOH	Ethanol
EPD	Eukaryotic promoter database
ER	Estrogen receptor
et al.	*et alii/aliae/alia* (English: and others)
FCS	Fetal calf serum
g	Gravity of Earth
G	Guanine

GC	Guanine-cytosine pair
gDNA	Genomic DNA
GSTP1	Glutathione S-transferase Pi 1
H_2O	Water
H_2O_2	Hydrogen peroxide
HER2	Human epidermal growth factor receptor 2
HRM	High resolution melting
IDC	Invasive ductal carcinoma
ILC	Invasive lobular carcinoma
kb	Kilo base
L	Liter
LOD	Limit of detection
LOQ	Limit of quantification
MCF-7	Michigan Cancer Foundation-7
mg	Milligram
Mg^{2+}	Magnesium ion
$MgCl_2$	Magnesium chloride
MGMT	O-6-Methylguanin-DNA-methyltransferase
min	Minute
mM	Millimolar
mL	Milliliter
MSP	Methylation specific PCR
MS-HRM	Methylation sensitive HRM
NCBI	National Center for Biotechnology Information
NCI	National Cancer Institute
NF	Normalized fluorescence
nM	Nanomolar
nm	Nanometer
n.s.	Not specified
n.v.	No value
Oligo Calc	Oligonucleotide Properties Calculator
PBS	Phosphate buffered saline
PCR	Polymerase chain reaction
PPi	Pyrophosphate
PR	Progesterone receptor
P/S	Penicillin/streptomycin
RARβ2	Retinoic acid receptor beta 2

Ras	Rat sarcoma
RASSF1A	Ras association domain-containing protein 1
RFU	Relative fluorescence units
RNA	Ribonucleic acid
RPMI 1640	Roswell Park Memorial Institute 1640
SAH	S-Adenosyl homocysteine
SAM	S-Adenosyl methionine
SD	Standard deviation
sec	Second
S/N	Signal/noise
SOD	Superoxide dismutase
SRB	Sulforhodamine B
ssDNA	Single stranded DNA
T	Thymine
T_a	Annealing temperature
Taq	*Thermus aquaticus*
TCA	Trichloroacetic acid
T_m	Melting temperature
U	Uracil
UV	Ultra violet
y	Years
µl	Microliter
µg	Microgram

1 Introduction

The global incidence of cancer is still increasing. In 2010, eight million people died of cancer, that is 38% more than 20 years ago. Aging and growth of the world population are the main causes of this development. Furthermore, a cancer-promoting lifestyle, such as smoking, low physical activity and high-fat diet, in economically developing countries causes this increase. Therefore, a lot of studies have been carried out focusing on the development of new methods for early detection and an efficient treatment of cancer. [1-3]

1.1 Cancer and Carcinogenesis

Cancer is not a single disease but a group of diseases characterized by an abnormal cell growth. The causes of this phenomenon are multiple changes in gene expression that can lead to a disturbed balance of cell proliferation and cell death. Subsequently, this cell population can invade tissues and metastasize to distant sites. Morbidity and, if untreated, death of the host is the final result. [4]

Briefly, carcinogenesis is an event in which a healthy body cell changes into a cancer cell. Many studies showed that carcinogenesis is a multi-step process triggered by genetic modifications. The two cancer researchers D. Hanahan and R. Weinberg described the six hallmarks of cancer as follows [5]:

- Self-sufficiency in growth signals
- Insensitivity to anti-growth signals
- Evading apoptosis
- Sustained angiogenesis
- Limitless replicative potential
- Tissue invasion and metastasis

Normal cells need to be activated by mitogenic growth signals that are transmitted into the cell by transmembrane receptors. Cancer cells, however, have the ability to stimulate themselves by oncogenes as they can mimic normal growth signaling. Oncogenes can result from mutations in the DNA sequence of proto-oncogenes, which are actually involved in cell growth, cell division and cell differentiation. The second group of mutated genes playing an important role in carcinogenesis are the tumor suppressor genes. Tumor suppressor genes code for specific proteins that are important for inhibiting growth and formation of tumors. A mutation, deletion or reduced transcription of these genes can increase the tumor incidence. [4-6]

According to Statistics Austria, cancer is the second leading cause of death after cardiovascular diseases. In 2010, there were 36 733 new cancer cases documented in Austria. The incidence of a cancer type is highly dependent on the sex of the individuals. While the most common cancer in men is prostate cancer, in women breast cancer is most frequently diagnosed. [7]

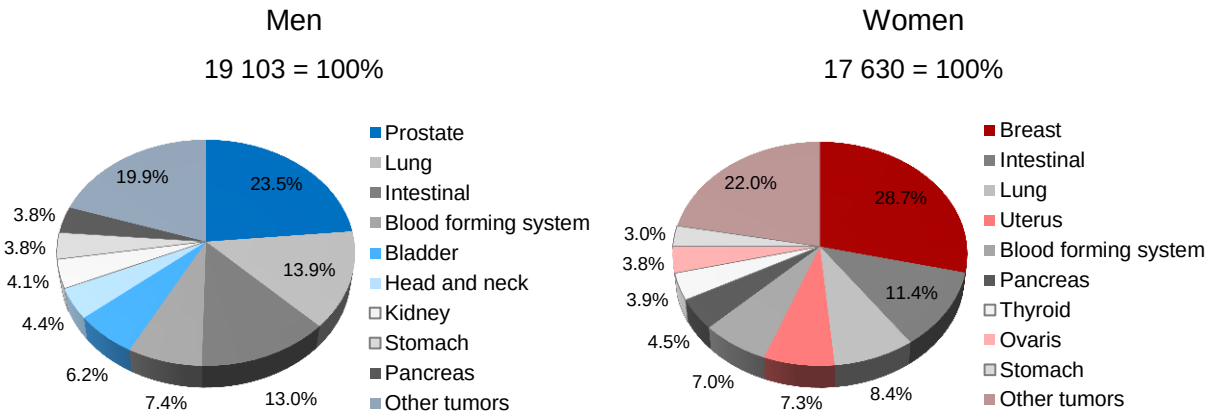

Figure 1: Incidence of new cancer cases by gender in Austria in 2010; from [7], modified

1.2 Epigenetics

In a multicellular organism every cell carries the same genetic material. But despite identical DNA sequence the cells differ greatly in their morphology and function. This fact can be explained by different gene expression. All heritable changes in gene expression without a change in the DNA sequence are described by epigenetics. The term epigenetics was first used by C.H. Waddington. With the Greek prefix *epi* (translated: over, above) all cell processes are meant that take place "in addition" to genetic processes. In other words, the genetic information provides the blueprint for protein biosynthesis and the epigenetic information gives instructions on how and when the genetic information should be used. [8-10]

The conjecture on the important role of epigenetic processes is confirmed by studies on monozygotic twins that show differences in their phenotype in spite of having an identical genotype. M.F. Fraga and co-workers identified global and locus specific differences in DNA methylation and histone acetylation in a large group of monozygotic twins. These differences increase with the age of the twins. [11]

Epigenetic phenomena are caused by a variety of molecular mechanisms. The most common epigenetic modifications are DNA methylation and histone modifications (such as acetylation and methylation). These different mechanisms often occur together and stabilize each other. A transmission of the epigenetic status from the parent cell to the daughter cell is possible. However, the epigenetic status of a genome is not irreversible and especially aging of an organism and environmental influences can change the status. An imbalance in the epigenetic status can either lead to increased expression of a gene or to gene silencing. Several studies have shown that epigenetics is involved for example in carcinogenesis, viral infections and X chromosome inactivation. Actually, DNA methylation is the most frequently studied epigenetic modification. [3, 8, 9]

1.3 DNA Methylation

In general, the term DNA methylation denotes covalent binding of a methyl group at a nucleotide of the DNA. This type of modification is found in different variants in a variety of organisms including prokaryotes, fungi, plants and animals. In humans and other mammals DNA methylation predominantly occurs at the C5 position of cytosines (C) directly followed by a guanine (G), so called CpG dinucleotides (CpGs). These CpGs are underrepresented in the human genome, due to spontaneous deamination of 5-methylcytosine to thymine. Diverging from this regularity, CpG rich clusters of length of approximately 1-4 kilo bases (kb), so called CpG islands, exist. CpG islands show an increased G+C content (more than 50%) and are located at the promoter region and first exons in 60-70% of all human genes. The human genome has an unequal methylation status, as there are found unmethylated regions separated by methylated ones. Usually, the CpG islands are unmethylated to ensure the maintenance of an open chromatin structure and a potentially active state of transcription. In contrast, scattered CpGs are often methylated. [3, 8, 10]

The process of DNA methylation is enzymatically driven by DNA methyltransferases (DNMTs). Current consensus of knowledge emphasizes that in mammals at least three independently encoded DNMTs are responsible for DNA methylation: DNMT1, DNMT3A and DNMT3B. Methylation can be carried out for the maintenance of the methylation status, when CpG dinucleotides are methylated on one strand, or *de novo*, when CpG dinucleotides are unmethylated on both strands. Maintenance enzymes preserve methylation patterns during cell division. DNMT1 has both maintenance and *de novo* methyltransferase activity. DNMT3A and DNMT3B are two important *de novo* methyltransferases. Additional types of DNMTs with other functions have already been identified. S-Adenosyl methionine (SAM) serves as universal methyl donor. Catalyzed by DNMT, a methyl group is transferred from SAM to the C5 position of a cytosine base, producing S-adenosyl homocysteine (SAH) (see *Figure 2*). High concentrations of SAH can inhibit the DNMT activity. [3, 8, 10]

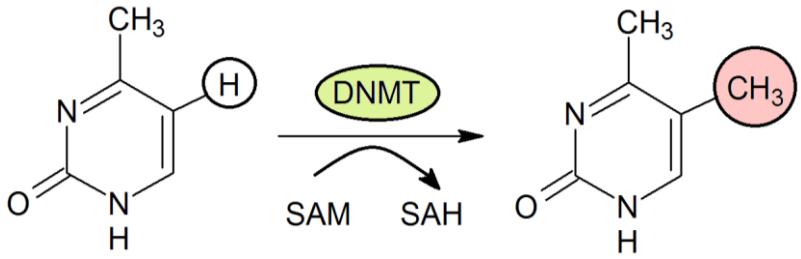

Cytosine 5-Methylcytosine

Figure 2: Cytosine methylation catalyzed by DNMT; from [12], modified

In prokaryotic organisms DNA methylation is primarily a mechanism for protection against foreign DNA. In contrast, in eukaryotes DNA methylation predominantly serves for regulation of gene expression. Gene expression regulated by DNA methylation plays an important role in processes such as genomic imprinting, X chromosome inactivation in females and silencing of repetitive, noncoding DNA sequences. However, it should be noted that the methylation status of the promoter region of a gene does not necessarily correlate with its transcription. An unmethylated CpG island only indicates that the gene is potentially activated and promoter methylation does not necessarily induce gene silencing. In many cases hypermethylation of only a specific part of the promoter is associated with gene expression. [8, 13]

It is known that tumor cells exhibit different DNA methylation patterns in contrast to normal cells. Two abnormalities are observed in tumor cells: global hypomethylation of the genome and local hypermethylation. The total amount of methylated CpGs is lower and at specific regions the methylation status is higher in tumor cells compared to normal cells. Sometimes repetitive and parasitic elements are hypomethylated in tumor cell, whereas normal cells show a high methylation status in these sequence fragments. Global hypomethylation can result in excessive transcription of oncogenes and genomic instability and thus increase the risk of cancer. Hypermethylation of the promoter region of a gene often leads to its silencing, as certain signal proteins cannot, or only with difficulty bind at these sites. The list of known tumor suppressor genes that become hypermethylated during carcinogenesis is already very long and continues to grow. Some tumor suppressor genes are found to be hypermethylated in different types of cancer, whereas other genes are hypermethylated only in specific tumor types. [10]

1.4 Tumor Suppressor Genes

As already mentioned tumor suppressor genes play an important role in the prevention of the formation of cancer. Various studies have shown correlations between aberrant DNA methylation of the promoter region of a gene and its transcriptional silencing. A decreased transcription of tumor suppressor genes is associated with cancer. [6, 14-16]

The tumor suppressor genes that were investigated during this master thesis are described in the following paragraphs.

1.4.1 Adenomatous Polyposis Coli (*APC*)

The *APC* gene encodes the multidomain APC protein, which is involved in degradation of β-catenin in the Wnt signaling pathway. Defects in this pathway are known to be implicated in the pathogenesis of different tumor types, including breast cancer. Several studies have demonstrated that *APC* expression is correlated with the DNA methylation status and promoter hypermethylation occurs in 35-54% of breast tumors. [17-23]

1.4.2 Breast Cancer 1, Early Onset (*BRCA1*)

The *BRCA1* gene is expressed in breast cells and some other cells. It encodes a protein of 1863 amino acids that plays an important role in the maintenance of genome stability with a crucial impact on DNA repair. In addition, the BRCA1 protein is involved in transcriptional regulation and cell cycle progression. *BRCA1* is a tumor suppressor gene because a reduced expression of this gene, e.g. caused by hypermethylation of the promoter region, increases the probability of the formation of cancer. [24-27]

1.4.3 Cyclin D2 (*CCND2*)

CCND2 encodes a protein that is a member of the D-type cyclins. These proteins are involved in cell cycle regulation, differentiation and malignant transformation. *CCND2* is a tumor suppressor gene. Several studies have shown that hypermethylation of the promoter region is a potential biomarker for breast cancer detection. [28-30]

1.4.4 Cyclin-Dependent Kinase Inhibitor 2A (*CDKN2A*)

CDKN2A encodes the protein p16, which binds to the cyclin-dependent kinases CDK4 and CDK6 and thereby inactivates these enzymes. Subsequently p16 is involved in the regulation of the cell cycle and is thus known as a tumor suppressor gene. Several studies have shown the inactivation of *CDKN2A* by DNA methylation in different tumor types, including breast cancer. [31-33]

1.4.5 Glutathione S-Transferase Pi 1 (*GSTP1*)

The *GSTP1* gene codes for a protein of the glutathione S-transferases (GSTs) family. These enzymes have an important influence on detoxification of carcinogenic compounds. Correlations between promoter methylation and the development of cancer, e.g. breast cancer, were found. [21, 34, 35]

1.4.6 Ras Association Domain Family Member 1, Isoform A (*RASSF1A*)

Ras GTPases regulate various cell functions, such as proliferation, differentiation, motility and apoptosis in response to extracellular signals. Ras effectors are proteins that specifically bind to the active form of Ras and can thereby influence complex signal cascades. In addition to the two well known Ras effectors Raf and PI3-K eight new genes encoding proteins similar to the Ras effector proteins have been identified and termed the Ras association domain family (*RASSF*) 1-8. The *RASSF1* gene encodes several isoforms of this protein (RASSF1A-G) due to alternative transcript variants of this gene. Loss or altered expression of *RASSF1A* is one of the most frequent events in a variety of cancers, indicating its tumor suppressor function. Aberrant promoter methylation has been reported in at least 37 tumor types, including breast cancer. [20, 21, 36]

1.5 DNA Methylation as Biomarker for Tumor Diagnosis and Prognosis

According to the National Cancer Institute (NCI) a biomarker in medicine is defined as a biological molecule found in blood, other body fluids or tissue samples that is characteristic for a normal or rather an abnormal process/condition or a disease. A biomarker can be used to monitor the body response to the treatment of a disease or condition. [37]

Various biomarkers on protein, RNA or DNA level can be used. DNA-based biomarkers show some advantages, e.g. the stable and amplifiable nature of DNA enables an easy transformation from laboratory research into routine clinical diagnostics. In addition, DNA can be obtained from a wide range of sources. [8, 38]

An early detection is crucial for successful treatment of many cancer types. As DNA methylation is an early event in carcinogenesis it is a promising biomarker for the detection of cancer in an early state. Different DNA methylation patterns could be observed in various tumor types and may be used to classify tumors. Furthermore, this nucleic acid modification is chemically and biologically stable over time. In addition to the stability of the sample material, biomarkers must meet further requirements. In order to differentiate diseased cells from healthy ones biomarkers must be sensitive and specific. In this context, the term sensitivity means to identify a diseased cell and the term specificity stands for the ability to distinguish a healthy cell from a diseased cell. To be useful as biomarker, age-associated

DNA methylation changes need to be excluded. In addition, sampling must be carried out under minimally invasive procedures to be clinically applicable. [3, 8]

Examination of the DNA methylation pattern depends on the sample material that carries disease-specific characteristics. In this respect, tissue samples should be taken for analysis. However, samples from many tissues are difficult to obtain and taking biopsy samples is an invasive procedure. Therefore, an easily accessible, universal substitute is needed, one of them is cell-free circulating DNA (cfcDNA) in blood plasma. CfcDNA can reflect a methylation pattern that is specific for a particular disease. CfcDNA-based biomarkers are now explored for cancer diagnosis and additional applications as tumor classification and monitoring of treatment efficacy. [38-40]

Many researches have focused on promoter hypermethylation of tumor suppressor genes, as the occurrence of hypermethylation is highly linked with transcriptional activity. However, also many promoters of genes without tumor suppressor activity become hypermethylated during carcinogenesis. In this case, DNA methylation can probably also be used as a biomarker for tumor diagnosis given that the methylation pattern is specific for a tumor type. [8]

1.6 Field Effect in Cancer

The concept of field effect was created to explain the recurrent formation of a tumor in the same organ. The reason for this phenomenon could be either of genetic or epigenetic nature. [41, 42]

Several studies have shown that the DNA methylation status of various genes changes in response to the distance of the primary tumor. Shen and co-workers compared the methylation status of the *MGMT* promoter in colorectal tumor and corresponding normal-appearing mucosa. They found out that colorectal mucosa located 1 cm away from the tumor was more frequently hypermethylated than colorectal mucosa located 10 cm away from the tumor [43]. Yan *et al.* showed differences in the DNA methylation status in the promoter of *RASSF1A* extending as far as 4 cm away from primary breast tumors. These position-dependent alterations may explain the high risk of local recurrence [44].

1.7 Nutrition and DNA Methylation

The diet has a major impact on the development of cancer. A number of dietary components have the ability to modify DNA methylation. They can be clustered in four different groups with respect to their mode of action [45]:

- B vitamins as coenzymes of one-carbon metabolism, e.g. vitamin B12, vitamin B6 and folate
- Dietary methyl donor nutrients, e.g. methionine and choline
- Micronutrients that can modify one-carbon metabolism, e.g. zinc and selenium
- Bioactive food compounds that can modify the activity of DNA methyltransferases, e.g. genistein, epigallocatechin gallate (EGCG) and lycopene

The dietary components of the first three groups are involved in one-carbon metabolism. One-carbon metabolism is a network of interconnected reactions in which a single carbon group is transferred from a methyl donor molecule into biochemical and molecular pathways, being especially important for DNA synthesis. The role of these substances is obvious in this context as the process of DNA methylation is also a one-carbon reaction (see *Chapter 1.3*). [45]

The substances of the fourth group, bioactive food components, have the ability to modulate metabolic processes. Several studies have reported a positive influence of bioactive food components on DNA methylation [45]. Lee *et al.* [46] showed a concentration-dependent inhibition of DNMT-mediated DNA methylation *in vitro* by tea polyphenols (catechin, epichatechin and EGCG) and bioflavonoids (quercetin, fisetin and myricetin). Bioflavonoids are a subgroup of polyphenols [46]. The basic structure of flavonoids and the structure of quercetin can be seen in *Figure 3*.

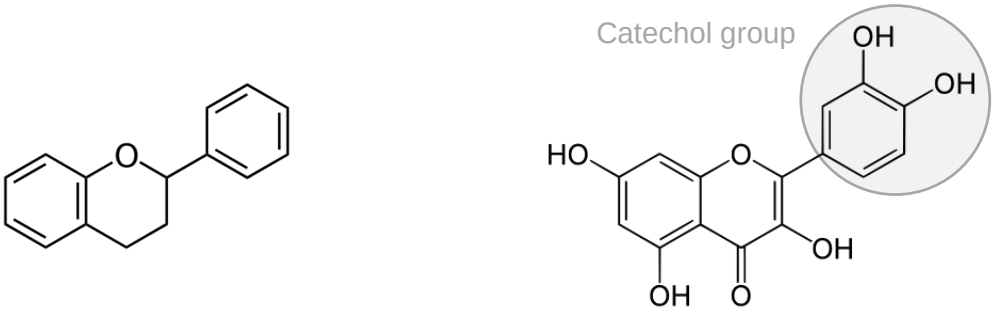

2-Phenylchroman Quercetin

Figure 3: Basic structure of flavonoids (2-phenylchroman) and quercetin structure

All dietary polyphenols investigated by Lee *et al*. contained a catechol group, therefore being excellent substrates for O-methylation catalyzed by catechol-O-methyltransferase (COMT). This is a competitive reaction to DNA methylation. Furthermore, SAH (that inhibits DNMTs) is formed during COMT-mediated methylation. Therefore, it is hypothesized that large amounts of catechol-containing dietary polyphenols reduce DNA methylation. [46]

King-Batoon *et al.* [47] monitored the change in DNA methylation of breast cancer cells as a result of treatment with lycopene, a potent antioxidant carotenoid. A significant demethylation of *GSTP1* was observed in MDA-MB468 cells, but no effect was found in MCF-7 cells. Lycopene is a phytochemical found in tomatoes and other red fruits and vegetables [47]. The lycopene structure is shown in *Figure 4*.

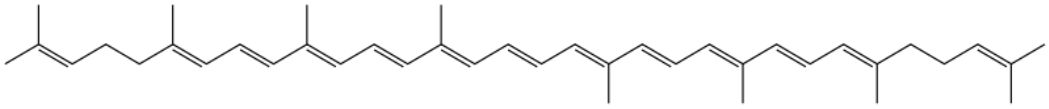

Figure 4: Structure of lycopene

1.8 Dietary Supplements

Dietary supplements often contain bioactive food components in large amounts [48]. In the present work the influence of two dietary supplements (propolis and tomato extract) on the DNA methylation status of MCF-7 breast cancer cells was investigated.

1.8.1 Propolis

Propolis is a resinous substance that is produced by honeybees from various plant sources, beeswax and secretions. The chemical composition of propolis depends on region of origin and time of removal. In any case, large amounts of fatty and aliphatic acids, flavonoids, sugars and aromatic acids are contained. Because of its complex and diverse chemical composition it is reported to have a broad spectrum of pharmacological effects, including antitumor properties. Propolis exhibit positive effects in anticancer therapy as for example it initiates apoptosis in cancer cells. Flavonoids are known as DNA methylation inhibitors (see *Chapter 1.7*). [46, 49, 50]

1.8.2 Tomato Extract

Tomatoes contain large amounts of lycopene, which was identified as a natural chemopreventive agent. [51]

2 Aim of the Master Thesis

Breast cancer is the most commonly diagnosed cancer in women and is lethal in every third case. In addition to genetic changes epigenetic modifications, in particular changes in DNA methylation, can affect the formation of cancer. Since hypermethylation of the promoter region of tumor suppressor genes occurs as an early event in carcinogenesis, it is plausible that aberrant DNA methylation patterns could be potential biomarkers. Field effect studies investigate the reasons for local recurrence of tumors. Tumor distance-dependent differences in DNA methylation pattern of normal-appearing tissues have already been reported. However, to date only little research was performed on this topic.

The main object of the present master thesis was the analysis of different breast tissue samples (tumor, adjacent and surrounding normal tissue) with respect to their DNA methylation status. The aim of this investigation was to determine whether there are position-dependent differences between the breast tissue samples. Sample pretreatment should consist of DNA isolation followed by bisulfite treatment. The sequence of interest should be amplified by polymerase chain reaction (PCR) and the DNA methylation status should be determined by using methylation sensitive high resolution melting (MS-HRM) analysis. The focus was the investigation of the promoter region of tumor suppressor genes. The gene promoters that should be examined are *APC*, *BRCA1*, *CCND2*, *CDKN2A*, *GSTP1* and *RASSF1A.* As part of this work a new MS-HRM method should be designed for *CCND2*.

In addition, incubation experiments with propolis and a commercially available tomato extract should be carried out with MCF-7 breast cancer cells. The effect of propolis on the DNA methylation pattern should be examined as this dietary supplement contains large amounts of flavonoids, which are known as DNA methylation inhibitors. Tomatoes contain large proportions of lycopene which is reported to have demethylating capacity. After DNA isolation and bisulfite treatment the methylation status should be determined by MS-HRM. The aim of these experiments was to investigate if the dietary supplements influence the methylation pattern of selected genes.

3 Theoretical Background

3.1 Polymerase Chain Reaction (PCR)

PCR is a method to copy specific DNA sequences *in vitro*. The obtained PCR product is commonly called amplicon. Kary Mullis had the idea for artificial DNA synthesis in 1983 and ten years later he was awarded the Nobel Prize in Chemistry for his work on PCR. Today, PCR is one of the most important methods for DNA analysis in the laboratory. The PCR method is based on native DNA replication of living cells. [52]

3.1.1 Reaction Components

PCR is performed in small PCR tubes with each tube containing the following reagents: DNA polymerase, forward and reverse primer, deoxynucleoside triphosphates (dNTPs), DNA template, Mg^{2+} and certain buffers. The first commonly used DNA polymerase was the thermostable DNA polymerase isolated from the thermophilic bacteria *Thermus aquaticus*. It is therefore known as *Taq* polymerase. In general, DNA polymerases have the ability to synthesize a new DNA strand, complementary to a template. The synthesis of the new DNA strand is carried out from 5' to 3' end. Today, different modified DNA polymerases for various applications are commercially available, such as the *HotStarTaq Plus DNA Polymerase* produced by Qiagen. This modified enzyme is provided in an inactive state and needs to be activated by a 5-minute incubation step at 95°C. The advantage of *in situ* activation is the prevention of formation of misprimed products and primer-dimers during the reaction setup. [53-55]

Primers are oligonucleotides that serve as a starting point for the DNA polymerase. A primer set consists of a forward primer and a reverse primer, with each of the primers binding to the respective complementary DNA strand. Each primer consists of 12-50 bases, depending on the length of the amplicon. The dNTPs are the substrates for the DNA polymerase. There are four different building blocks for DNA strands: deoxyadenosine triphosphate (dATP), deoxyguanosine triphosphate (dGTP), deoxycytidine triphosphate (dCTP) and deoxythymidine triphosphate (dTTP). The dNTPs are individually attached to the 3' end of the primers by the DNA polymerase. As template DNA, the genomic DNA of the sample is used. The template DNA has to be pure and intact. Mg^{2+} is essential for the function of the DNA polymerase. Commercially available kits usually contain Mg^{2+}. However, the optimal concentration is slightly different for each method and has to be determined experimentally. High Mg^{2+} concentrations result in high amplification yield but too much Mg^{2+} ions lead to the formation and amplification of unspecific PCR products. In addition to its influence on the enzymatic activity, the Mg^{2+} concentration also influences the melting temperature (T_m) of

dsDNA. The composition of the buffer solution is adjusted to achieve high efficiency of the DNA polymerase at specific temperatures. [52, 54]

3.1.2 PCR Steps

First, the DNA polymerase is activated by incubation at 95°C for 5 minutes, in a so called initialization step. Then 30-50 PCR cycles are carried out with three temperature-dependent steps during each cycle: denaturation, annealing and elongation. During the denaturation step the reaction mixture is heated up to 95°C. The high temperature breaks the hydrogen bonds, leading to two complementary strands, which form the PCR template. Next, the reaction is cooled to the primer specific annealing temperature. In general, the annealing temperature should be 5°C below the T_m of the primers to allow the hybridization between primers and template DNA. The annealing temperature is usually between 48 and 60°C. In the third step the temperature is increased to the optimum working temperature of the DNA polymerase, which is 72°C. This is the so called elongation step in which the actual DNA synthesis occurs. [52, 54]

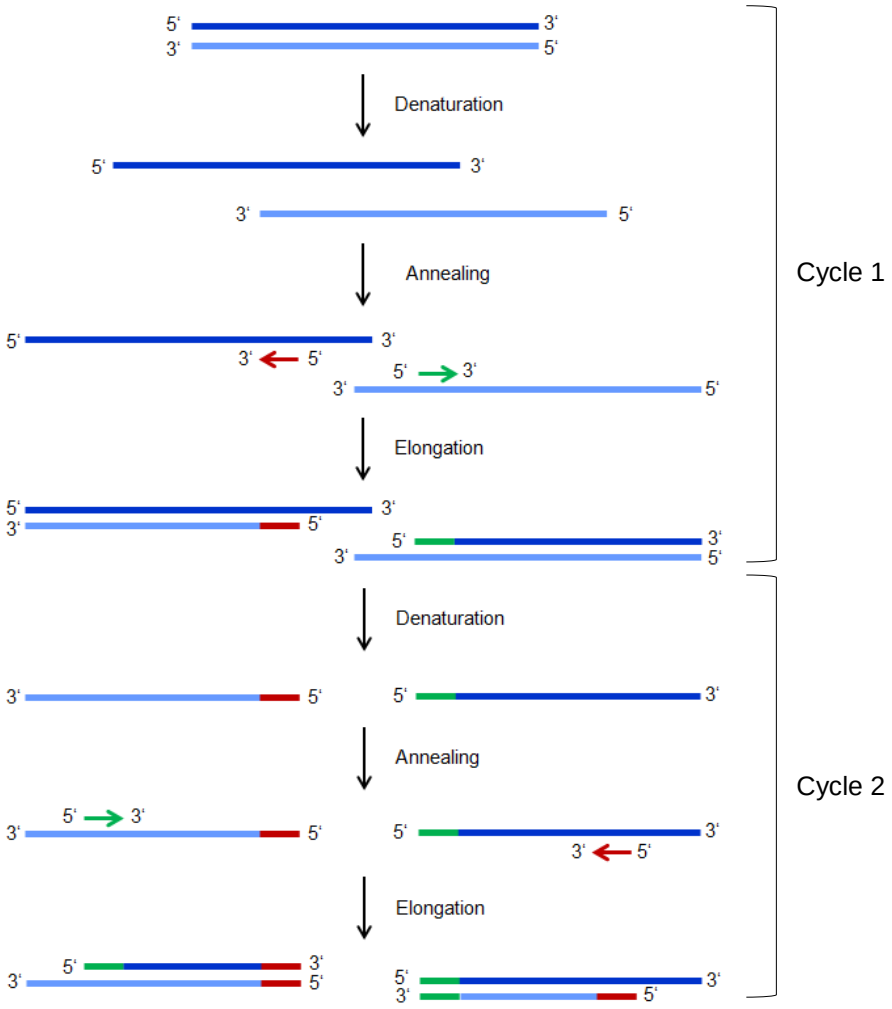

Figure 5: Schematic flow of PCR; from [54], modified

In *Figure 5*, the schematic flow of the first two cycles of PCR are demonstrated. It shows that the number of DNA strands is doubled after cycle 1. However, the two newly synthesized strands, so called daughter strands, are shorter than the strands of the DNA template, but are still longer than the length of the desired amplicon. The reason for this is that the synthesis by the DNA polymerase starts from the site where the primers anneal and ends when the elongation step is over. During the second cycle single DNA strands are obtained with the defined length of the amplicon, but paired with longer DNA fragments. [54]

3.1.3 Kinetics of PCR

As a result of doubling the number of copies during each PCR cycle, after 20 cycles $2^{20} = 1\,048\,572$ copies are obtained. Since in practice the amplification efficiency is commonly below 100%, the actual copy number is lower. *Figure 6* shows the progression of an amplification curve. During the early cycles no increase of the PCR product concentration can be detected, as the amount of newly synthesized DNA is very low compared to the amount of genomic DNA. After a few cycles an increase of the signal can be observed. Due to DNA doubling the DNA concentration increases exponentially at the beginning of the mid cycles phase. Later on, the amount of DNA polymerase is the limiting factor of the PCR kinetics, which leads to a linear curve profile. Then, the curve flattens due to reaction inhibition by pyrophosphate, damaged DNA polymerase and by re-annealing of synthesized DNA strands. Finally, the amplification curve reaches a plateau because the primers and/or dNTPs are consumed. [52, 54]

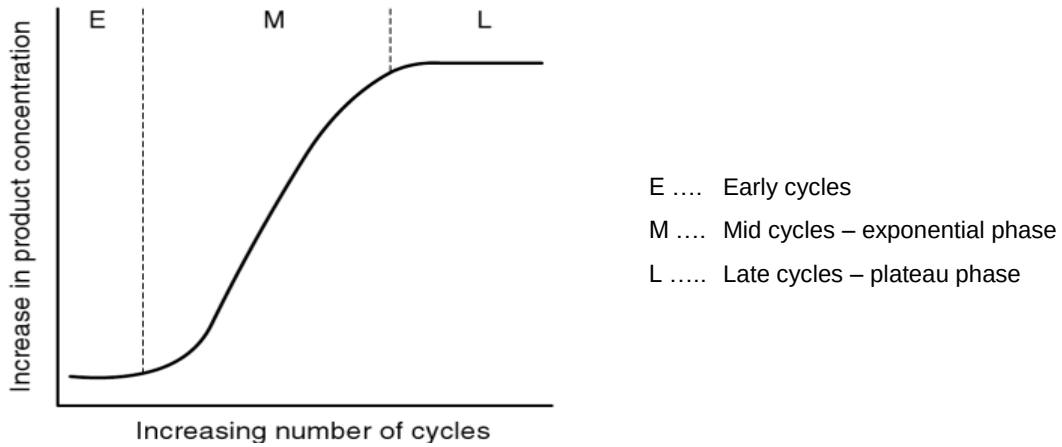

Figure 6: Progression of a typical amplification curve; from [52]

Depending on the aim of analysis, the reaching of a plateau is either intended or should be avoided. For carrying out HRM analysis, for example, it is necessary to reach the plateau because the amount of DNA influences the melting temperature of the sample and has therefore to be similar in all PCR tubes. [56]

3.1.4 Real-Time PCR

There are several options to detect PCR products, such as ethidium bromide/gel electrophoresis or the use of radioactive probes. Novel methods allow monitoring of PCR in real-time by the use of fluorescence markers. The increase of the fluorescence signal is proportional to the increasing number of PCR products. Real-time PCR is also called quantitative PCR, as these methods are very suitable for DNA quantification. Two different kinds of fluorescence markers are available: dsDNA binding dyes (intercalating dyes, e.g. SYBR Green I, LCGreen® or EvaGreen) and fluorescent reporter probes (e.g. TaqMan probe). Intercalating dyes can be used universally for any DNA sequence. The disadvantage of intercalating dyes is that non-specific sequences, e.g. primer dimers, are detected as well. [57]

The detection is based on the fact that the dye molecules intercalate into double stranded DNA resulting in an increase of the fluorescence signal. When the dye molecules are dissolved in solution or bind to ssDNA the signal is very weak. *Figure 7* illustrates the principle of intercalation by means of the dsDNA binding dye EvaGreen. [57]

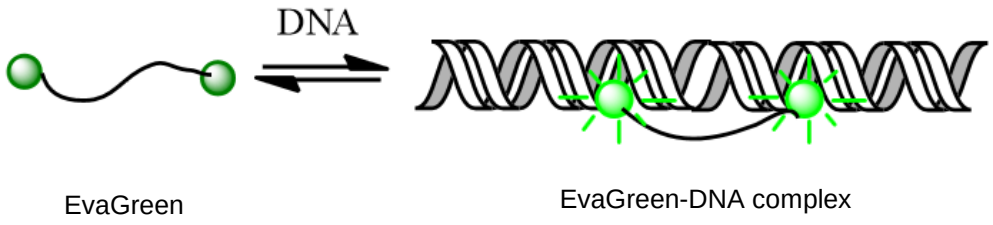

Figure 7: Intercalation of the dsDNA binding dye EvaGreen, from [58]

EvaGreen is a saturating intercalating dye that can be used in high amounts during PCR without inhibiting the DNA polymerase. This is the major advantage compared to some other dsDNA binding dyes, such as SYBR Green I. [57, 58]

3.2 Bisulfite Conversion

During DNA amplification by PCR the information on the DNA methylation status is lost since DNA polymerases do not distinguish between methylated and unmethylated cytosines and the reaction mixture does not contain any DNMTs. However, it is possible to determine DNA methylation after PCR by converting the gDNA with bisulfite before amplification. [59]

Under optimal conditions, bisulfite treatment results in conversion of unmethylated cytosines (C) into uracils (U), whereas methylated cytosines remain unchanged. During PCR, uracil is misunderstood as thymine by the DNA polymerase and therefore adenine is incorporated into the daughter strand. Ultimately, unmethylated cytosines are replaced by thymines (T) and methylated cytosines are found as cytosines in the DNA sequence. Thus, bisulfite treatment leads to different DNA sequences for methylated and unmethylated DNA. *Figure 8* illustrates the principle of bisulfite conversion. [60, 61]

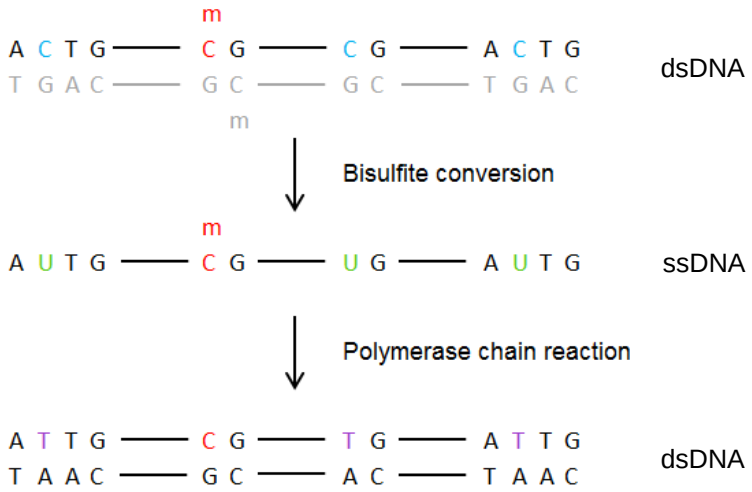

Figure 8: Principle of bisulfite conversion; from [61], modified

The reaction is highly specific for single-stranded DNA, thus in a first step the gDNA is heated to become denatured. Under weak acid conditions, sulfonation occurs on C6 position of cytosine by sodium bisulfite. 5-Methyl cytosine shows very low reactivity under specific conditions. Next, hydrolytic deamination is carried out to obtain uracil sulfonate and finally uracil is received by alkaline desulfonation. [60, 61]

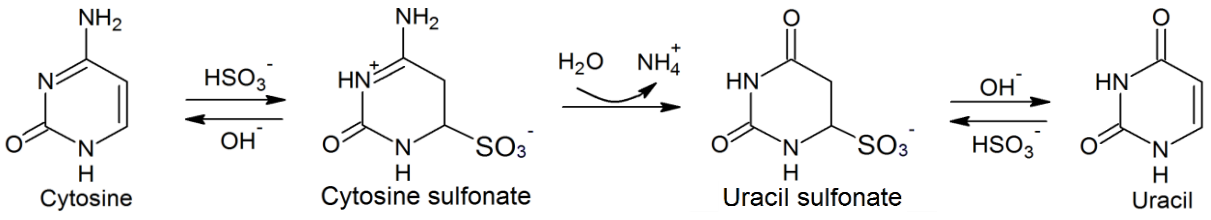

Figure 9: Scheme of bisulfite conversion reaction; from [61], modified

3.3 Methylation Sensitive High Resolution Melting (MS-HRM) Analysis

Historically, melting analysis has been used for different applications, primarily to detect primer dimers or other non-specific by-products of PCR. Meanwhile, the resolution of this method has been improved and today a temperature gradient of 0.1°C/sec can be realized. Since it is possible to detect a variation in a single base, HRM is frequently used as a post-PCR method for DNA analysis, such as genotyping, mutation scanning and sequence matching. MS-HRM is based on differences in the base composition of PCR products derived from sodium bisulfite modified templates. Within HRM analysis the melting profile of a PCR product is generated by monitoring the fluorescence signal of a saturating dye. [59, 62, 63]

3.3.1 Principle of MS-HRM

The melting temperature (T_m) of a double stranded DNA is defined as the temperature at which half of the duplexes are dissociated to its two single strands. This can be achieved by breaking hydrogen bonds and stacking interactions. Guanine (G) and cytosine (C) have three hydrogen bonds while between adenine (A) and thymine (T) there are only two hydrogen bonds (see *Figure 10*). Hence, more energy is needed to dissociate G and C than to dissociate A and T. As a consequence, sequences with a high GC content melt at higher temperature than AT rich sequences. Since bisulfite conversion is carried out before PCR, distinguishing between methylated and unmethylated DNA is possible. Furthermore, the melting curve of a PCR product depends on its length, sequence and heterozygosity. [64, 65]

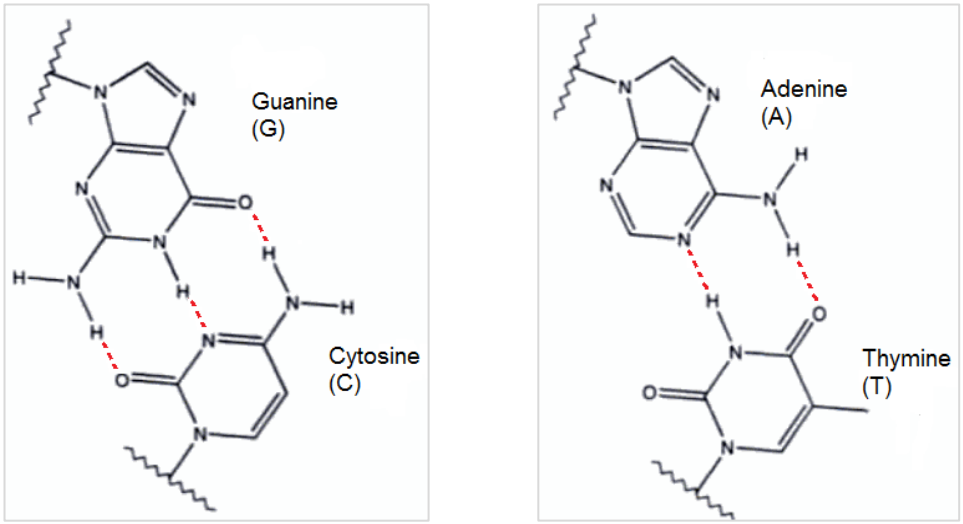

Figure 10: Base pairing; from [66], modified

HRM analysis is carried out by gradually increasing the temperature after PCR. At the beginning, the fluorescence signal is high because of the presence of a high number of double stranded amplicons. With increasing temperature the hydrogen bonds between the

two complementary strands break up, the intercalating dye molecules are released and a decrease of the fluorescence signal is observed. Finally, melting curves are obtained by plotting the intensity of the fluorescence against the temperature [62]. In *Figure 11* an example of a HRM curve is shown.

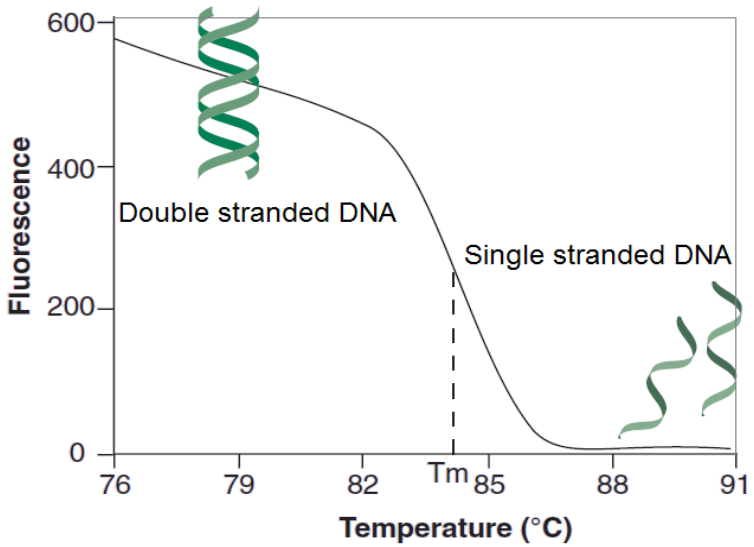

Figure 11: HRM curve; from [62], modified

3.3.2 Data Analysis

After background subtraction, the fluorescence signals of the HRM curves are normalized between 0 and 100%. This step of data processing is performed to compensate for initial variations caused by different amounts of amplicons in the PCR tubes. The DNA methylation status of an unknown sample can be determined by comparing the melting profile of the unknown sample with those of methylated and unmethylated control DNA standards. [59, 62]

In *Figure 12* an example of HRM curves obtained for DNA standards and an unknown sample is shown.

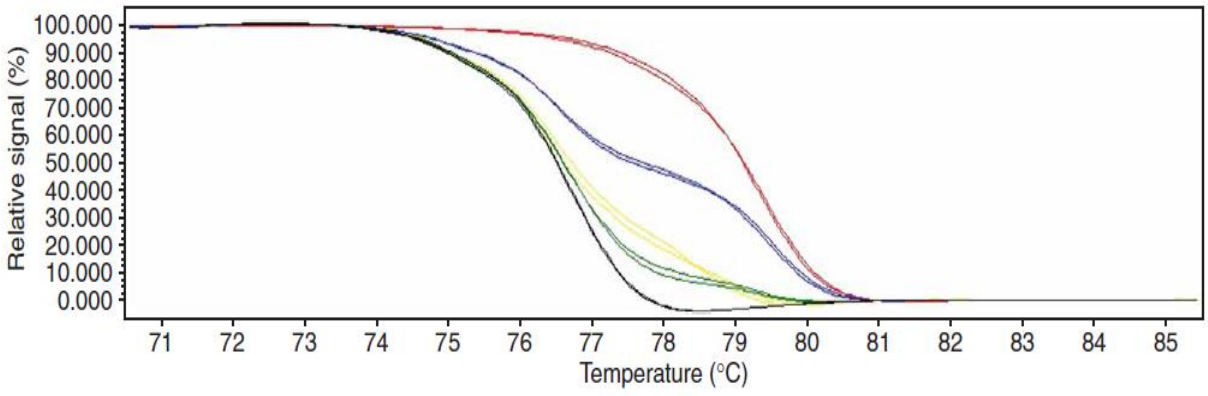

Figure 12: Normalized HRM curves of DNA standards; from [59]
(100% methylated DNA red, 10% methylated DNA blue, 1% methylated DNA green, 0% methylated DNA black) and an unknown sample (yellow)

For determination of the DNA methylation status of an unknown sample different methods can be used. For example, a differential plot with respect to the 0% methylated DNA standard can be registered and the peak heights of the DNA standards can be used for establishing the calibration function [59].

Another method was described by Migheli *et al.* [67]. *Figure 13* shows the melting curves of two DNA standards. The average of the normalized relative fluorescence units (RFU) was calculated at chosen temperature points (circled sites). These average values were used for establishing the calibration function. [67]

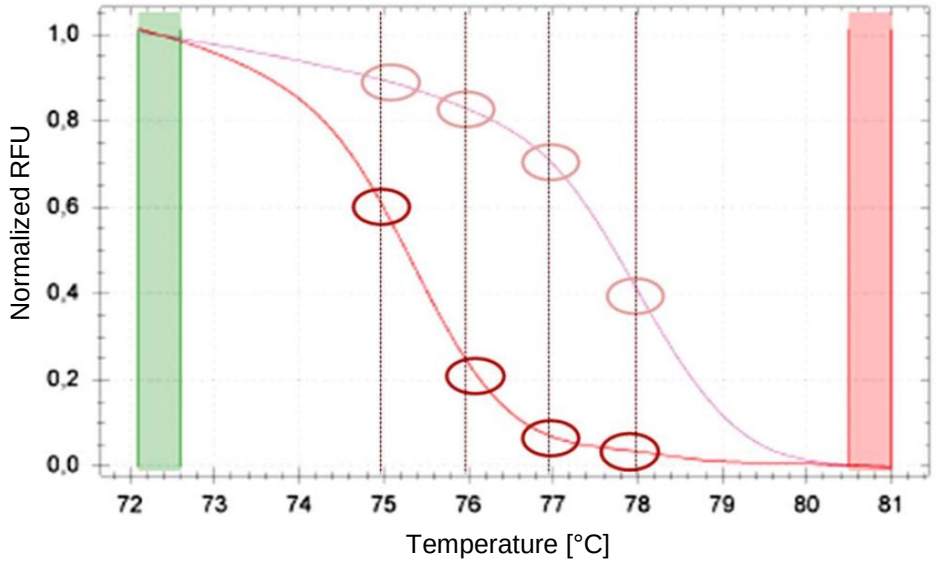

Figure 13: Chosen temperatures to obtain the average of normalized RFU values for the HRM curve of each sample; from [67]

The advantage of the method proposed by Migheli *et al.* is that samples with partially methylated DNA sequences can also be analyzed. The amplicons of a partially methylated allele result in a normalized HRM curve of different shape compared to standards with a mix of methylated and unmethylated alleles. In this case, a shift of the peak maximum is observed in the difference plot. Calculation of the DNA methylation status from the peak maximum would therefore cause a systematic error.

3.3.3 Melting Profile

The first negative derivative of fluorescence with respect to temperature (-dF/dT) gives the melting profile of the amplicons. *Figure 14* gives an example of melting peaks.

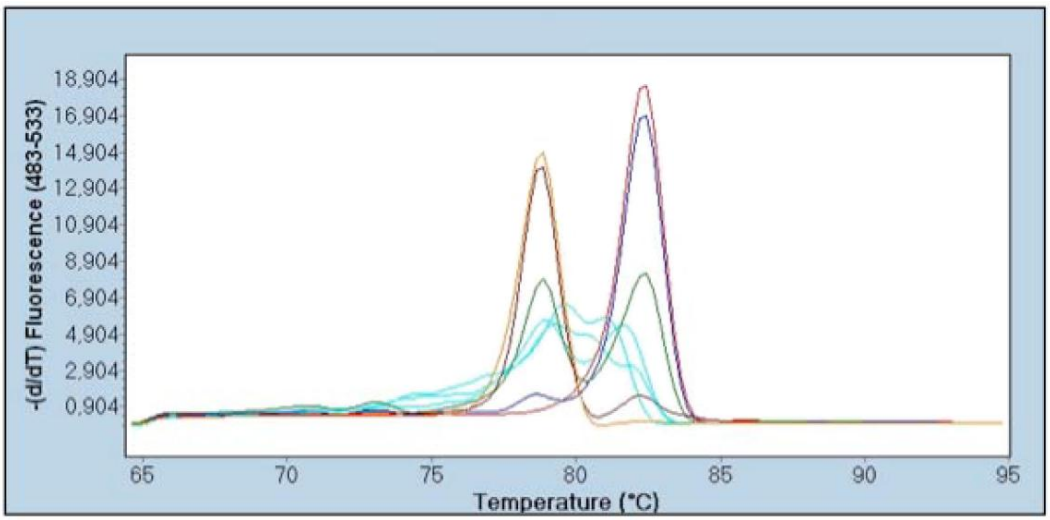

Figure 14: Melting profiles of DNA standards and heterogeneously methylated samples; from [68] (100% methylated DNA red, 10% methylated DNA blue, 1% methylated DNA green, 0.1% methylated DNA brown, 0% methylated DNA orange, samples are shown in turquoise)

It can be seen that the melting profile of both the unmethylated and the methylated standard show a single peak with the peak maximum representing the T_m of the amplicon. For standards with a mix of methylated and unmethylated DNA two peaks are obtained. The figure shows that the melting profile of the 1% methylated DNA standard (green curve) has a peak at the T_m of the unmethylated DNA and a peak at the T_m of the methylated DNA. Both peaks have the same height, indicating that this method has a bias towards the methylated template. Furthermore, an example of heterogeneously methylated DNA (turquoise curves) is shown in this figure. PCR products of DNA sequences in which some CpG sites are methylated while others are unmethylated sometimes have a complex melting profile. Homoduplexes and heteroduplexes will be formed after PCR. The heteroduplexes do not have fully complementary sequences and hence they begin to melt at lower temperature. The intermediate and later melting are likely to be the melting of various homoduplexes. [68]

In addition, by considering the melting profile of the PCR products primer dimers can be discovered easily as they melt usually at lower temperature than the amplicons. [59]

3.4 Development of MS-HRM Methods

3.4.1 Primer Design

Primer design for PCR based analysis of the DNA methylation status using bisulfite converted DNA is much more complex than primer design for regular PCR. The selection of the primers plays a key role in the development of a MS-HRM method. [69]

There are two general groups of techniques using PCR amplification of bisulfite converted DNA. One group is based on primers that amplify only the methylated or the unmethylated templates, e.g. methylation specific PCR (MSP). The other group utilizes primers that amplify the templates regardless of their methylation status and combine it, for example, with HRM analysis. When using this primer type care must be taken on proportional amplification of methylated and unmethylated templates, because a preferential amplification of one template (referred to as PCR bias) can cause misinterpretation of the results. However, a PCR bias can also be applied intentionally to make a method more sensitive in a selected DNA methylation range. [59]

First, some general guidelines for primer design are given by McPherson and Møller [52]:

- The primers should consist of 16-30 nucleotides and both primers should have approximately the same length. Short sequences promote unspecific binding whereas long sequences facilitate the formation of secondary structures and primer dimers.
- The primers should bind specifically to the desired template, especially the 3' end of the primers should be fully complementary as the DNA polymerase starts with elongation from this point.
- The sequence of the primers should be very complex, meaning that the same nucleotide does not occur more than four times in series.
- The primers should not form secondary structures or primer dimers.

Wojdacz *et al.* have published some additional guidelines for primer design when carrying out MS-HRM analysis [59, 69]:

- Each primer should contain one or two CpG dinucleotides. These CpGs should be located as close as possible to the 5' end of the primer to avoid PCR bias towards the methylated template.
- The T_m of the primers should be very similar, preferably about 65°C and the difference should be less than 1°C.
- The inclusion of Ts originally from non-CpG Cs at the 3' end of the primer ensures the amplification of only bisulfite converted templates.

- The primers should not form secondary structures and the formation of primer dimers should be avoided.
- The length of the amplicon should be around 100 bp to reduce the complexity of the melting profile.

3.4.2 Optimization

For each MS-HRM method the PCR conditions need to be optimized. Following parameters can be varied [52, 59, 69, 70]:

- **Annealing temperature (T_a)**
  The ideal T_a of a MS-HRM method depends on the sequence of the primers and should be tested in a first run 5°C lower than the T_m of the primers. By varying the T_a a PCR bias can be controlled. Lowering the temperature also causes the formation of unspecific products and therefore a reduction of a PCR bias towards the methylated template. However, unspecific amplification also leads to the formation of by-products.

- **$MgCl_2$ concentration**
  Commercially available PCR kits contain Mg^{2+}, however, this concentration is frequently not sufficient for efficient amplification of bisulfite converted DNA. An increase to 2.5-3.0 mM Mg^{2+} is recommended. At the same time, care must be taken that no amplification of by-products occurs.

- **Primer concentration**
  Both primers should be used in equal concentrations within a range of 0.1-1.0 µM. Too high amounts of the primers favor the formation of primer dimers and other unspecific by-products.

In addition, the designed primer set should be tested with regard to the formation of primer dimers by including a reaction mixture without template DNA. Furthermore, it should be verified that non-bisulfite treated DNA is not amplified. [70]

4 Results and Discussion

The present master thesis addresses two issues related to DNA methylation. In the first part, I determined the DNA methylation status in the promoter region of various tumor suppressor genes in order to investigate if there are position-dependent differences between tumor, adjacent and normal breast tissue of breast cancer patients. In the second part, I carried out incubation experiments with MCF-7 breast cancer cells and examined the influence of dietary supplements on DNA methylation.

Furthermore, I developed analytical methods based on MS-HRM for determining the DNA methylation status in the gene promoter. In addition, I analyzed the obtained MS-HRM data and compared the results with existing studies.

4.1 Development of MS-HRM Methods

As part of this master thesis, MS-HRM methods were developed to determine the DNA methylation status of gene segments, mainly parts of the promoter region, of breast cancer-related tumor suppressor genes. Details on carrying out primer design and method optimization are given in *Chapter 5.7*.

4.1.1 *BRCA1*

The DNA sequence was taken from the database of the *National Center for Biotechnology Information* (*NCBI*) [71]. The accession number of this sequence is NG_005905.2. Two primer sets were designed according to the guidelines mentioned in *Chapter 3.4.1*.

Primer set 1

The primers fulfilled almost all criteria for primer design. In *Table 1*, the characteristics of primer set 1 are summarized. The forward primer contains one CpG (shown in red) and has a T that was a C in the gDNA at the 3' end (shown in blue). The reverse primer has two CpGs (shown in red), wherein one is located at the 5' end and the other one at the 3' end. The CpG at the 3' end is rather unfavorable because an extreme bias in favor of the methylated template has to be expected. According to the web server *RNAfold* [72], both primers do not show the formation of secondary structures. The calculated T_m for the primers deviates slightly in the various calculations. Details on calculation of T_m can be found in *Chapter 5.7.2*. However, the melting temperature of the forward and reverse primer is rather similar.

Table 1: Characteristics of primer set 1 for *BRCA1*

	Primer forward (BRCA1f1)	**Primer reverse** (BRCA1r1)
Sequence (5' → 3')	TAGTGGATTTTGCGTAGGGTTG	ACGTAACCTAAACCTCCCCGA
Number of CpGs	1	2
Secondary structures		
T_m [°C] calculated according to Wallace rule	64.0	64.0
T_m [°C] calculated with *Oligo Calc* [73]	60.1	61.2

Characteristics of the amplicon:

- Length: 119 bp
- Number of CpGs: 7
- T_m: 77.5°C for the unmethylated DNA
  80.5°C for the methylated DNA

In a first run, the primer set 1 was tested with bisulfite treated human control DNA using in-house standard PCR mixtures (see *Chapter 5.8.1*). The concentration of each primer in the reaction mixture was 250 nM. The $MgCl_2$ concentration was increased by 2 mM. Each reaction mixture contained 10 ng of DNA. The annealing temperature was set at 55°C with a touchdown of 1°C per cycle for the first seven cycles, resulting in a final annealing temperature of 49°C. Further settings for PCR amplification and HRM analysis can be seen in *Chapter 5.8.2*.

As it is shown in *Figure 15*, the DNA templates were amplified well. An increase of the fluorescence signal was observed already at the 25th cycle and a plateau was reached for all samples. Interestingly, the increase of the fluorescence signal occurred for all samples at similar cycle numbers. Because of the three CpGs in the primer sequences a preferred amplification of the methylated DNA template was expected, which should be visible in an increase of the fluorescence signal at lower cycle number compared to the unmethylated DNA template. The reason for this unexpected result was perhaps the low annealing temperature, which results in unspecific amplification of several different templates with similar sequence.

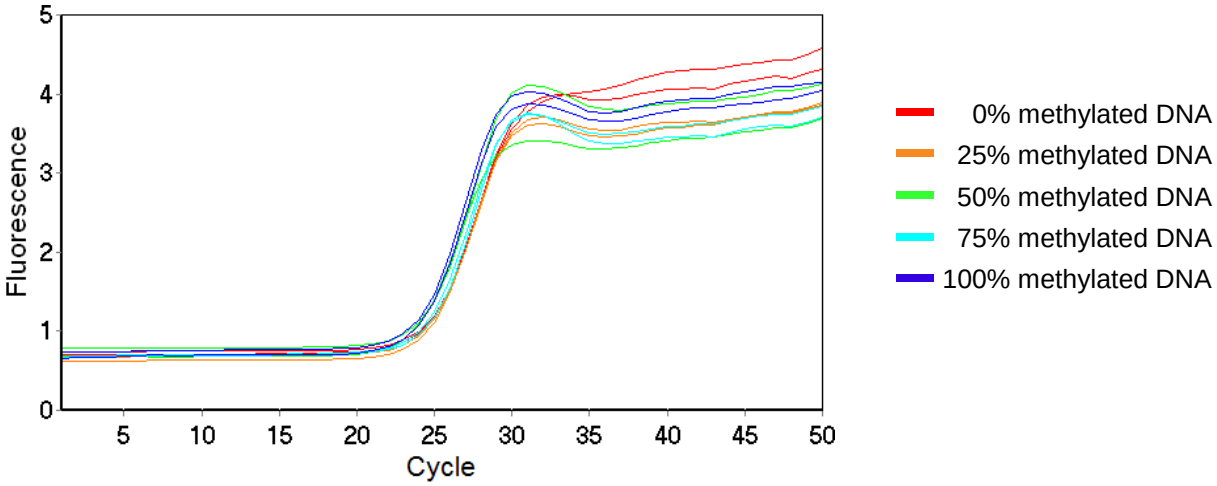

Figure 15: Amplification curves obtained with primer set 1 for *BRCA1*

In *Figure 16* the melting profile derivative plot is shown. The first negative derivative of fluorescence with respect to temperature (-dF/dT) is plotted against temperature. This type of representation shows the melting profile of the PCR products of a sample. It can be seen that both the reaction batches with unmethylated (0% methylated DNA, red curves) and those with methylated human control DNA (100% methylated DNA, blue curves) show only one peak. Thus, only the desired DNA fragment and no other sequences were amplified. The unmethylated and the methylated amplicons melt at a similar temperature. The unmethylated amplicon has the peak maximum at about 79.0°C, the methylated at about 80.5°C. Thus, the temperature difference was only 1.5°C. In addition, the relatively broad peaks make it difficult to quantify methylation differences.

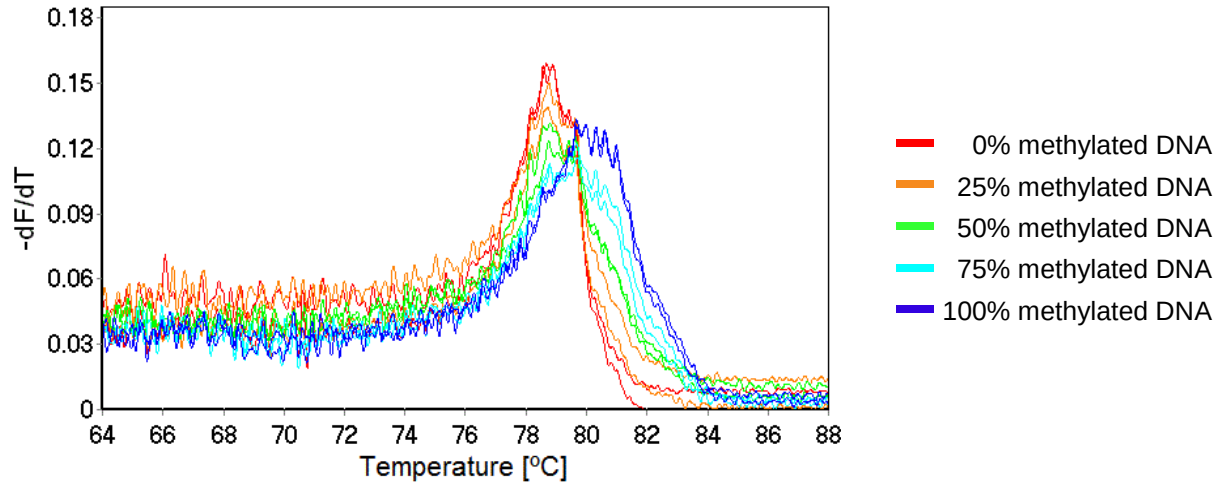

Figure 16: Melting profiles of the PCR products using primer set 1 for *BRCA1*

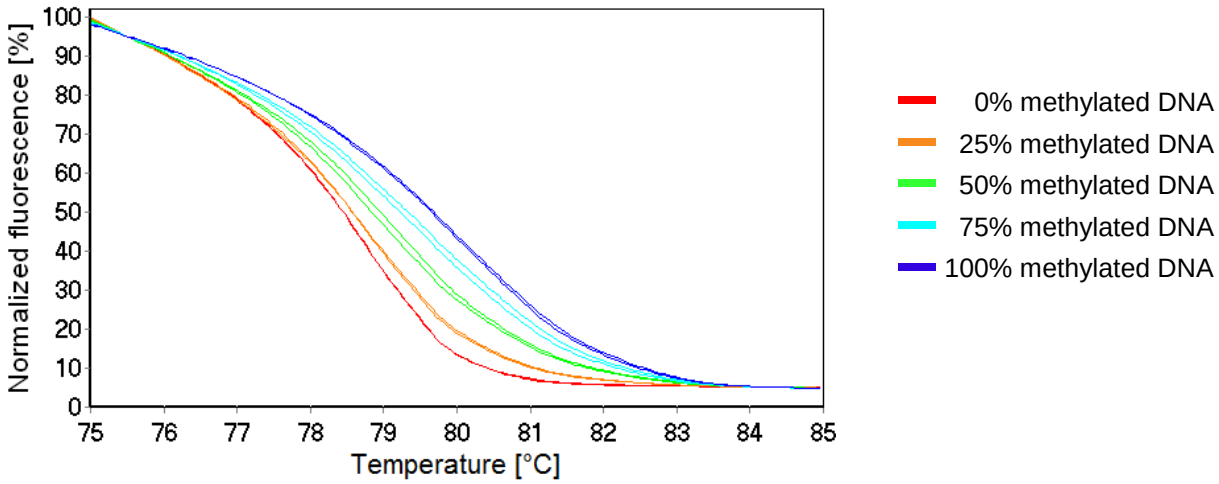

Figure 17: Normalized HRM curves of the PCR products using primer set 1 for *BRCA1*

Figure 17 shows the normalized HRM curves of the PCR products obtained with primer set 1. This figure shows again low differences in the melting behavior of the unmethylated and methylated DNA. Because of this poor result, the design of the primers was checked again. It turned out that primer set 1 targets the *neighbor of BRCA1 gene 2* (*NBR2*) but not the desired sequence. This mistake happened because the sequence selected for primer design consisted of several genes. As a consequence, no further investigations were performed with primer set 1.

Primer set 2

Table 2 summarizes the characteristics of primer set 2. These primers did not fulfill all criteria established for primer design. The forward primer does not contain a T that corresponds to a C in the gDNA before bisulfite conversion. Therefore, unspecific amplification of not bisulfite converted DNA can occur. Furthermore, the forward primer shows a low tendency to form secondary structures, which may result in poor annealing of the primer. Since there are only three base pairs involved in the formation of dumbbell-shaped structure of the forward primer and the 3' end of the primer is not affected, the primer was tested yet. In addition, the melting temperatures of the two primers differ in 4°C according to Wallace rule *(Equation 1*, see *Chapter 5.7.2*). However, according to *Oligo Calc* [73] the primers should have the same T_m.

Table 2: Characteristics of primer set 2 for *BRCA1*

	Primer forward (BRCA1f2)	**Primer reverse** (BRCA1r2)
Sequence (5' → 3')	**C**GGTGG**C**GTATGTTTGTAAT	C**G**AAATTTCACCATACTAACCA
Number of CpGs	2	1
Secondary structures	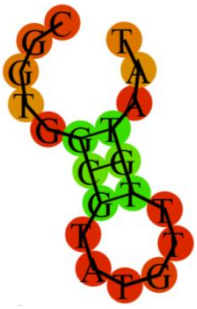	
T_m [°C] calculated according to Wallace rule	58.0	62.0
T_m [°C] calculated with *Oligo Calc* [73]	56.4	56.4

Characteristics of the amplicon:

- Length: 101 bp
- Number of CpGs: 5
- T_m: 79.5°C for the unmethylated DNA
  83.0°C for the methylated DNA

The primer set was tested in a first run with human control DNA using in-house standard MS-HRM conditions (see *Chapter 5.7.4*). The annealing temperature was set at 55°C with a touchdown of 1°C per cycle for the first seven cycles.

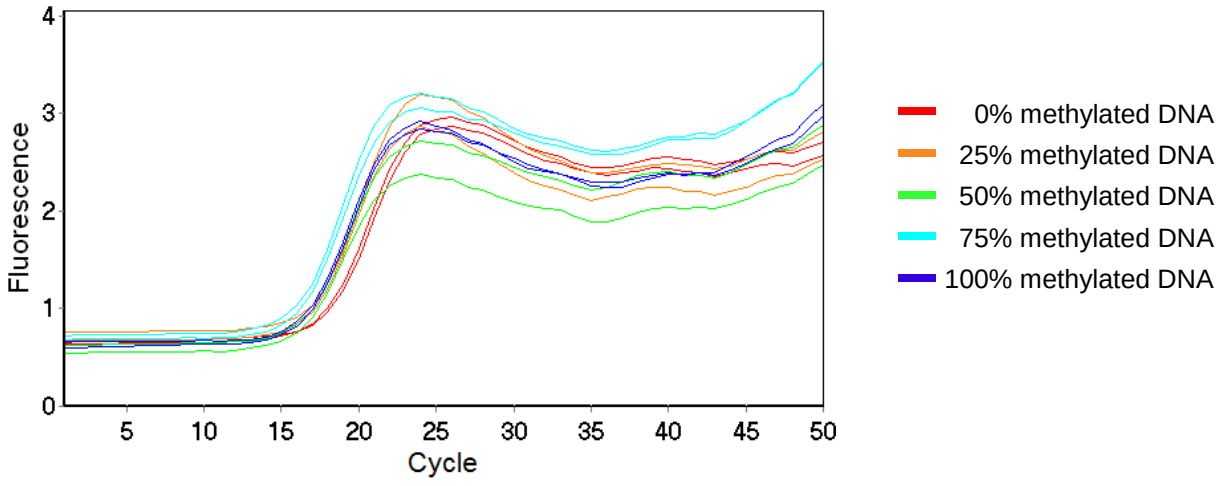

Figure 18: Amplification curves obtained with primer set 2 for *BRCA1*

The amplification curves in *Figure 18* show an atypical profile. First, the increase of the fluorescence signal is observed already at the 15th cycle, which is rather early. In my opinion there are two explanations: an extremely efficient amplification of the target sequence or co-amplification of non-specific template sequences or formation of primer dimers. The curves show a particularly strange course at higher cycle number: instead of reaching a plateau the fluorescence signal fluctuates.

Maybe the partial decrease of the fluorescence signal can be explained as follows: Because of unspecific annealing of the primers, by-products are formed during PCR amplification. These by-products show partially complementary sequence to the actual amplicon, since at least the sequence given by the primers is equal. As a result of rapid cooling after the denaturation step, unspecific hybridization of different products can occur and an incomplete base pairing of DNA sequences can be the consequence. Therefore, less of the fluorescent dye molecules are incorporated into the DNA and the signal is therefore lower. When hybridization of the DNA sequences occurs more specific, more dsDNA is formed and more fluorescent dye molecules can be incorporated, which results in a higher fluorescence signal.

Figure 19 shows that a broad peak from 70 to 75°C was obtained for all samples. The fact that there are amplicons in all samples which melt at the same temperature (65-75°C) can be an indication for the presence of primer dimers. This observation is in accordance with the previous described conjecture of the formation of primer dimers during PCR amplification.

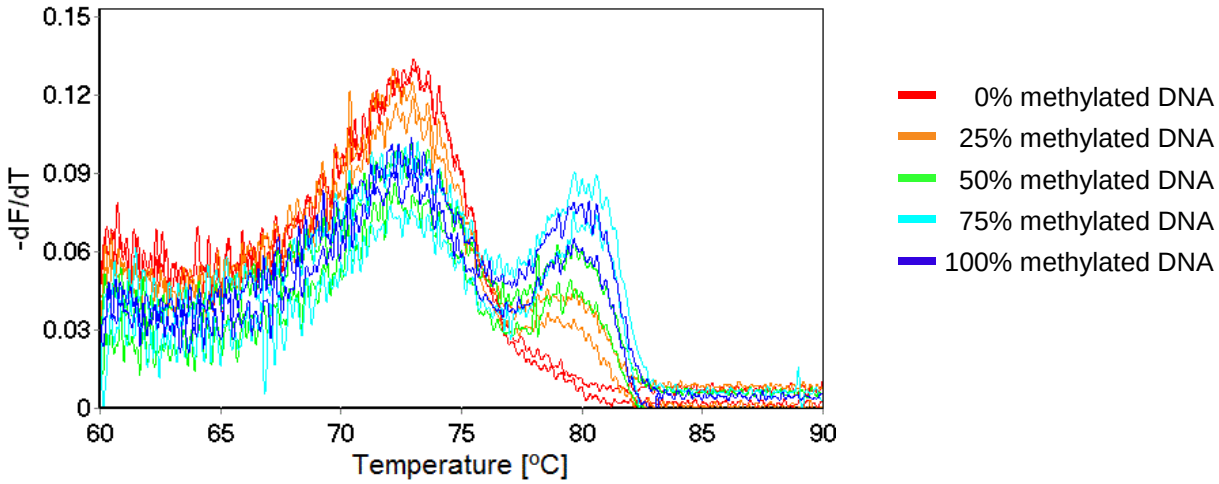

Figure 19: Melting profiles of the PCR products using primer set 2 for *BRCA1*

Due to the presence of by-products that have similar melting temperature as the unmethylated target sequence it is difficult to normalize the fluorescence signals. As it can be seen in *Figure 20*, the melting curves of the 75% standards are above those obtained for the 100% standards. This behavior can be explained by the fact that in the individual reaction

batches different numbers of targeted products and by-products were formed, and the ratio of these products is not uniform.

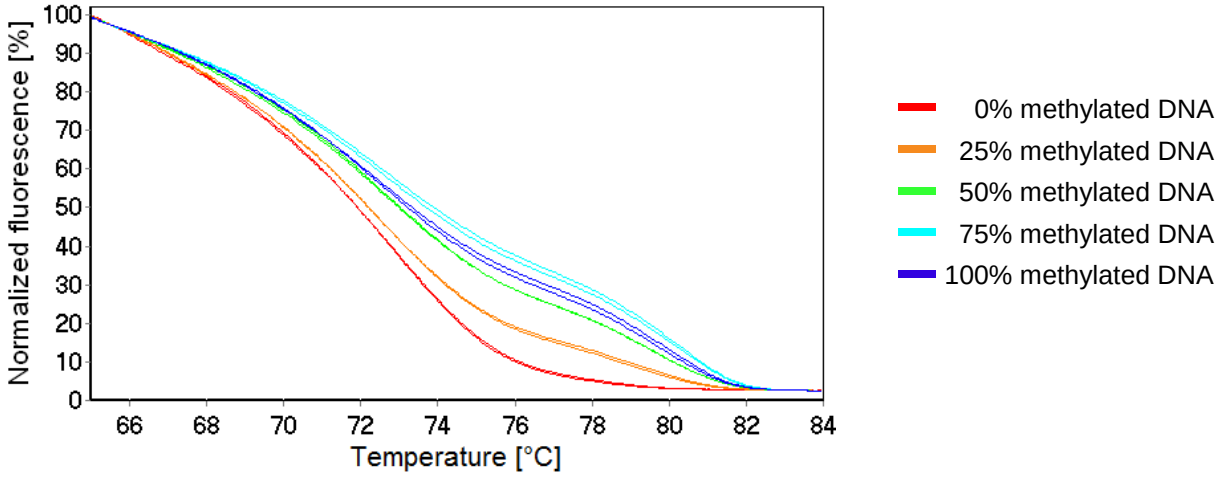

Figure 20: Normalized HRM curves of the PCR products using primer set 2 for *BRCA1*

Further investigation of the position of the primers has revealed that primer set 2 is located in a non-coding sequence between exon 17 and 18 of *BRCA1* and is therefore not suitable for our examinations.

Since in the literature an appropriate MS-HRM method was found from Wong *et al.* [26], no further primers were designed for *BRCA1*.

4.1.2 *CCND2*

The DNA sequence was taken from *NCBI* [71] and the accession number is CM000263.1 (location: 6 004 981 – 6 036 585).

Two primer sets were designed and tested.

Primer set 1

In *Table 3* the characteristics of primer set 1 for *CCND2* are given. Both primer sequences include one CpG (shown in red). According to *RNAfold* [72], the primers do not show the formation of secondary structures. The T_m calculated with two different algorithms are very similar for both primers.

Table 3: Characteristics of primer set 1 for *CCND2*

	Primer forward (CCND2f1)	**Primer reverse** (CCND2r1)
Sequence (5' → 3')	GTTTTAGAGCGGAGAAGAG	AACAAAACCTCGAAACTACC
Number of CpGs	1	1
Secondary structures		
T_m [°C] calculated according to Wallace rule	56.0	56.0
T_m [°C] calculated with *Oligo Calc* [73]	55.0	54.3

Characteristics of the amplicon:

- Length: 89 bp
- Number of CpGs: 4
- T_m: 83.0°C for the unmethylated DNA
  86.5°C for the methylated DNA

The primers were, however, designed without strictly following the guidelines (see *Chapter 3.4.1*). In *Figure 21*, the schematic primer annealing for the first two PCR cycles is shown. First, the sequences of the primer positions for the methylated DNA are shown. The CpGs in the gDNA are highlighted in red and all other Cs are highlighted in green. It can be seen that all unmethylated Cs are replaced by Ts in the bisulfite converted DNA (bcDNA). Due to bisulfite conversion, only the reverse primer can anneal to the DNA in the first PCR cycle and therefore this DNA strand can be amplified. Attention was paid that there are As (shown in blue) that correspond to Gs in the gDNA before bisulfite treatment at the 3' end of the reverse primer to ensure the amplification of only bisulfite converted DNA. Since the forward primer contains Gs, it is not completely complementary to bisulfite converted DNA and cannot bind to the DNA in the first PCR cycle. In the second PCR cycle, the forward primer can anneal to the DNA strand that was synthesized during the first PCR cycle and the complementary sequence can be amplified. If the forward primer contains only As and Ts at its 3' end the primer could anneal during the first PCR cycle. However, consequently several different PCR products and therefore rather complex melting profiles would be obtained.

Figure 21: Schematic illustration of primer annealing in the first two PCR cycles

In a first run, primer set 1 was tested with fully methylated and fully unmethylated human control DNA. The composition of the reaction mixtures is explained in detail in *Chapter 5.8.1*. Two different conditions were tested: 0 and 1 mM additional $MgCl_2$, respectively. The final primer concentrations of the reaction mixture were 250 nM. The annealing temperature was set at 56°C with a touchdown of 1°C per cycle for the first seven cycles. Further settings for PCR amplification and HRM analysis can be seen in *Chapter 5.8.2*.

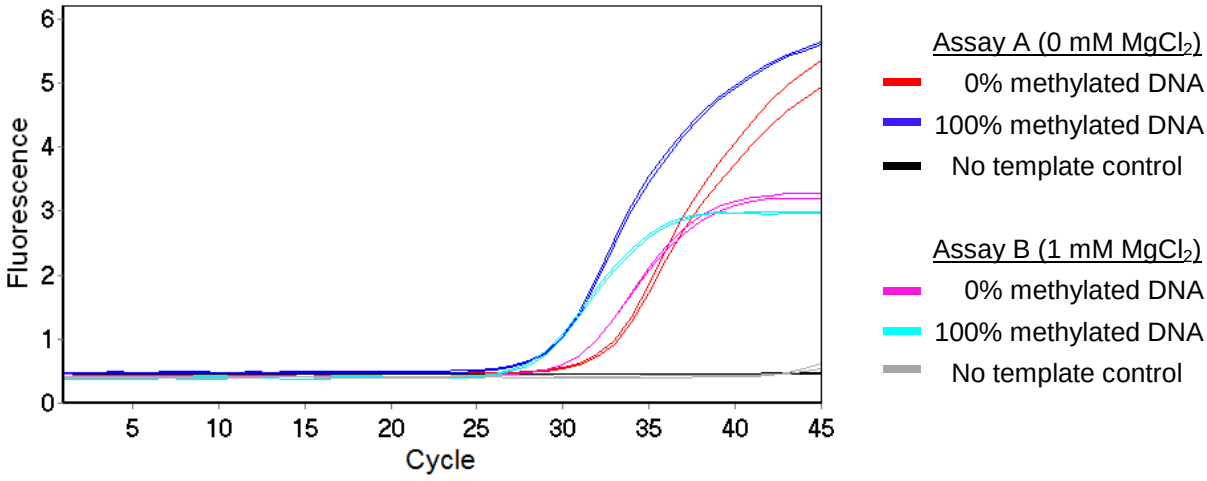

Figure 22: Amplification curves of the PCR products using primer set 1 for *CCND2*

Figure 22 shows the amplification curves of the PCR products for the two assays. When no $MgCl_2$ was added (assay A) the no template control (see *Chapter 5.8.1*) did not result in an increase of the fluorescence signal within 45 PCR cycles, indicating that no primer dimers were formed. In contrast, an increase of the $MgCl_2$ concentration resulted in a slight increase of the fluorescence signal in the last PCR cycles. This can be explained by the formation of some non-specific products.

An increase of the fluorescence signal can be observed for the samples with human control DNA between the 25th and the 30th cycle. Without the addition of $MgCl_2$ (assay A) higher fluorescence signals were obtained than after adding $MgCl_2$ (assay B). However, an increase of the $MgCl_2$ concentration was necessary in order to obtain amplification curves reaching the plateau within 45 cycles. Alternatively, the number of cycles could be increased up to 50 cycles in order to ensure that the amplification curves reach the plateau without additional $MgCl_2$.

Under both conditions, the methylated DNA is amplified slightly better than the unmethylated DNA. This difference is reduced by the addition of $MgCl_2$ in assay B.

The melting profiles in *Figure 23* show that independent of the condition and the methylation status only one peak was obtained. It can be assumed that only the desired PCR products are formed. The amplicons of assay B melt at higher temperature than the amplicons of assay A. This fact is most probably caused by the addition of $MgCl_2$ which is known to influence the melting behavior of DNA. As seen in the amplification curves, the signal is higher in assay A than in assay B. The curves obtained for the no template control in assay A is hardly visible in this figure because the signal overlaps with the bottom axis. In the presence of additional $MgCl_2$ (assay B), a small broad peak with its maximum at 75°C can be seen. This is in accordance with the conjecture of the formation of primer dimers.

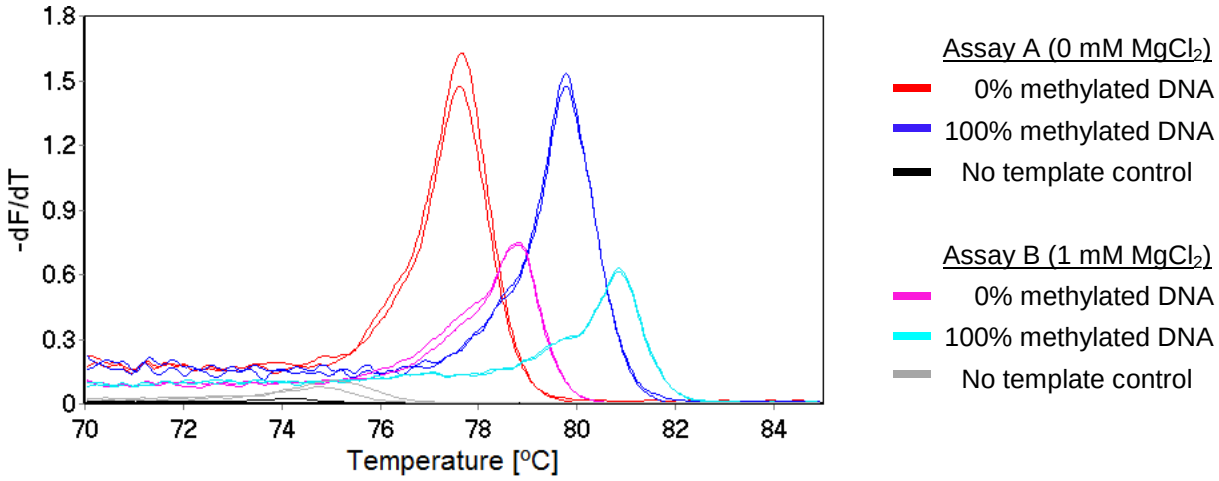

Figure 23: Melting profiles of the PCR products using primer set 1 for *CCND2*

The normalized HRM curves for the two assays are shown in *Figure 24* and *Figure 25*. In both assays, the difference in the melting point between the fully unmethylated DNA and the fully methylated DNA is about 2.5°C. Compared to other MS-HRM methods used in this thesis, the temperature difference is quite low. The low difference in the melting point is caused by the low CpG to base number ratio in the amplicon. However, since the melting profiles of the respective duplicates are very similar, differences in the methylation status can be detected in spite of the low difference in the melting point.

In *Figure 24* the normalized HRM curves of assay A can be seen. For both the unmethylated and the 100% methylated DNA, the curves overlap exactly. The melting curves of the 50% methylated DNA standard indicate that the MS-HRM method has a strong bias towards the methylated template.

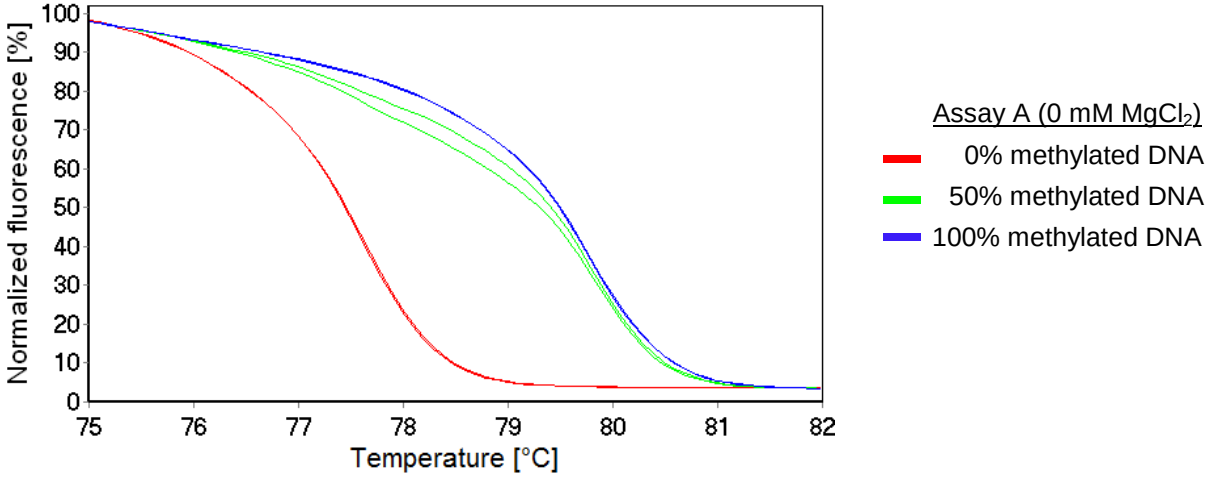

Figure 24: Normalized HRM curves of the PCR products using primer set 1 for *CCND2*, 0 mM $MgCl_2$

Figure 25 shows that the increase of the $MgCl_2$ concentration in the reaction mixture reduced the bias towards the methylated template.

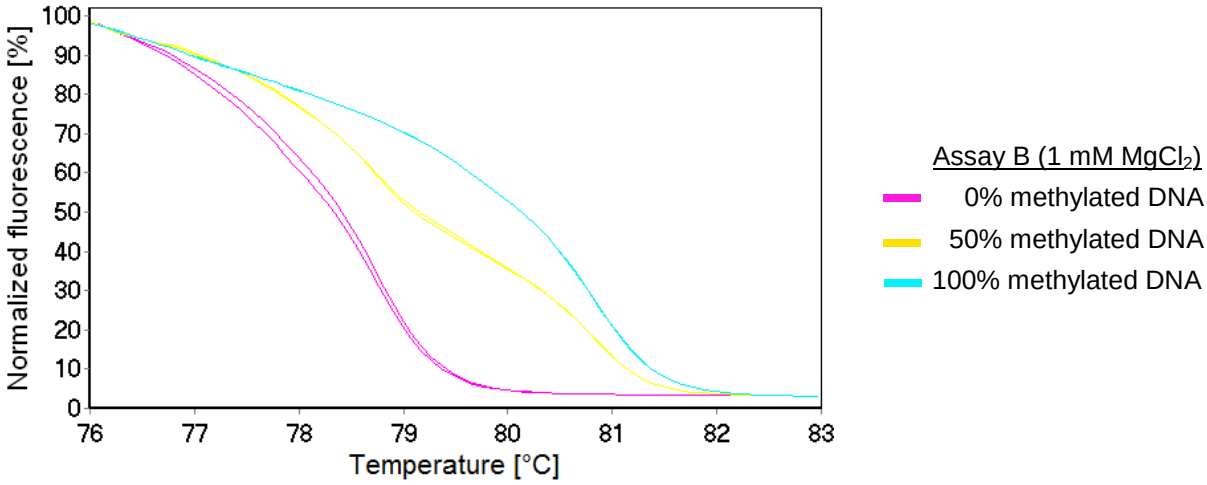

Figure 25: Normalized HRM curves of the PCR products using primer set 1 for *CCND2*, 1 mM $MgCl_2$

As a conclusion it can be said that by the use of primer set 1 the formation of primer dimers can be avoided when the addition of $MgCl_2$ is omitted. Furthermore, in case of low DNA methylation a stronger bias towards the methylated DNA would be advantageous. Therefore, it was decided to analyze the samples without additional $MgCl_2$. The annealing temperature of 50°C yielded good results and was therefore maintained.

In a second run, a standard series was measured. Standards differing in the methylation status were prepared by mixing unmethylated and 100% methylated human control DNA. The results can be seen in *Figure 26.*

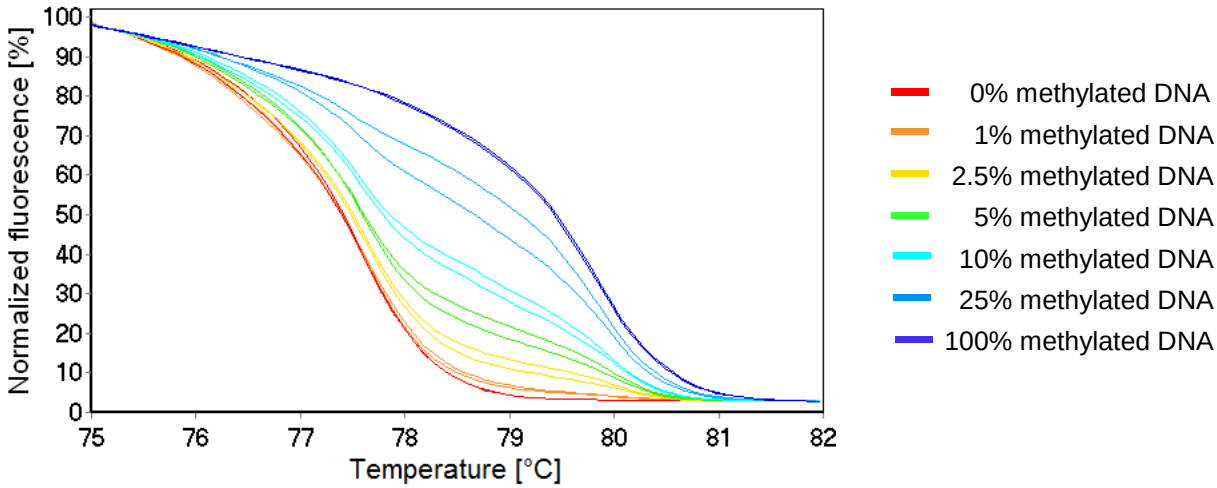

Figure 26: Normalized HRM curves of a standard series using primer set 1 for *CCND2*

To determine the methylation status of the samples, a calibration curve had to be established. Further details on the calibration function for this method can be found in *Chapter 4.3.6.* General information on how I established the calibration functions are written in *Chapters 4.3.1* and *5.9.2*.

Primer set 2

The forward and reverse primer of primer set 2 contained two and one CpGs at the 3' end of the sequence, respectively. Due to the extreme bias towards the methylated DNA alleles (25% and 100% methylated standard overlapped), no further experiments were carried out with this method.

4.2 A New Approach for Analysis of Heterogeneous DNA Methylation

With HRM analysis, heterogeneously methylated DNA can be detected, however, it is not possible to quantify the methylation status with the use of this analytical method (see *Chapter 3.3.3*). Within this work, heterogeneous methylation of sample DNA was observed in certain genes. Among the genes investigated, particularly *CCND2* showed heterogeneous methylation. Heterogeneous DNA methylation is characterized by an onset of melting at lower temperature in HRM analysis, as incorrect base pairing occurs during hybridization of dsDNA after PCR. The hybridization of not fully complementary DNA strands is probably caused by fast temperature decrease before HRM analysis.

The idea was to modify the settings in that way that the amplicons have more time for hybridization and thus exact base pairing can occur. Therefore two further HRM steps were added. In the following application of the modified temperature program for *CCND2* the sample analysis will be discussed. The first steps were set according to the protocol (see *Chapter 5.8.2*) inclusive HRM step A (73-83°C). Next, the new HRM step B from 83-73°C (with 0.1°C/2sec) was added for slow cooling of the samples. Immediately afterwards, during the HRM step C the samples were melted again from 73-83°C.

Figure 27 shows the melting profiles obtained for the unmethylated and methylated human control DNA and the tumor samples of patient 12 and 15 of the two HRM steps A and C. It can be seen that there is nearly no difference in the melting profiles of the human control DNA standards between the HRM steps. However, the melting profile of the PCR products of tumor 15 has changed by the additional hybridization step. The sample shows an onset of melting at 74°C in the HRM step A (black curve) whereas it begins to melt at 75°C in the HRM step C (gray curve).

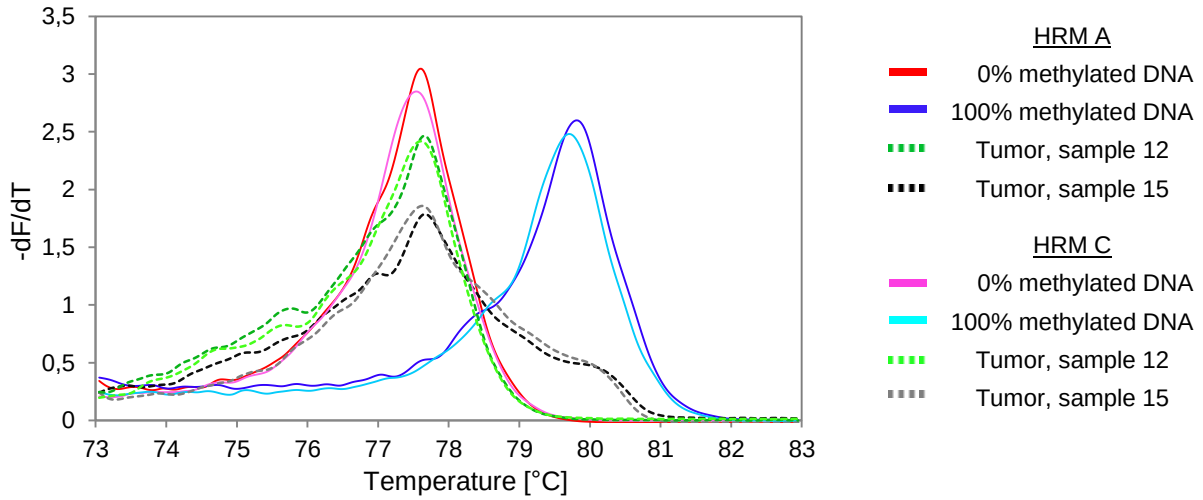

Figure 27: Comparison of the melting profiles obtained in HRM steps A and C; Replicate view

In contrast, the melting profile of the amplicons of tumor 12 (green curves) does not change significantly. In both HRM steps, the sample starts melting before the unmethylated DNA. However, at the melting point of the methylated DNA no peak can be seen in the melting profile of the PCR products of tumor 12. This indicates that the abnormal melting behavior of tumor 12 is not caused by heterogeneous methylation, but perhaps by a mutation in the sequence of this sample. A mutation could be easily proven by sequencing.

The normalized HRM curves are shown in *Figure 28*. It can be seen that the melting curve of tumor 15 runs optimal (no early onset of melting) in the HRM step C, but no improvement can be observed in case of tumor 12.

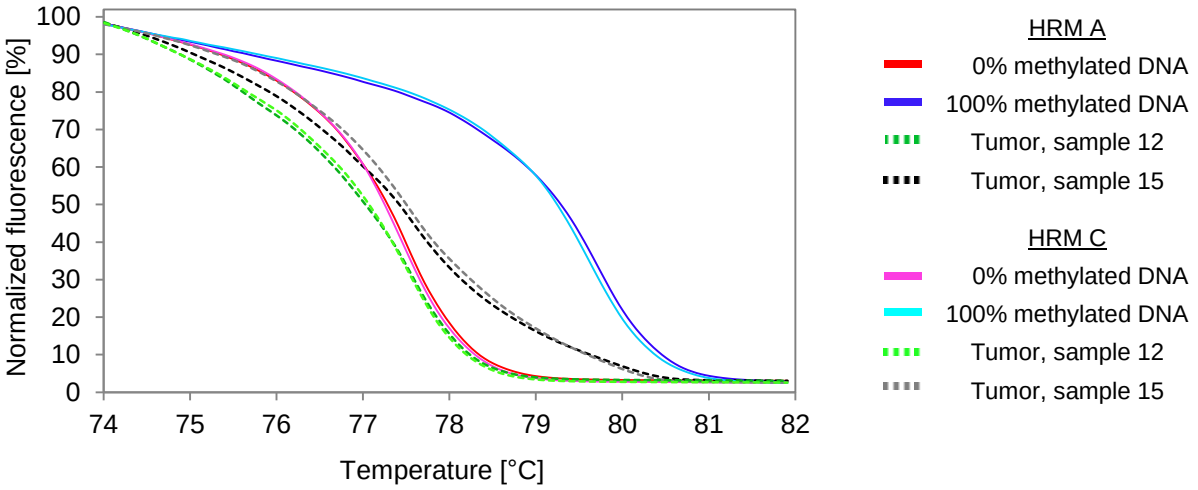

Figure 28: Comparison of the normalized HRM curves of the two HRM steps A and C; Replicate view

In my opinion, the novel analysis approach gives more correct results for heterogeneously methylated DNA samples and thus it should be used for subsequent measurements. However, the parameters could still be improved. For example, the hybridization step was carried out with a temperature reduction of 0.1°C per 2 sec. A higher speed could be tested in order to save time during the measurements.

4.3 Determination of the DNA Methylation Status in Tumor Suppressor Genes of Biopsy Samples from Breast Cancer Patients

Many studies have addressed their investigations on the methylation profile of breast tumors. However, little is known about how the methylation status in normal-appearing breast tissue differs in dependence of the distance to the tumor.

Biopsy samples from breast cancer patients were obtained from Ass. Prof. Dr**.** Georg Pfeiler, Department of Obstetrics and Gynecology, Medical University of Vienna. From each patient, a biopsy sample was taken from the tumor, the adjacent and the surrounding normal tissue (details can be found in *Chapter 5.4.2*). Ethical approval for the project was received and all patients gave written informed consent.

In the present study a total of 15 cases with invasive breast cancer (age range 39-76) were examined. Clinicopathological data were available for all patients, among whom 14 cases were classified as invasive ductal carcinomas and one as invasive lobular carcinoma. The hormone receptor status was assessed for 14 patients, 93% of the cases being ER positive, 86% were PR positive and 29% were HER2 positive. The details are summarized in *Appendix A, Table A2*.

After DNA extraction (see *Chapter 5.4.2*) and bisulfite treatment (see *Chapter 5.6*) of the samples, the DNA methylation status of selected tumor suppressor genes was determined by PCR and MS-HRM analysis (see *Chapter 5.8*). In *Appendix A, Table A1* a list of applied MS-HRM methods, including the parameters, can be found.

In the following sections the results for each gene are presented and discussed.

4.3.1 *APC*

The primer sequences for amplifying a fragment of the promoter of *APC* were taken from Balic *et al*. [74]. The amplicon has a length of 149 bp and contains 10 CpGs. The primer concentrations were 500 nM, as described in the literature. Although the sequence of the forward primer contains a CpG, the bias could be compensated by applying a relatively low annealing temperature (53°C). Details on this method can be found in *Appendix A, Table A1* and PCR and HRM conditions are described in *Chapter 5.8*.

Figure 29 shows representative normalized HRM curves obtained for a series of methylated DNA standards and the tumor samples 8 and 14. The shape of the melting curve obtained for tumor sample 14 is similar to that of the 50% methylated DNA standard. Thus it can be assumed that the DNA in the tumor tissue has fully methylated and fully unmethylated alleles. The presence of unmethylated and methylated alleles is also reflected in the melting profiles of the samples shown in *Figure 30*. The melting profile obtained for tumor 14 shows two peaks, one overlapping with the peak of the unmethylated DNA and one overlapping with the peak of the methylated DNA.

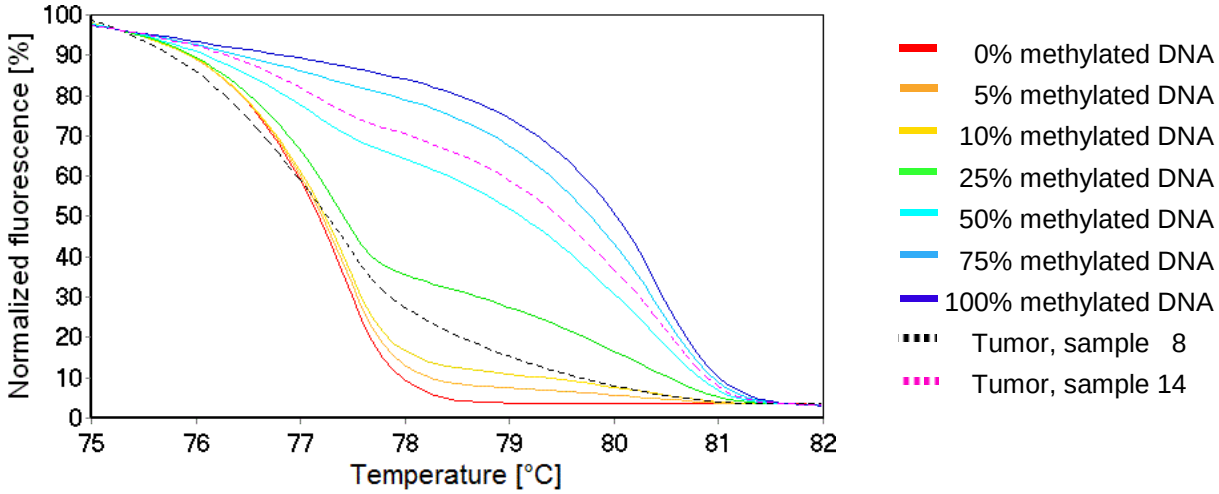

Figure 29: Normalized HRM curves of the PCR products for *APC;* Replicate view (Human control DNA standards and tumor samples 8 and 14)

In contrast, the normalized HRM curve and the melting profile obtained for tumor 8 are slightly different. The PCR products of the sample began already to melt at lower temperature than the amplicons of the 0% methylated standard. Furthermore, instead of a peak at the position of the methylated DNA in the melting profile a decrease of the curve can be observed. This indicates heterogeneous methylation of DNA in tumor sample 8. Details on heterogeneous DNA methylation can be found in *Chapter 3.3.3*. Due to heterogeneous DNA methylation, formation of dsDNA without exact complementarity will occur after PCR. The dsDNA begins to denature at lower temperature and thus the calculated methylation status of the sample is lower than the actual methylation status would be.

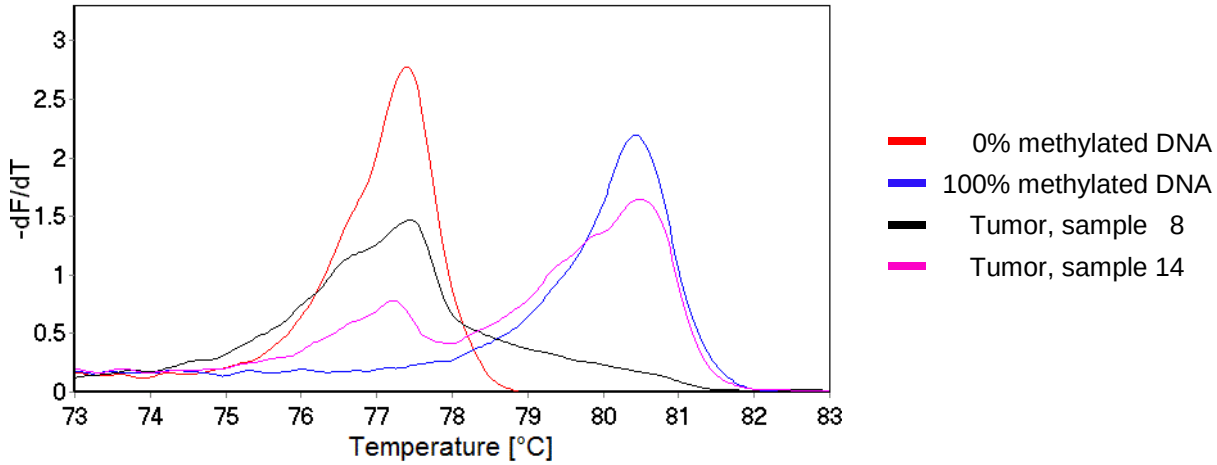

Figure 30: Melting profile of the PCR products for *APC*; Replicate view
(Human control DNA standards and tumor samples 8 and 14)

In order to establish a calibration function, PCR and HRM analysis of DNA standards differing in their methylation status were carried out in duplicate on three different days. Biopsy samples were analyzed in two runs in duplicate. The data of HRM step A were used for determination of the methylation status. To calculate the methylation status, I have modified the evaluation method of Migheli *et al.* [67] (see *Chapter 3.3.2*). For this purpose, I also used the dataset of the normalized HRM curves. However, I calculated the average of the normalized fluorescence signal for each standard over the entire temperature interval instead of using single values at chosen temperature points. The obtained values were standardized between 0-100% with respect to the unmethylated and methylated human control DNA standards. Further details on the calculation of the standardized values can be found in *Chapter 5.9.2*.

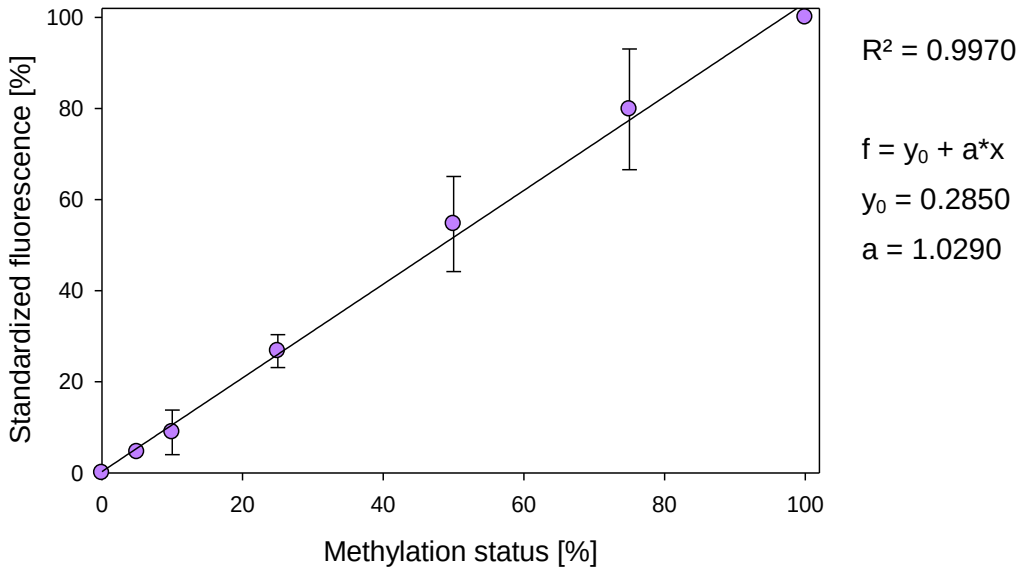

Figure 31: Calibration function for *APC;* Mean and standard deviation of n = 6 measurements

Figure 31 shows the calibration function for the method. A linear calibration function could be taken since no bias was observed. The repeatability of the method was acceptable, but not very good.

By using the calibration equation, the methylation status of the samples was calculated. In *Appendix B, Table B1* a list of the individual values can be found. In *Figure 32*, the results of the investigation on the methylation status of the 15 biopsy samples for the gene *APC* are summarized. For each breast cancer patient the DNA methylation status of tumor, adjacent and normal tissue was determined. By repeatedly analyzing the unmethylated standard a limit of detection (LOD, S/N = 3) of 0.7% and a limit of quantification (LOQ, S/N = 10) of 3.0% was determined. The determination of LOD and LOQ is described in *Chapter 5.9.4*. In addition, the significance test analysis of variance (ANOVA) was carried out, comparing the methylation status of the adjacent or normal tissue with that of the tumor tissue (see *Chapter 5.9.5*). The results of the significance test are shown in the graphic.

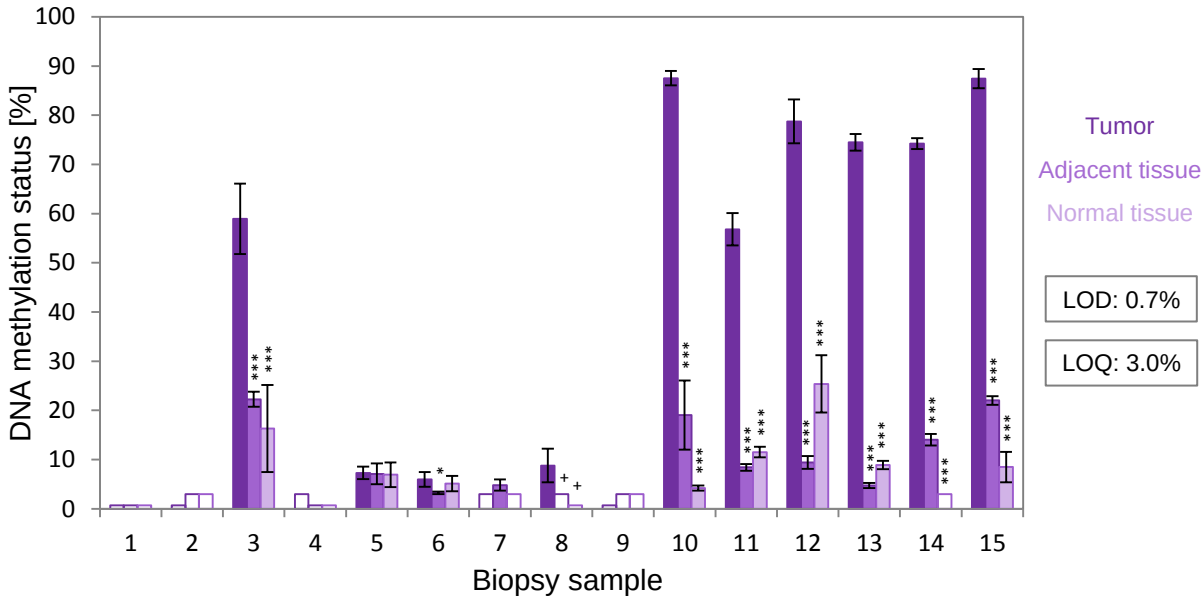

*P ≤ 0.05, **P ≤ 0.01, ***P ≤ 0.001, $^{+}$significant (no test possible)

Figure 32: DNA methylation status [%] of *APC* for biopsy samples*;* Mean and standard deviation of n ≥ 4 measurements; Empty boxes denote a DNA methylation ≤ LOD or ≤ LOQ

Some breast cancer patients show very low (patients 5, 6, 7 and 8) or even undetectable/ no quantifiable (patients 1, 2, 4 and 9) DNA methylation in the promoter region of *APC* in all three tissue types. Considering only the tumor tissue samples, 7 out of 15 patients (47%) show a methylation status higher than 50%. Highly significant differences in the DNA methylation status were found between tumor & adjacent tissue and tumor & normal tissue for these seven patients. As mentioned above, the methylation status of tumor sample 8 is rather uncertain due to heterogeneous methylation.

Interestingly, in some cases the methylation status of the adjacent tissues was found to be lower than that of the respective normal tissues, as it was observed for patients 11, 12 and 13. The adjacent tissues were expected to show higher or similar methylation status than/as the normal tissues.

There was no correlation observed between the methylation status of the tumor tissue and the hormone receptor status of the patients. In addition, no age-dependent correlation was observed.

The data indicate that 47% of the breast tumors show increased DNA methylation of the *APC* gene. This result is in good agreement with previous studies. Tserga *et al.* [21] determined the DNA methylation status of biopsy samples taken from patients with invasive breast cancer using MS-HRM analysis. 25 out of 46 tumors (54%) were identified to be hypermethylated.

Some other working groups analyzed invasive tumor samples with respect to the DNA methylation of *APC* using MSP. In a study from Jin *et al*. [22], the promoter region of *APC* was hypermethylated in only 18 out of 50 cases (36%). Virmani *et at.* [19] found a DNA methylation in 44% (34 out of 77) of the tumor samples and Dulaimi *et at.* [20] discovered 44% (15 out of 34) of the tumor samples to be hypermethylated. Even more frequently the tumor samples showed a DNA methylation of *APC* in a study of Sarrió *et al.* [23], as 54% (25 out of 46) were hypermethylated.

4.3.2 *BRCA1*

The sequences of the primer set for the *BRCA1*-method were taken from Wong *et al.* [26]. Care was taken that the primers were located in the promoter region of *BRCA1*. In addition, sequences were selected that differ as much as possible from the *pseudo-BRCA1* in order to avoid the amplification of by-products. The amplicon has a length of 122 bp and contains 9 CpGs [26, 75]. I optimized the PCR conditions for this method. Details on this method can be found in *Appendix A, Table A1. Figure 33* shows representative normalized HRM curves obtained for human control DNA standards and biopsy sample 12.

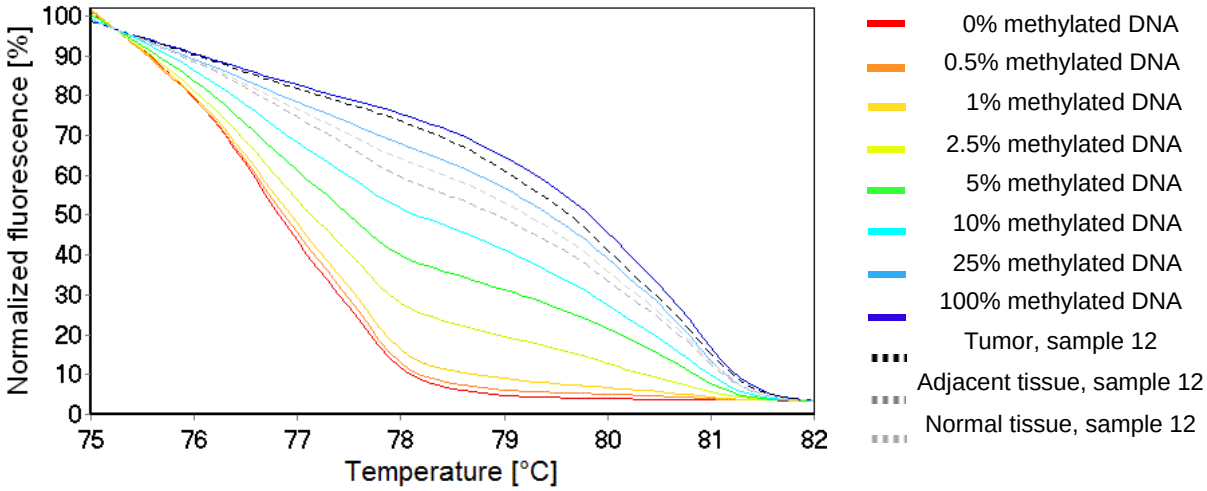

Figure 33: Normalized HRM curves of the PCR products for *BRCA1;* Replicate view (Human control DNA standards and biopsy sample 12)

A calibration function was established using a hyperbola function. In *Figure 34* the calibration function of this method is shown. The repeatability was quite good. The preferred amplification of the methylated template is most probably caused by the sequences of the primers and the high annealing temperature.

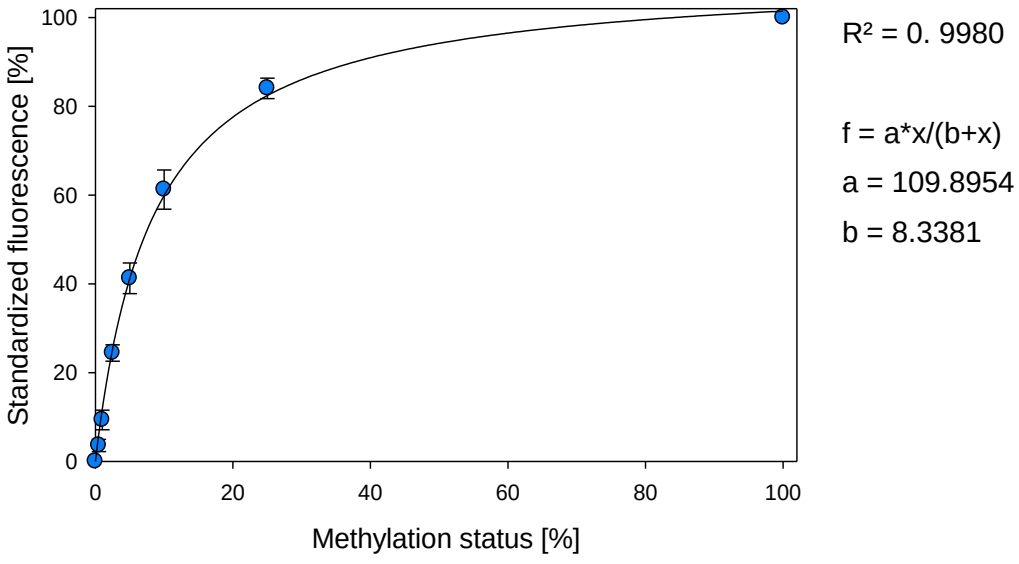

Figure 34: Calibration function for *BRCA1;* Mean and standard deviation of n = 6 measurements

In general, the DNA methylation status of the samples could be determined without any problems since they did not show any heterogeneous methylation patterns. Only the methylation status of the adjacent tissue of biopsy sample 15 could not be determined, as too high amounts of primer dimers were formed during PCR.

The results obtained for the biopsy samples are summarized in *Figure 35*. The methylation levels obtained in individual measurements are given in *Appendix B, Table B2*. A LOD (S/N = 3) of 0.4% DNA methylation and a LOQ (S/N = 10) of 1.6% DNA methylation were determined. The significance test ANOVA was performed for the different tissue types of biopsy samples 12 and 14. Details on data analysis can be found in *Chapter 5.9*.

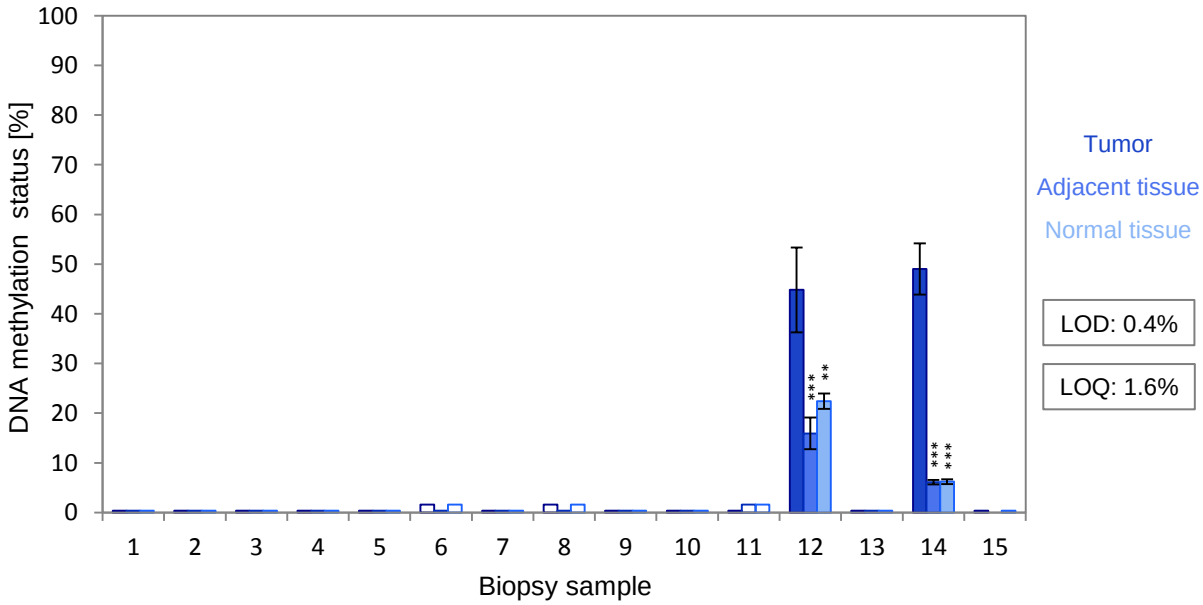

*P ≤ 0.05, **P ≤ 0.01, ***P ≤ 0.001, $^{+}$significant (no test possible)

Figure 35: DNA methylation status [%] of *BRCA1* for biopsy samples*;* Mean and standard deviation of n ≥ 4 measurements; Empty boxes denote a DNA methylation ≤ LOD or ≤ LOQ
(DNA methylation status could not be determined for the adjacent tissue of patient 15)

It can be seen in *Figure 35* that 13 out of 15 biopsy samples were methylated below the LOQ or even not methylated in the promoter region of *BRCA1*. Just two breast cancer patients showed a DNA methylation in this gene. Both patients had a methylation status of about 50% in the tumor sample. And in both cases, the methylation status of the tumor was significantly higher than in the adjacent and the normal surrounding tissue. Compared to the other patients, patient 12 and 14 showed not only a high methylation status in the tumor, but also a relatively high DNA methylation in the surrounding tissue.

As observed for *APC*, the adjacent tissue of patient 12 showed a higher methylation status than the normal tissue.

As a conclusion it can be said that the gene *BRCA1* is aberrantly methylated in a small number of breast cancer patients, namely only in approximately 13% (2 out of 15). However, these patients showed quite a high methylation status in the *BRCA1* promoter region.

Wong *et al.* [26] determined the DNA methylation status of *BRCA1* in tumor samples from breast cancer patients. The tumor samples (without germline *BRCA1* mutation) were clustered in three groups, based on *BRCA1* mutation-associated morphologic features. Group 1, which consisted of tumor tissues showing high *BRCA1* mutation-associated pathology, was hypermethylated in 45% of the cases (9 out of 20). In contrast, group 3 (having low *BRCA1* mutation-associated pathology) was hypermethylated in only 9% of the tumor tissues (3 out of 32).

4.3.3 *CDKN2A*

The sequences of the primers were taken from Migheli *et al.* [67]. The primers target a sequence of the promoter region of *CDKN2A*. The amplicon has a length of 73 bp and contains 7 CpGs. Primer concentrations and annealing temperature were used as described in the literature. Further PCR and HRM condition were applied according to our in-house protocol (see *Chapter 5.8*). Details on the method can be found in the *Appendix A, Table A1*.

In *Figure 36*, the melting profile of the PCR products of representative samples can be seen. In general, the peaks are quite broad. Espeacilly the peak of the methylated DNA is rather low and broad than high and narrow.

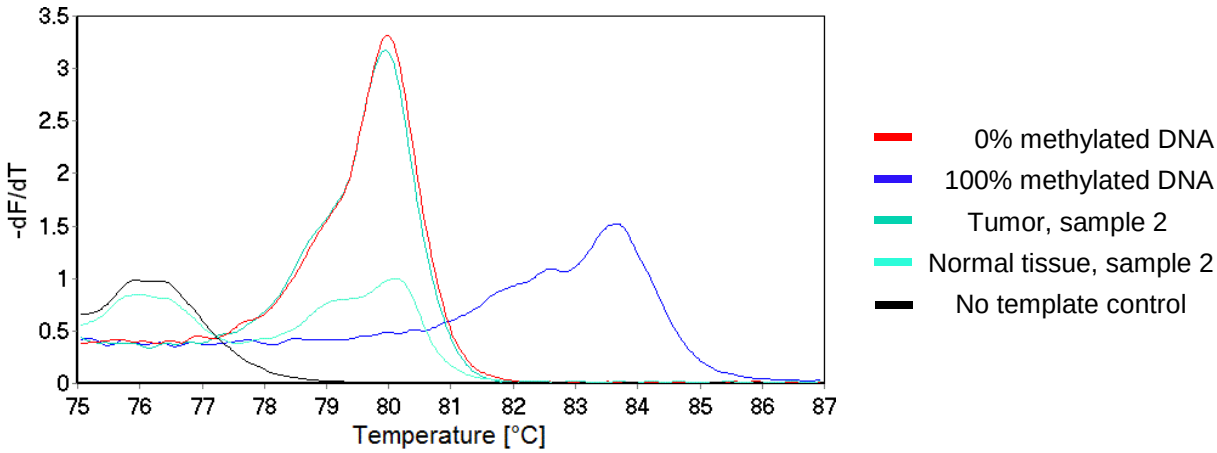

Figure 36: Melting profile of some samples for *CDKN2A*; Replicate view
(Human control DNA standards and tumor and normal tissue of biopsy sample 2)

The peak obtained for the no template control indicates that primer dimers have been formed in the absence of template DNA. Primer dimers are usually shorter than the desired amplicon and therefore melt at a lower temperature than the unmethylated and methylated DNA templates. The melting profile obtained for the tumor of biopsy sample 2 was virtually identical to the melting profile of the unmethylated DNA. The melting profile obtained for the normal tissue of biopsy sample 2 shows an additional peak at 76°C, indicating the formation of primer dimers. However, by starting the normalization process at 77°C, an influence on the melting profile of the amplicon could be avoided. Thus, the methylation status of the sample could be determined without systematic error.

Figure 37 shows an example of normalized HRM curves obtained for human control DNA standards and biopsy sample 12. The curves obtained for the tissue samples are parallel to the standard curves. Biopsy sample 12, and also all other biopsy samples, did not show any heterogeneous methylation patterns.

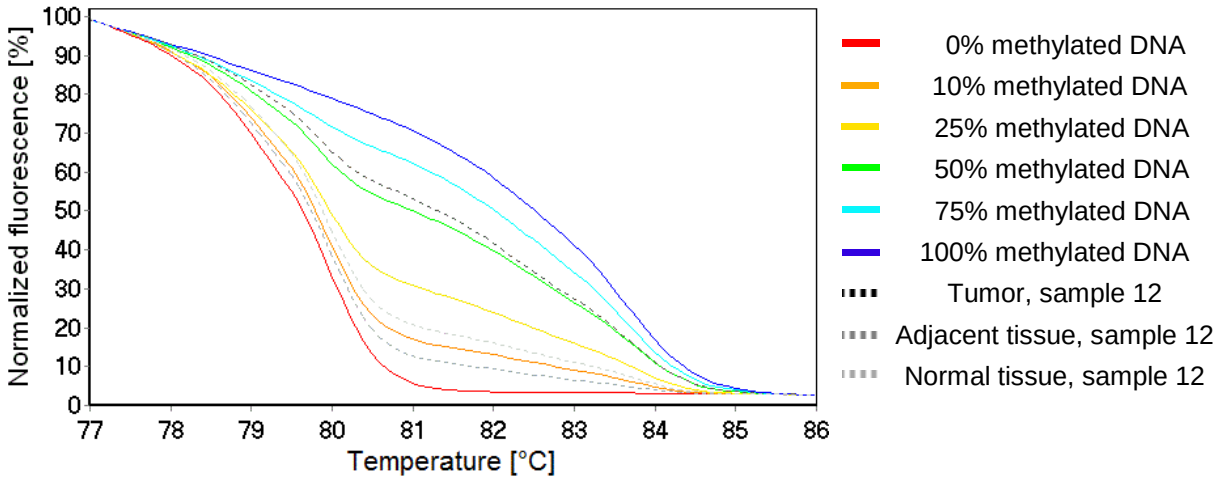

Figure 37: Normalized HRM curves of the PCR products for *CDKN2A;* Replicate view (Human control DNA standards and biopsy sample 12)

This method showed a low bias towards the methylated DNA and therefore a hyperbola was chosen for fitting the data. The calibration function for this method can be seen in *Figure 38*. The repeatability of this method was very good.

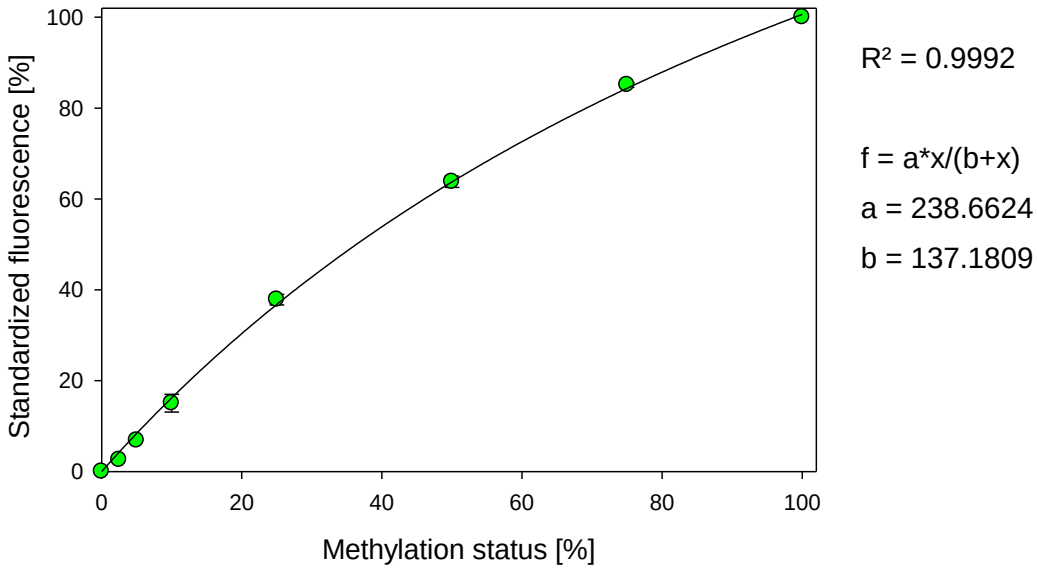

Figure 38: Calibration function for *CDKN2A;* Mean and standard deviation of n = 6 measurements

The biopsy samples of the 15 breast cancer patients were measured twice in duplicate. The methylation levels obtained in individual measurements are given in *Appendix B, Table B4*. The LOD and the LOQ of the method were found to be 1.0% and 3.3%, respectively. The significance test ANOVA was performed for the different tissue types of biopsy samples 12 and 14. Details on data analysis can be found in *Chapter 5.9*. *Figure 39* summarizes the results for the biopsy samples with respect to the methylation status.

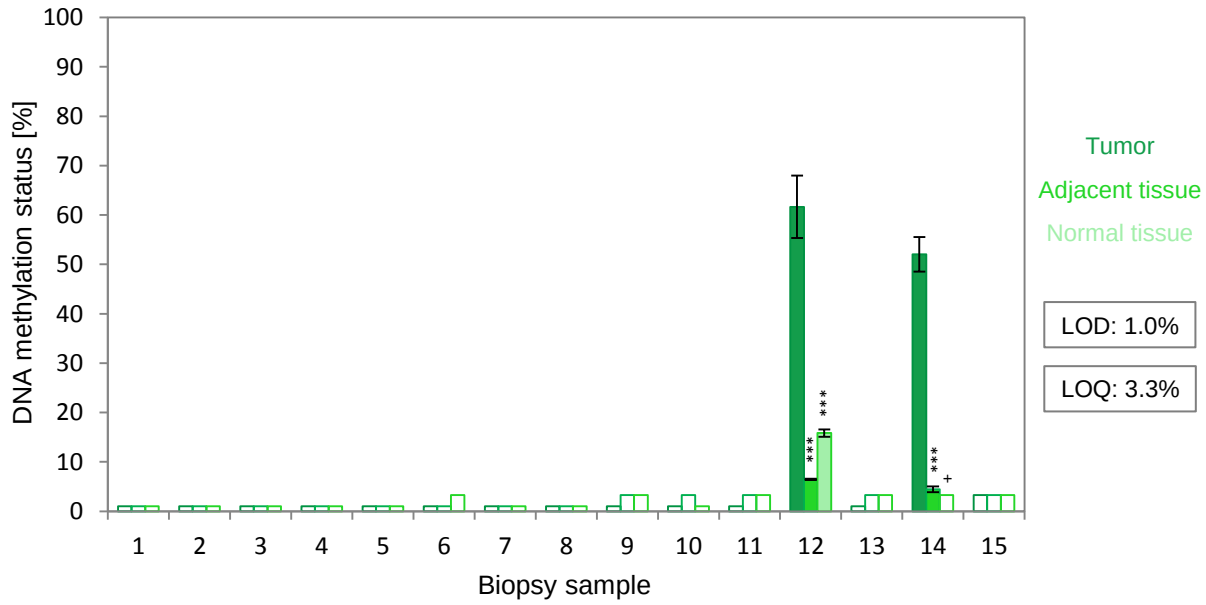

*P ≤ 0.05, **P ≤ 0.01, ***P ≤ 0.001, $^{+}$significant (no test possible)

Figure 39: DNA methylation status [%] of *CDKN2A* for biopsy samples; Mean and standard deviation of n ≥ 4 measurements; Empty boxes denote a DNA methylation ≤ LOD or ≤ LOQ

The results obtained for *CDKN2A* are very similar to those obtained for *BRCA1*. The same two breast cancer patients (patient 12 and 14) who had a high DNA methylation in the promoter region of *BRCA1* also showed a high methylation in the promoter of *CDKN2A*. For the tumor samples of both patients a methylation status > 50% was obtained. And in both cases, the methylation status of the tumor was significantly higher than that in the adjacent and the normal surrounding tissue. Patient 12 showed again a higher methylation status in the adjacent tissue than in the normal tissue.

In summary, the promoter region of *CDKN2A* was found to be methylated in 13% of the patients. However, in these patients the promoter region was highly methylated (> 50%). Patient 12 and 14 showed aberrant DNA methylation in the two genes *BRCA1* and *CDKN2A*.

Sinha *et al.* [31] determined the DNA methylation status in the *CDKN2A* promoter of 106 invasive breast carcinomas. 28% of group A (≤ 40 years, n = 47) and 31% of group B (> 40 years, n = 59) were hypermethylated. The frequency of DNA methylation in the promoter region of *CDKN2A* was thus higher than in the tumor samples analyzed in the present master thesis.

4.3.4 *CDKN2A*_Exon 3

The MS-HRM method was developed by Bettina Werner [76] in our research group as part of her master thesis. The amplicon has a length of 116 bp and contains 10 CpGs. The primers do, however, not target the promoter region but a region located in exon 3. Details on the method can be found in the *Appendix A, Table A1* and PCR and HRM conditions are described in *Chapter 5.8*.

In *Figure 40*, representative normalized HRM curves are shown. The curve obtained for the 100% methylated standard indicates that the amplicon has several melting domains. Furthermore, it is noticeable that the curves obtained for the biopsy samples have a different course compared to the curves obtained for the standards. Other biopsy samples also showed a different shape of the normalized HRM curve compared to the standards. However, the reason for this deviation is unclear.

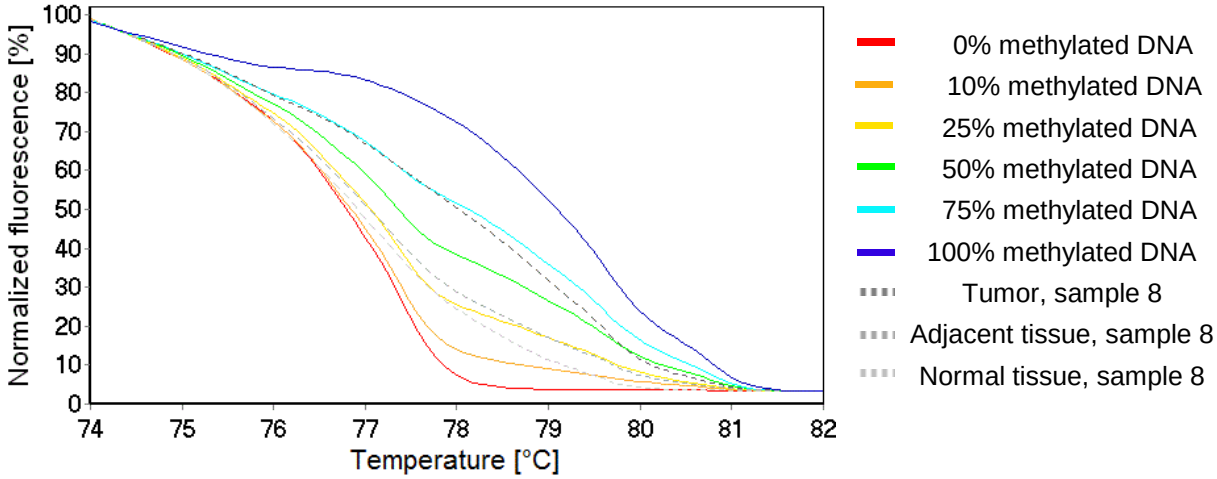

Figure 40: Normalized HRM curves of the PCR products for *CDKN2A*_Exon 3; Replicate view (Human control DNA standards and biopsy sample 8)

DNA standards differing in their methylation status were analyzed in duplicate in four different runs. The duplicates gave very similar values. However, larger differences were observed between various runs.

A calibration function was established by plotting the standardized values of the human control DNA standards against the methylation status, fitting the data by linear regression (shown in *Figure 41*).

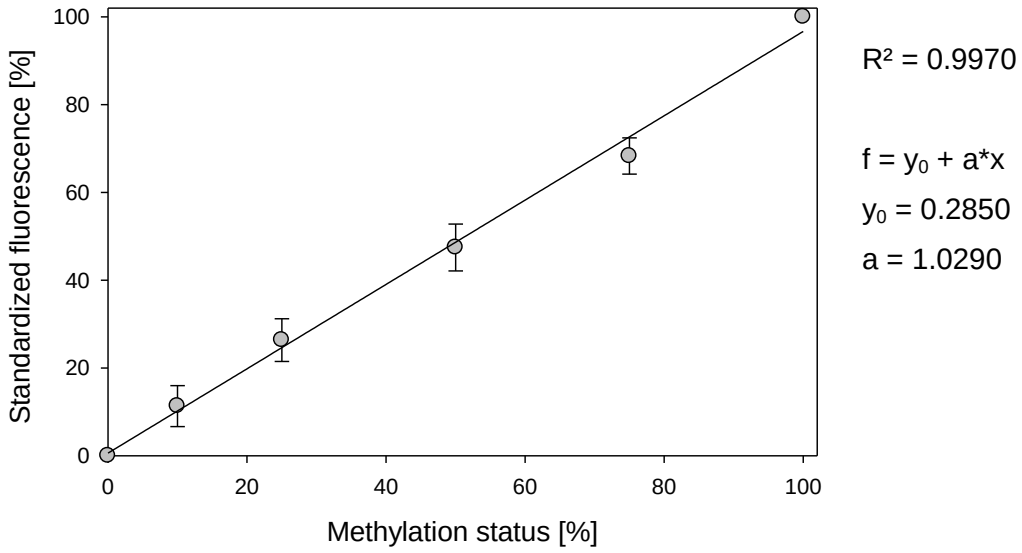

Figure 41: Calibration function for *CDKN2A*_Exon 3; Mean and standard deviation of n = 8 measurements

All biopsy samples were measured in two runs in duplicate. Details on data analysis can be found in *Chapter 5.9*. The methylation levels obtained in individual measurements are given in *Appendix B, Table B5*. In *Figure 42*, the results are summarized.

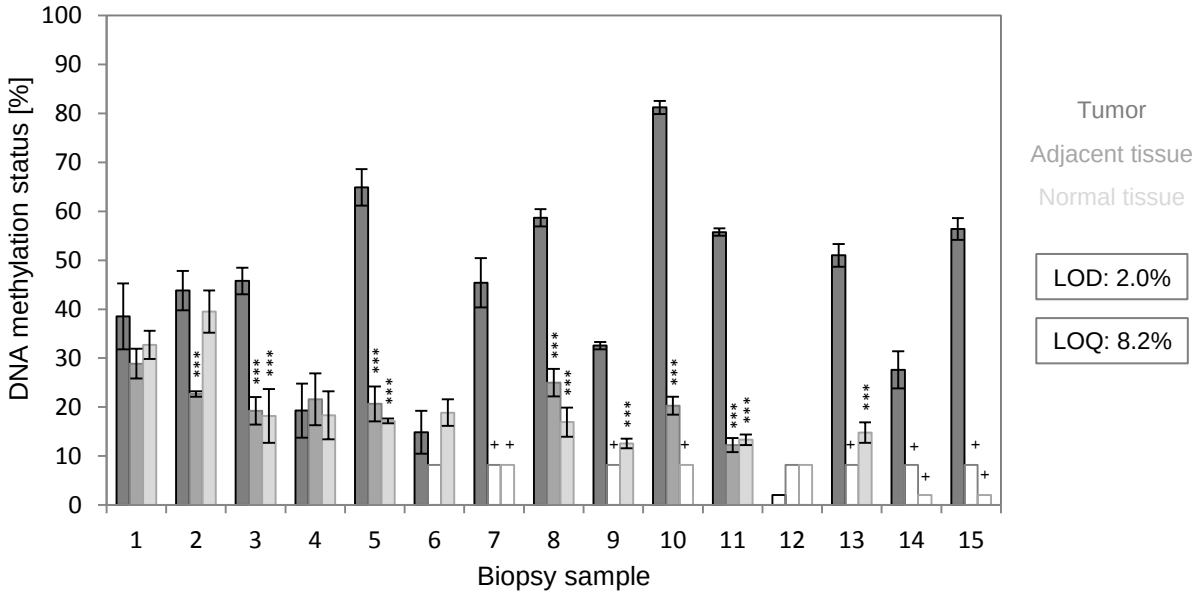

*P ≤ 0.05, **P ≤ 0.01, ***P ≤ 0.001, +significant (no test possible)

Figure 42: DNA methylation status [%] of *CDKN2A*_Exon 3 for biopsy samples; Mean and standard deviation of n = 4 measurements; Empty boxes denote a DNA methylation ≤ LOD or ≤ LOQ

Interestingly, the DNA methylation status in exon 3 was found to be very different from that in the promoter region. 14 out of 15 patients showed a DNA methylation in the tumor tissue. The highest DNA methylation was found in tumor 10 with a methylation status of 81 ± 1%. Only the tumor tissue of patient 12 was unmethylated in exon 3. The adjacent and normal tissue of patient 12 showed low DNA methylation (< LOQ).

In 73% of the patients, a significant difference between tumor and adjacent tissue and in 67% a significant difference between tumor and normal tissue was observed. There were 4 patients (1, 2, 4 and 6) who showed DNA methylation in the tumor, but there was no significant difference to the adjacent and/or normal tissue.

Since in 10 out of 15 cases a significant difference was found between the methylation status in the tumor and the respective normal tissue, the methylation status in exon 3 of *CDKN2A* can be considered as a potential biomarker for diagnosis of breast cancer. However, a number of breast tissue samples from healthy individuals as well as from breast cancer patients have to be analyzed in order to determine both its sensitivity and its specificity and thus the probability of obtaining false negative and false positive results, respectively.

4.3.5 *RASSF1A*

The method was developed by Anna Raab [77] in our research group as part of her diploma thesis. The primers are located in exon 1 of the gene. The amplicon has a length of 118 bp and contains 9 CpGs. Some investigations on biopsy samples were already performed by Anna Raab. Details on the method can be found in the *Appendix A, Table A1*. PCR and HRM condition were applied according to our in-house protocol (see *Chapter 5.7*).

In *Figure 43*, representative normalized HRM curves for *RASSF1A* are shown. The curves obtained for biopsy sample 8 are similar to those obtained for the standards. None of the samples showed any heterogeneous methylation in this gene segment.

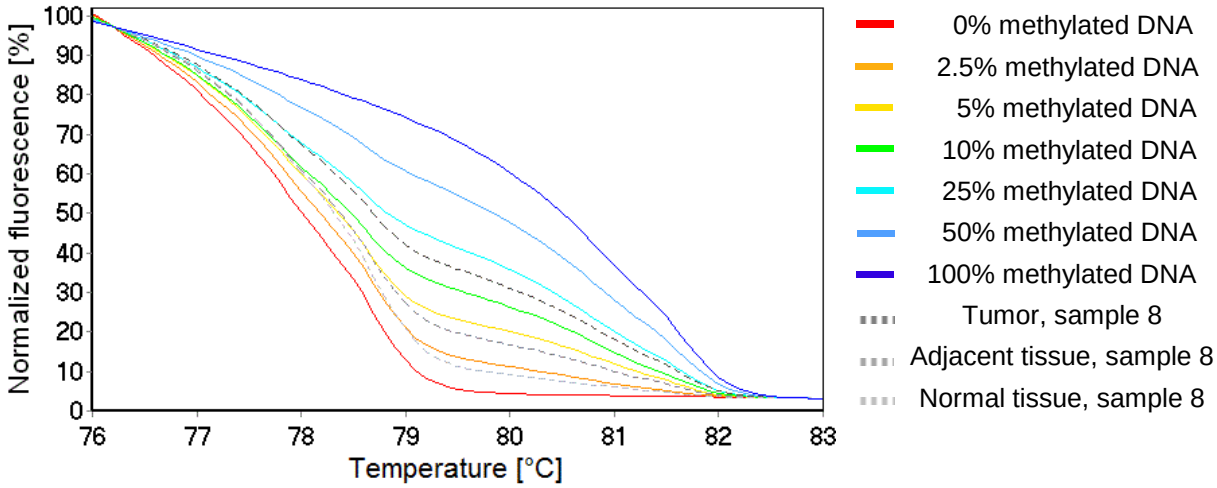

Figure 43: Normalized HRM curves of the PCR products for *RASSF1A*; Replicate view (Human control standards and biopsy sample 8)

The calibration function was established by plotting the standardized values against the methylation status and fitting the data by a hyperbola function (see *Figure 44*).

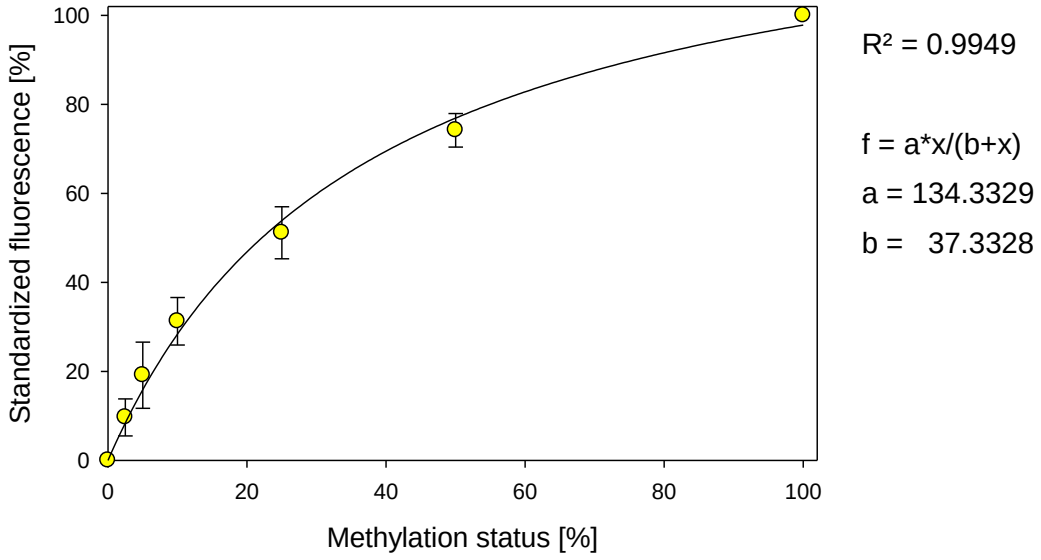

Figure 44: Calibration function for *RASSF1A;* Mean and standard deviation of n = 6 measurements

This method showed a moderate bias towards methylated DNA. The repeatability of this method was satisfactory. The biopsy samples of the 15 breast cancer patients were measured in two runs in duplicate. Details on data analysis can be found in *Chapter 5.9*. The methylation levels obtained in individual measurements are given in *Appendix B, Table B8*. *Figure 45* summarizes the results of the biopsy samples.

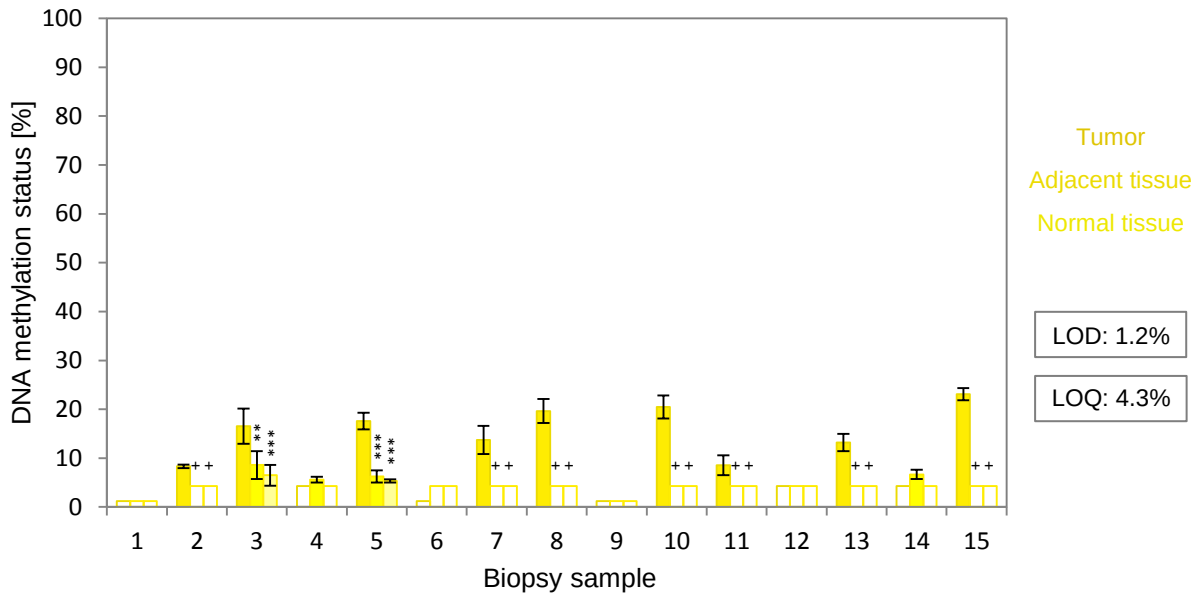

*P ≤ 0.05, **P ≤ 0.01, ***P ≤ 0.001, $^{+}$significant (no test possible)

Figure 45: DNA methylation status [%] of *RASSF1A* for biopsy samples*;* Mean and standard deviation of n = 4 measurements; Empty boxes denote a DNA methylation ≤ LOD or ≤ LOQ

In 9 out of 15 breast cancer patients (60%) the tumor sample was methylated. However, the methylation status of the tumors was relatively low. The tumor of patient 15 had the highest value with a DNA methylation of 23 ± 1%. In these nine patients significant differences between the tumor & the adjacent and/or normal tissue could be observed. A DNA methylation status above the LOQ could be observed in 27% of the adjacent tissue samples and only in 13% of the normal tissue samples.

Lewis *et al.* [30] determined the DNA methylation in the *RASSF1A* promoter of breast tissue samples using MSP. In this study a DNA methylation was found in 59% (n = 27) of the malignant tumor tissues. The frequency is in good agreement with the frequency found in the present master thesis. However, Lewis and co-workers also observed hypermethylation in 29% of benign breast tissue samples from the cancer patients and in 37% (n = 55) of breast tissue samples from unaffected women.

Dulaimi *et al.* [20] observed a hypermethylation of the *RASSF1A* promoter in 65% (22 out of 34) of invasive breast tumor samples using MSP. Tserga *et al.* [21] found a methylation in only 16 out of 48 (33%) of invasive breast carcinomas by the use of MSP.

4.3.6 *CCND2*

The method for *CCND2* was developed as part of this master thesis (see *Chapter 4.1.2*). Details on this method are summarized in *Appendix A, Table A1*. PCR and HRM conditions are described in *Chapter 5.8*.

A strong influence of the presence of ethanol residues on the melting temperature of DNA was observed. During bisulfite conversion the column is washed with ethanol (absolute) before eluting the DNA (see *Chapter 5.6.2*). The ethanol must be completely removed after the washing step to avoid matrix effects. In one batch of bisulfite conversion of biopsy samples, the ethanol was not completely removed. A PCR run was performed with both pure DNA samples and DNA samples contaminated with residues of ethanol (see *Figure 46*). The following figure shows the effect of ethanol on the melting behavior of the DNA using the example of the normal tissue of patient 3. It can be seen that without residues of ethanol the amplicon obtained for normal tissue 3 (black curve) shows the same melting behavior as the unmethylated human control DNA (red curve). HRM analysis of the same sample containing residues of ethanol (green curve) yielded a peak shift to lower temperature.

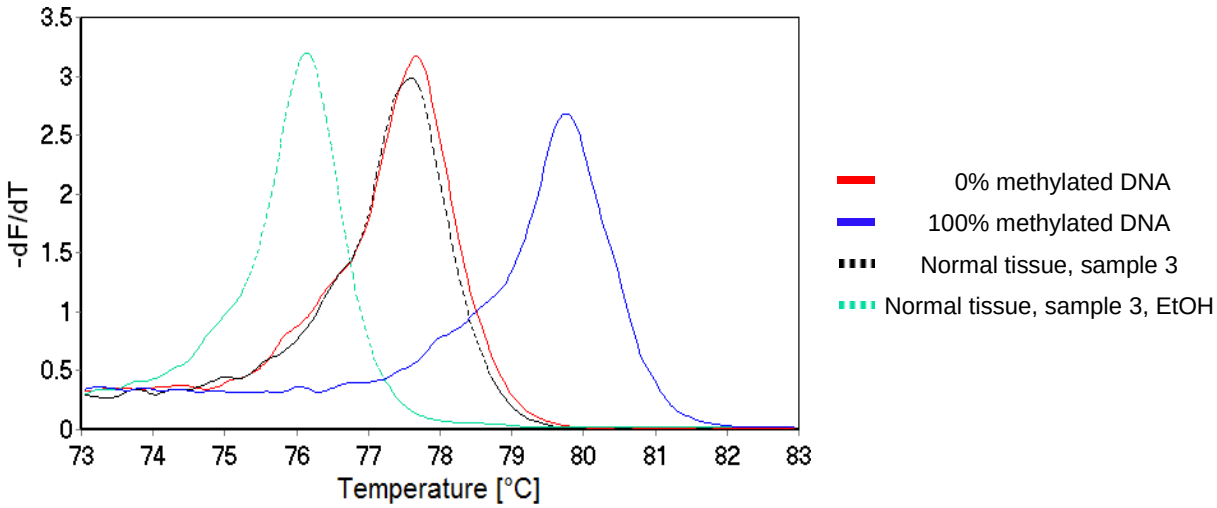

Figure 46: Melting profile of some amplicons of *CCND2*, showing the influence of ethanol on the melting temperature

The temperature difference of the two reaction batches was about 1.5°C, although it was the same biopsy sample. In this case, the effect of ethanol on the melting temperature of the DNA is enormously.

In *Figure 47*, representative normalized HRM curves for *CCND2* can be seen. The curve obtained for the tumor tissue of patient 10 showed a different progression than that for the standards. The reason for this may be a partial methylation of the DNA. Heterogeneous methylation was observed in some tumor samples in the HRM step A. However, the DNA methylation status of the samples could be determined since the biopsy samples did not melt

at lower temperature than the 0% methylated DNA standard in the HRM step C. For comparison of HRM step A and C see *Chapter 4.2*.

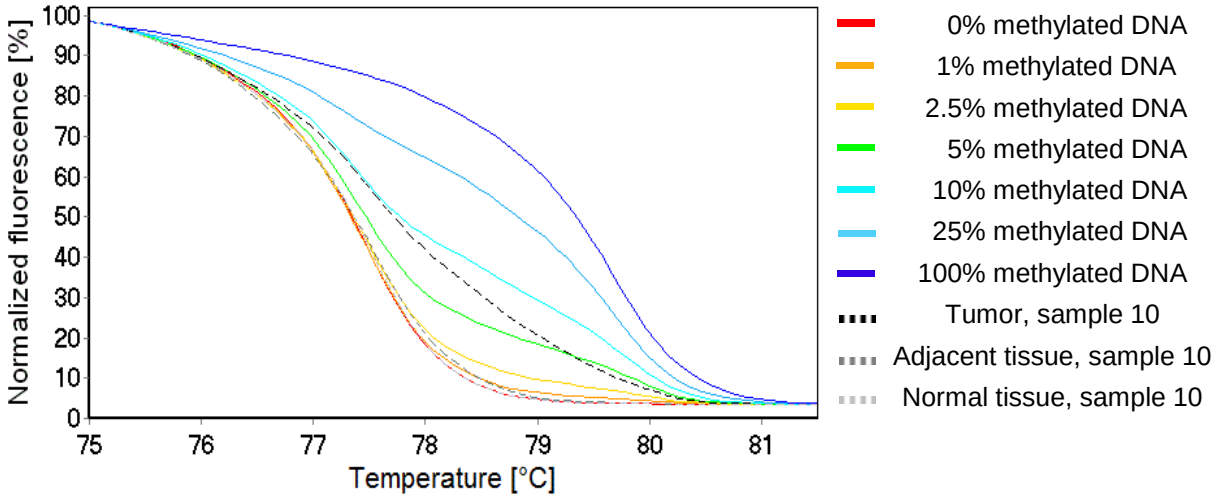

Figure 47: Normalized HRM curves of the PCR products for *CCND2*; Replicate view (Human control standards and biopsy sample 10)

The standard series was analyzed in three runs in duplicate. In *Figure 48* the calibration function obtained by fitting the data with a hyperbola function is shown. The repeatability was very good.

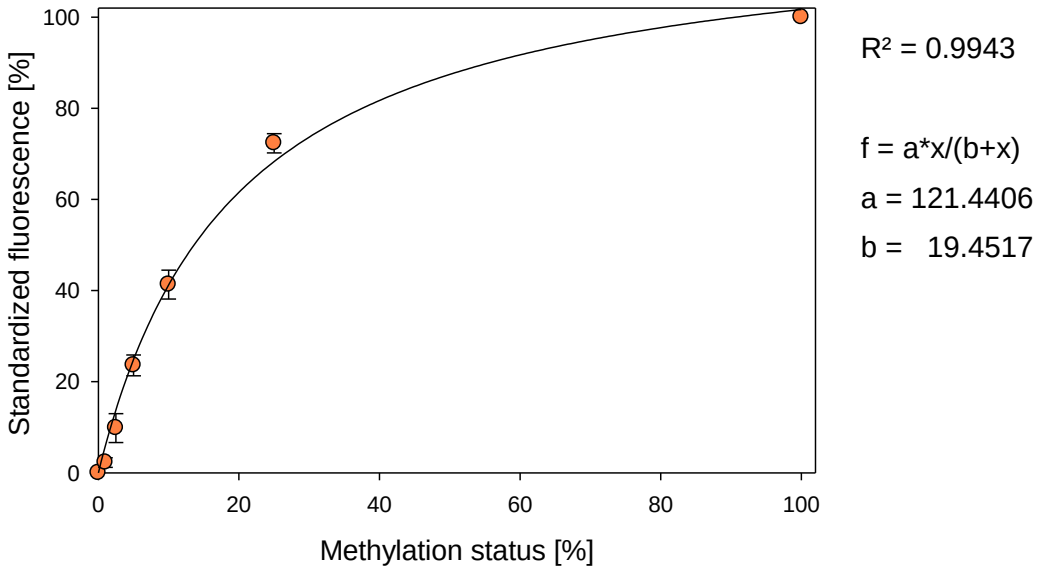

Figure 48: Calibration function for *CCND2;* Mean and standard deviation of n = 6 measurements

The biopsy samples of the breast cancer patients were measured twice in duplicate. Details on data analysis can be found in *Chapter 5.9*. The results of the methylation status obtained in individual measurements are given in *Appendix B, Table B3*. *Figure 49* summarizes the results of the biopsy samples.

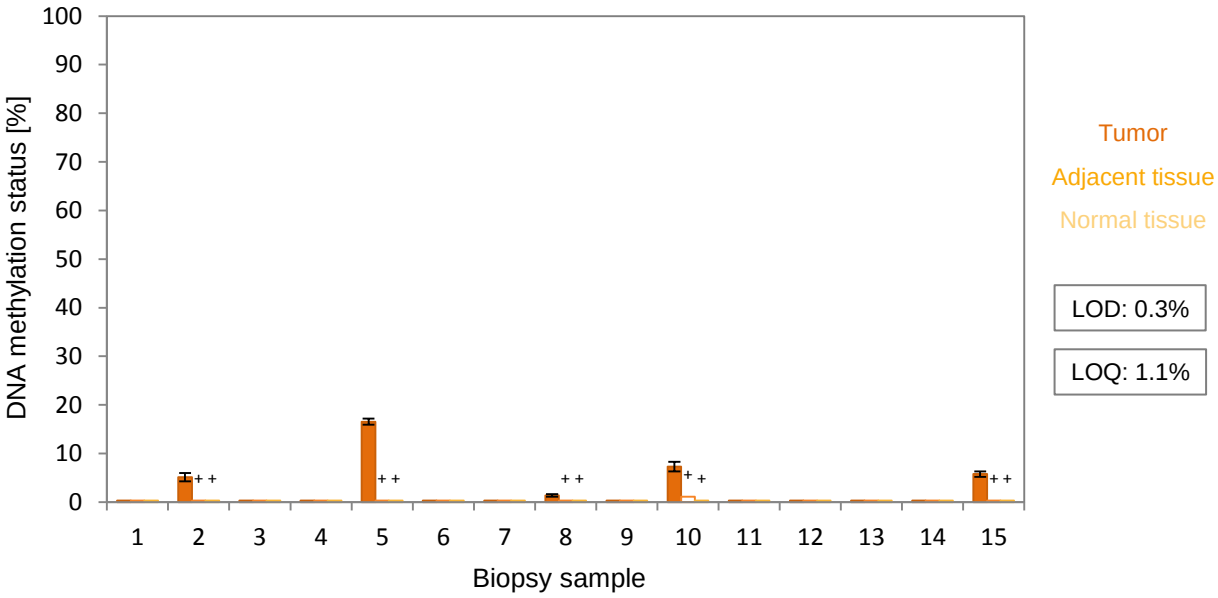

*P ≤ 0.05, **P ≤ 0.01, ***P ≤ 0.001, $^{+}$significant (no test possible)

Figure 49: DNA methylation status [%] of *CCND2* for biopsy samples; Mean and standard deviation of n = 4 measurements; Empty boxes denote a DNA methylation ≤ LOD or ≤ LOQ

The results indicate that in general the DNA methylation status of the promoter region is very low. Only five patients (33%) showed DNA methylation in the tumor. The highest level (17 ± 0.6%) was found for the tumor sample of patient 5. The adjacent and the surrounding normal breast tissues did not show a DNA methylation in the promoter region of *CCND2*, except the adjacent tissue of patient 10, which had a DNA methylation below the LOQ.

Evron and co-workers [28] investigated the DNA methylation status of *CCND2* in different breast tissue types from breast cancer patients using MSP. They detected DNA methylation in 46% (49 out of 106) of the analyzed primary breast carcinomas. None of the 11 corresponding normal breast tissues analyzed showed DNA methylation in the promoter of *CCND2*. Based on these results, the authors concluded that *CCND2* promoter-methylation can be considered as a tumor specific phenomenon.

Lewis *et al.* [30] determined the methylation status of biopsy samples from invasive breast tumors and breast tissue samples from unaffected women using MSP. 57% (13 out of 23) of the tumor samples were hypermethylated and DNA methylation was found in only 2% (1 out of 53) of breast samples from unaffected women.

The results of the present master thesis are in good agreement with those previous studies.

4.3.7 *GSTP1*

The sequences of the primers were taken from Tserga *et al*. [21]. The primers target a sequence of the promoter region of *GSTP1*. The amplicon has a length of 120 bp and contains 12 CpGs. I optimized the method (details can be found in *Appendix A, Table A1*). PCR and HRM analysis were carried out under the in-house conditions (see *Chapter 5.7*).

Figure 50 shows normalized HRM curves obtained for human control DNA standards and for tumor, adjacent and normal tissue from patient 13.

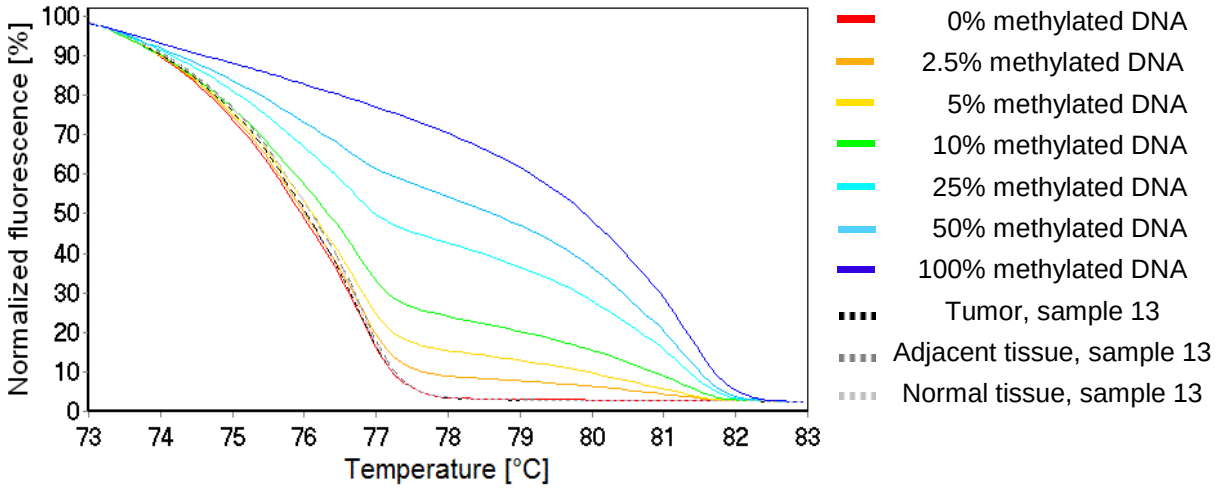

Figure 50: Normalized HRM curves of the PCR products for *GSTP1*; Replicate view (Human control standards and biopsy sample 13)

This method showed a low bias towards the methylated DNA. In *Figure 51* the calibration function obtained by fitting the data with a hyperbola function is shown.

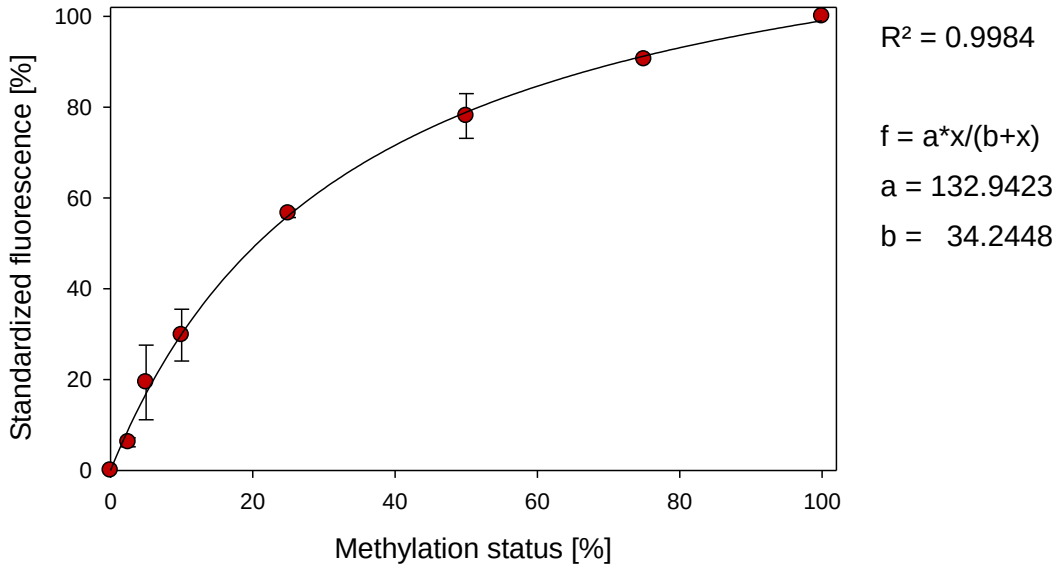

Figure 51: Calibration function for *GSTP1;* Mean and standard deviation of n = 6 measurements

In *Appendix B, Table B6,* the DNA methylation levels obtained in the individual measurements are listed. The results of the biopsy samples are summarized in *Figure 52*. By repeatedly analyzing the unmethylated standard a LOD of 1.3% and a LOQ of 3.5% were determined.

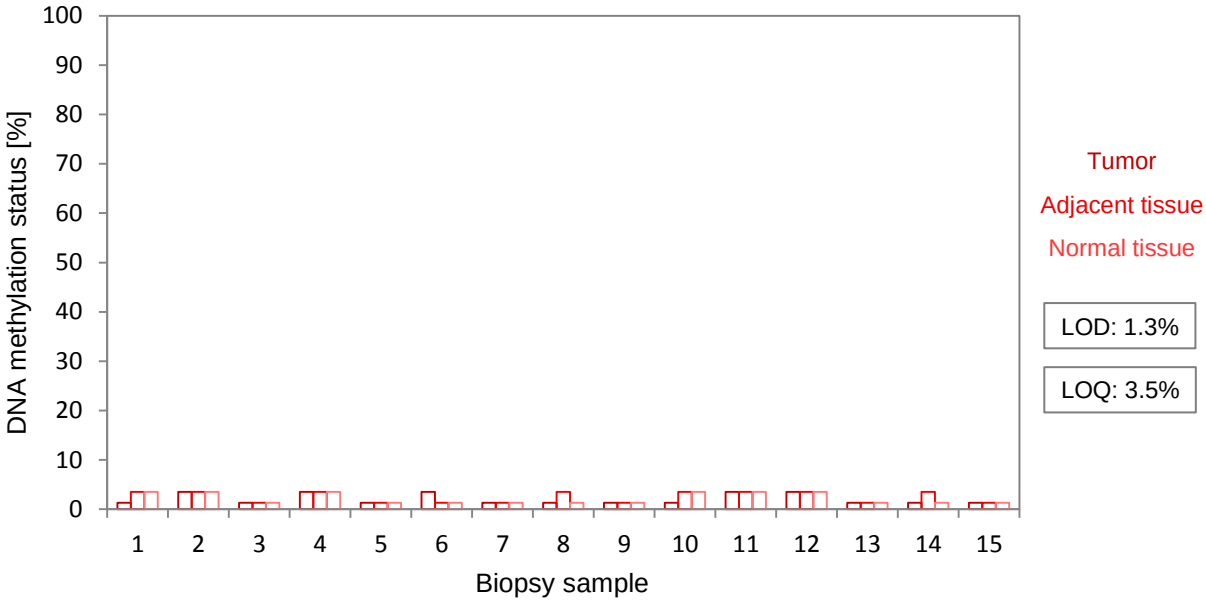

Figure 52: DNA methylation status [%] of *GSTP1* for biopsy samples; n = 4 measurements; Empty boxes denote a DNA methylation ≤ LOD or ≤ LOQ

Figure 52 indicates that none of the tissue samples (neither tumor, nor adjacent or normal tissue) from the 15 patients are methylated above the LOQ.

In a study by Tserga *et al*. [21], 17% (8 out of 48) of invasive breast tumors were found to be methylated. However, in that study it was only distinguished if the samples are methylated or not, but the methylation status was not quantified.

In the study of Shargh *et al.* [35], the methylation of *GSTP1* was determined by DNA sequencing after PCR. DNA methylation was detected in 41% (19 out of 46) of the breast tumor samples. However, 13% of the corresponding normal tissues (about 3 cm away from the tumor) were also found to be methylated. These results are different from the results obtained in the present master thesis.

4.3.8 Comparison of the Methylation Status of the Genes Investigated

The *Figure 53-55* show the methylation status in the promoter region of the different genes for each individual tissue type.

Figure 53 compares the DNA methylation status of the tumor tissues taken from the 15 breast cancer patients. It is obvious that there are big differences in the DNA methylation status in the tumor tissues between different patients in the same gene and between different genes in the respective tumor tissue. For example, the gene *APC* was more than 50% methylated in about half of the tumor tissues, whereas the other tumors were very low methylated or even unmethylated. *BRCA1* and *CDKN2A* showed a DNA methylation status of about 50% in the tumor samples from two patients, whereas the other tumor samples were methylated below the LOQ or even unmethylated. *RASSF1A* and *CCND2* had, if any, low DNA methylation in the promoter region. In none of the patients, the methylation status of the gene *GSTP1* was above the LOQ.

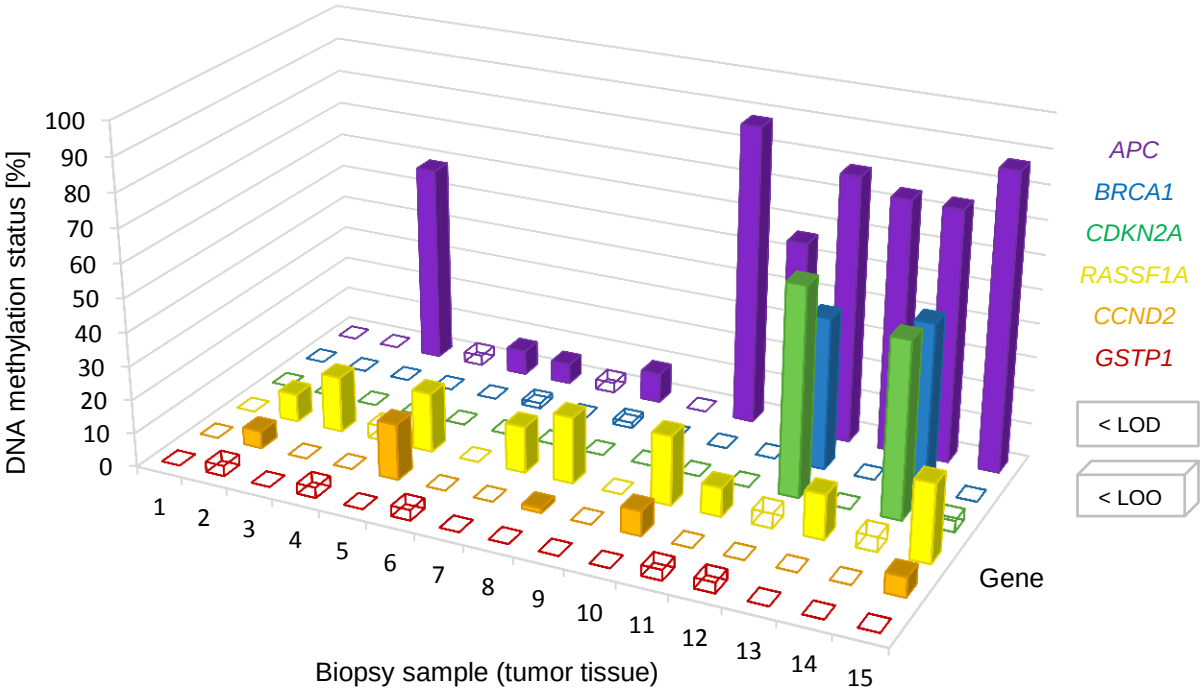

Figure 53: DNA methylation status [%] of the tumors in different tumor suppressor genes

Patients 12 and 14 showed very similar DNA methylation patterns in the different genes. In both patients *APC*, *BRCA1* and *CDKN2A* were very highly methylated, whereas in the other three genes no or no quantifiable DNA methylation was detected. From the clinicopathological data (see *Appendix A*, *Table A2*) it could be found out that patient 12 had a triple negative hormone receptor status and patient 14 was PR and HER2 negative and ER positive. All other patients were at least twofold positive. (For patient 3 no data on hormone receptor status were available.)

Similarities with respect to the methylation patterns were also found between patients 3, 11 and 13 and between patients 10 and 15. Patients 3, 11 and 13 showed high methylation of *APC* and low methylation of *RASSF1A* and patients 10 and 15 showed additionally low methylation of *CCND2*. In three patients (1, 4 and 9) none of the genes was found to be methylated above the LOQ. However, no correlation between these patients and their hormone receptor status could be found. In addition, no age dependent correlation was observed.

In *Figure 54*, the results for the adjacent tissue samples are shown. In general, the DNA methylation status is much lower than that in the tumor tissue. *APC* is more frequently and also higher methylated than the other genes. Furthermore, *BRCA1*, *CDKN2A* and *RASSF1A* are slightly methylated in some adjacent tissues. Neither *CCND2* nor *GSTP1* were methylated above the LOQ in any of the adjacent tissue samples.

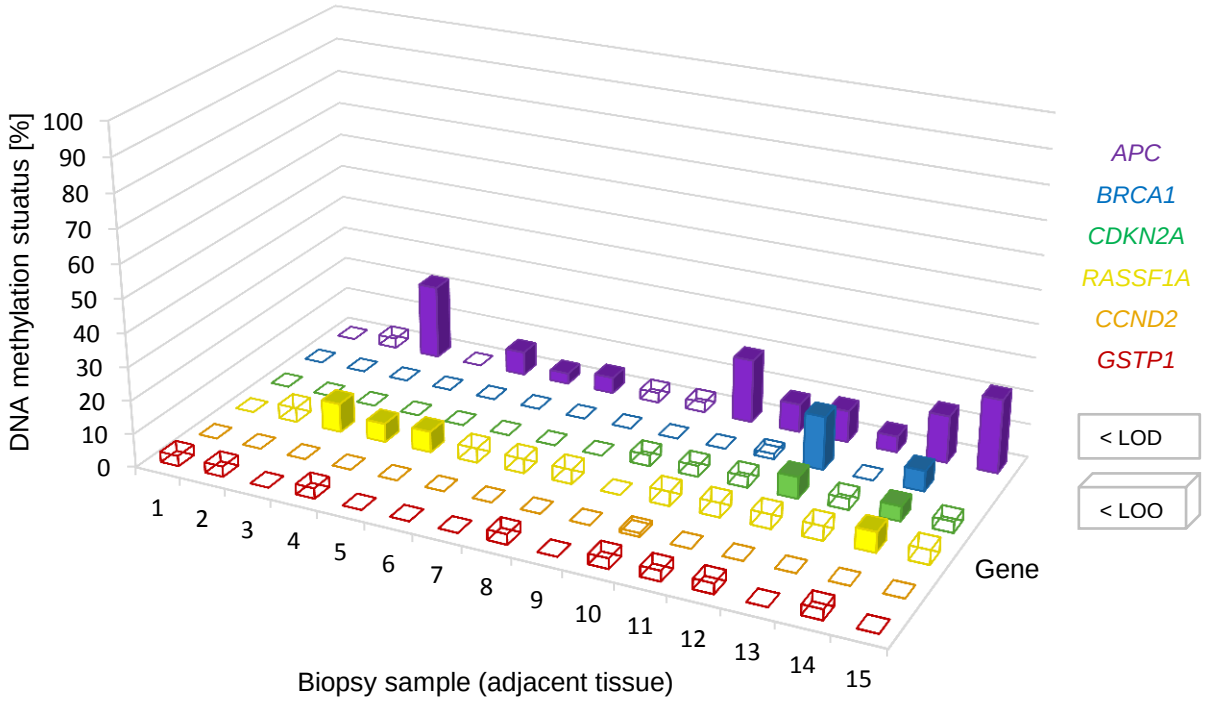

Figure 54: DNA methylation status [%] of the adjacent tissues in different tumor suppressor genes (DNA methylation status could not be determined for the adjacent tissue of patient 15)

Due to the generally low DNA methylation status, no clear correlations between the patients could be observed. However, a trend can be seen that those patients that have a highly methylated tumor tissue also have a somewhat higher DNA methylation in the adjacent tissue.

The normal tissues in *Figure 55* show a similar DNA methylation profile as the adjacent tissue samples, however, the DNA methylation of the normal tissues is somewhat lower.

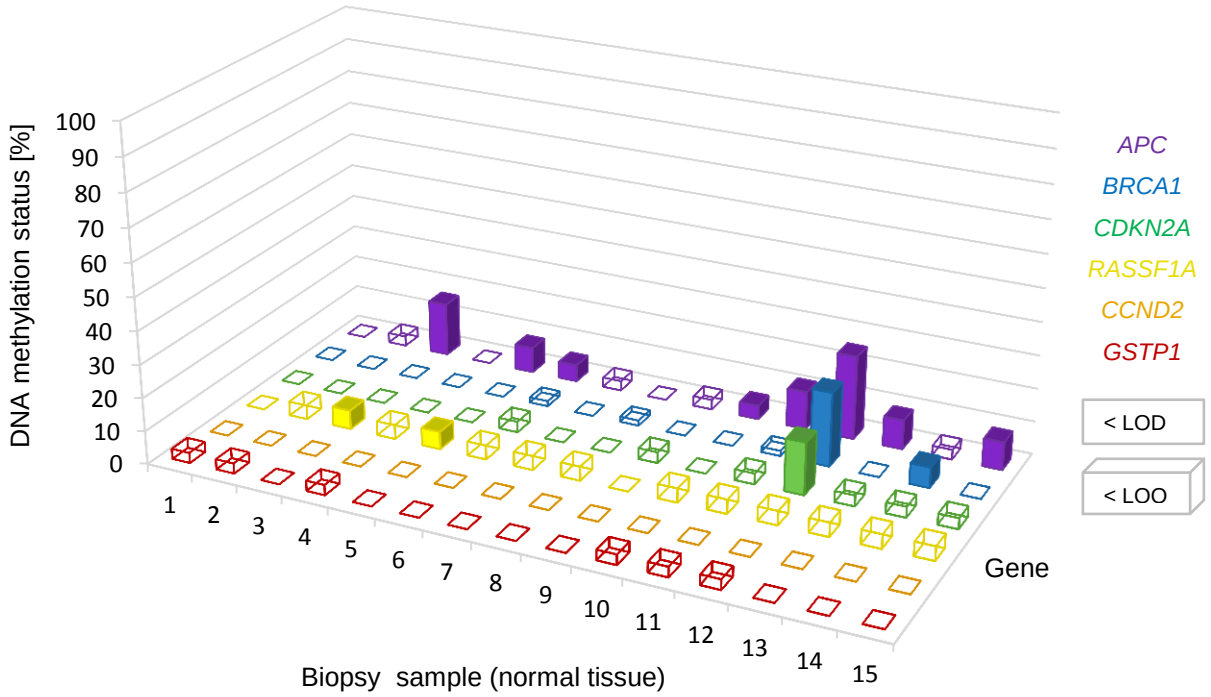

Figure 55: DNA methylation status [%] of the normal tissues in different tumor suppressor genes

Due to the small differences in the methylation status between the adjacent and normal tissues and the comparatively large differences between the tumor and adjacent tissues it can be concluded that the adjacent tissue samples do not have an abnormal DNA methylation status.

Table 4 gives an overview of the frequency of significant difference in the DNA methylation status between tumor & adjacent tissue and tumor & normal tissue.

Table 4: Frequency of significant difference in the DNA methylation status

	Tumor & adjacent tissue		**Tumor & normal tissue**	
RASSF1A	60%	(9/15)	60%	(9/15)
APC	60%	(9/15)	53%	(8/15)
CCND2	33%	(5/15)	33%	(5/15)
BRCA1	13%	(2/15)	13%	(2/15)
CDKN2A	13%	(2/15)	13%	(2/15)
GSTP1	0%	(0/15)	0%	(0/15)

4.4 Influence of Dietary Supplements on the DNA Methylation Status of Tumor Suppressor Genes in MCF-7 Cells

The aim was to determine if the DNA methylation status in tumor suppressor genes in MCF-7 breast cancer cells changes by incubating them with the dietary supplements propolis or tomato extract. In *Chapter 1.8* the two dietary supplements are described.

At the beginning, I incubated the MCF-7 breast cancer cells with different amounts of the dietary supplements to determine at which concentration the substances are toxic to the cells. Incubation experiments were performed as described in *Chapter 5.2.4*. In *Table 5* and *Table 6* details on the incubation experiments, e.g. final concentrations of the substances and incubation period, are given. The DNA methylation status in some tumor suppressor genes was determined. Due to time reasons only a few MS-HRM analysis were carried out.

4.4.1 Cytotoxicity Test of Dietary Supplements on MCF-7 Cells

The cytotoxicity of dietary supplements on MCF-7 cells was determined by the sulforhodamine B (SRB) assay. The protocol for carrying out the SRB assay is described in *Chapter 5.3*. Two dietary supplements, propolis and tomato extract, were tested.

Propolis

The propolis concentration ranged from 1-500 mg/L. In addition, a control sample with 1% DMSO was prepared. MCF-7 cells were incubated for either one, three or five days, changing the incubation solution every 24 hours. The samples were standardized with respect to the control sample. The results of the SRB assays are shown in *Figure 56*.

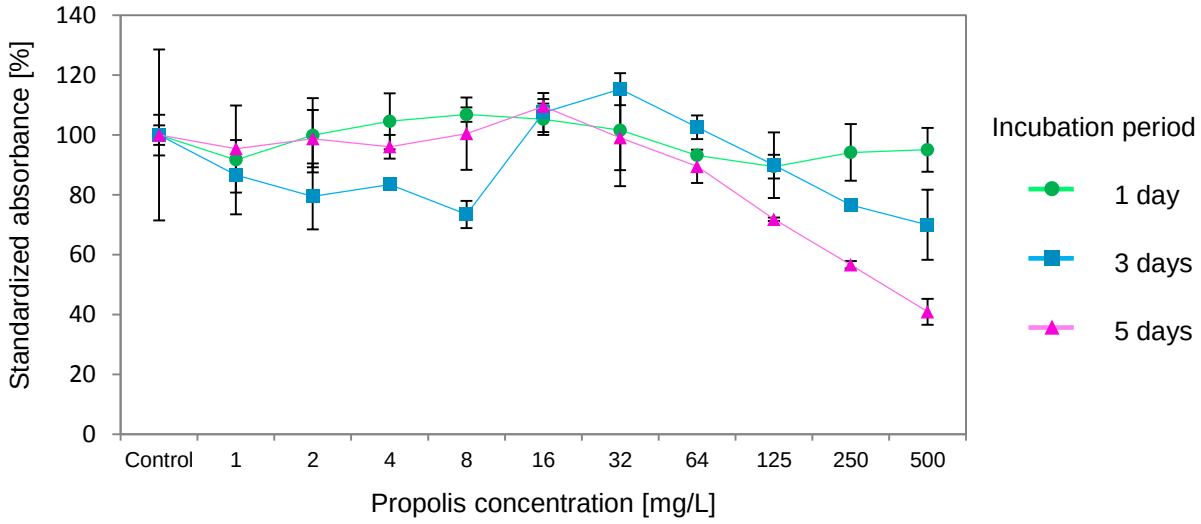

Figure 56: Result of the SRB assays for propolis; Mean and standard deviation of the standardized absorbance of n = 2 measurements

It can be seen that after one day of propolis incubation no drastic change in cell density was found compared to the control sample. Incubating the cells with propolis for three days led to rather strange results. Low propolis concentrations (1-8 mg/L) seem to reduce the cell density whereas higher concentrations (16-64 mg/L) seem to increase the cell growth. Above a propolis concentration of 125 mg/L the cell growth is decreased again. This experiment should be repeated to confirm the result. When the incubation experiment lasted five days, propolis concentrations of 64 mg/L and higher resulted in a decrease of the cell density. Based on these results, a propolis concentration of 20 mg/L was used for carrying out further incubation experiments to determine any influence of propolis on the DNA methylation status in MCF-7 cells.

Tomato Extract

The tomato extract concentration ranged from 0.16-80 mg/L. In the samples with higher tomato extract concentrations (20-80 mg/L) small red crystals were visible under the microscope. Maybe the concentration was too high and due to oversaturation of the medium some components of the tomato extract crystallized. In addition, a control sample with 1% DMSO was prepared. MCF-7 cells were incubated with tomato extracts for five days by adding new incubation solution every 24 hours. Cells were fixed 72 hours after the last incubation step. The result of the SRB assay is shown in *Figure 57*.

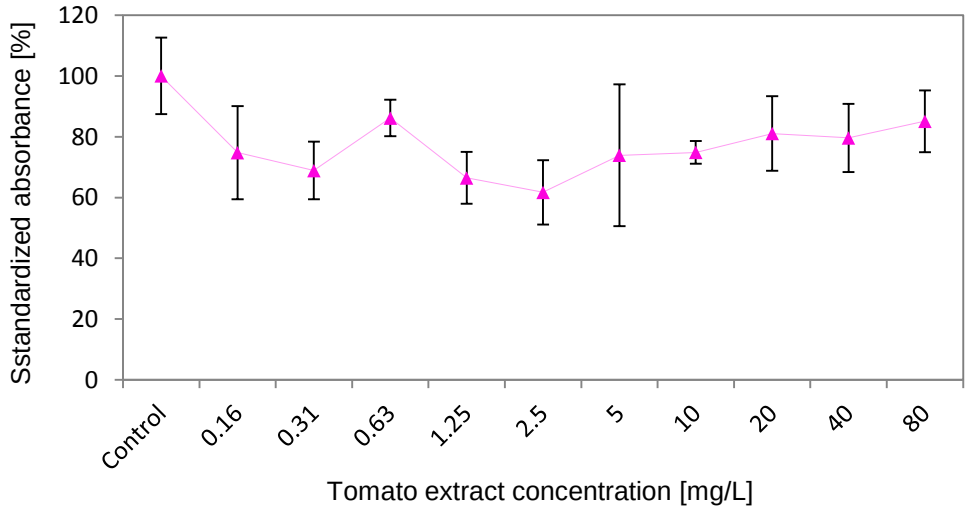

Figure 57: Result of the SRB assay for tomato extract; Incubation period of 5 days; Mean and standard deviation of the standardized absorbance of n = 4 measurements

It can be seen that the control sample showed the highest absorbance, indicating that the tomato extract resulted in a decrease of the cell number. However, the effect was rather independent of the concentration of the tomato extract. Since at higher concentrations (20-80 mg/L) a recrystallization of tomato extract components occurred, the following incubation experiments were carried out with concentrations lower than 10 mg/L.

4.4.2 *CDKN2A*_Exon3

The MS-HRM method had already been used to determine the DNA methylation status of the biopsy samples (see *Chapter 4.3.4*). Details on the method can be found in the *Appendix A, Table A1* and PCR and HRM conditions are described in *Chapter 5.8*.

In *Figure 58*, the melting profiles of PCR products of unmethylated and methylated human control DNA and MCF-7 cells after incubation with tomato extracts can be seen. The melting profile of the amplicons of the 100% methylated DNA shows a peak minimum at about 77°C and a peak maximum at 80°C with a shoulder of the peak at 81°C. The melting profiles of the amplicons of MCF-7 DNA showed a different shape than that of the 100% methylated DNA standard. These melting profiles have a broad single peak with a maximum at 80°C. MS-HRM analysis of DNA isolated from MCF-7 cells after incubation with propolis also resulted in atypical melting curves. The reason for this different melting behavior could not be found within the course of this work. Because of the different melting behavior of the amplicons from MCF-7 cells it was not possible to calculate the absolute DNA methylation status of the MCF-7 cells. Nevertheless, the DNA methylation status of incubated MCF-7 cells could be compared with that of untreated MCF-7 cells.

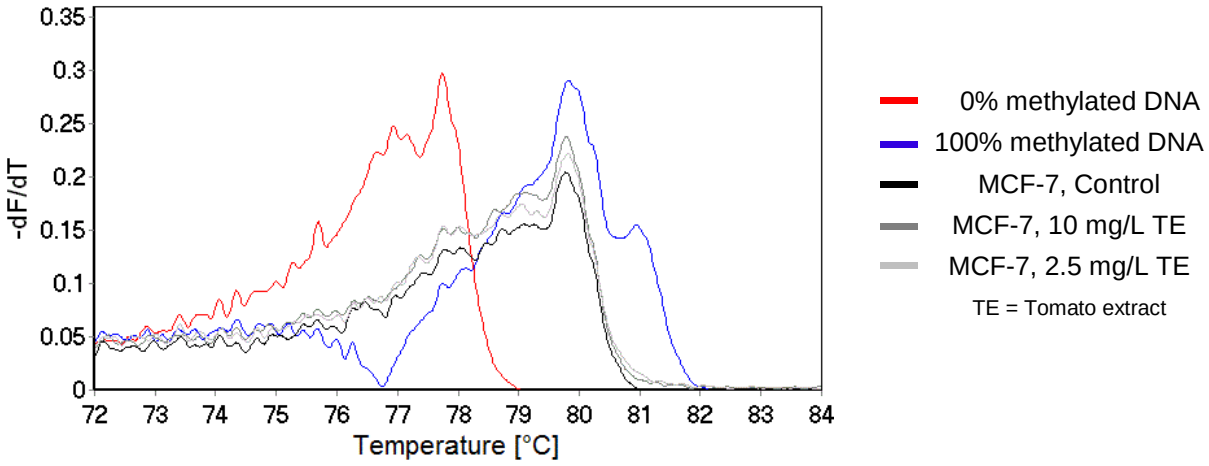

Figure 58: Melting profile of PCR products of *CDKN2A*_Exon 3; Replicate view (Human control DNA standards and MCF-7 DNA)

For the calculation of the relative DNA methylation status the calibration function of *Chapter 4.3.4*, *Figure 41* was used. The relative DNA methylation status of propolis incubated MCF-7 cells was determined with respect to the control sample. The DNA methylation status was calculated as described in *Chapter 5.9*. *Figure 59* summarizes the results of the incubation experiment P1 (first incubation experiment with propolis). The relative DNA methylation levels obtained in the individual measurements are listed in *Appendix C, Table C3*. Details on the incubation experiment P1 can be found in *Chapter 5.2.4*. The MCF-7 cells of incubation experiment P1 were incubated twice with a

fresh prepared mixture of culture medium and propolis (dissolved in DMSO) every 48 hours. The control group was incubated with culture medium and DMSO. The propolis concentration range was from 15-150 mg/L (150 mg/L was above the critical cytotoxic concentration observed in the SRB assay experiments). *Figure 59* indicates that the incubation with propolis resulted in an increase of the DNA methylation.

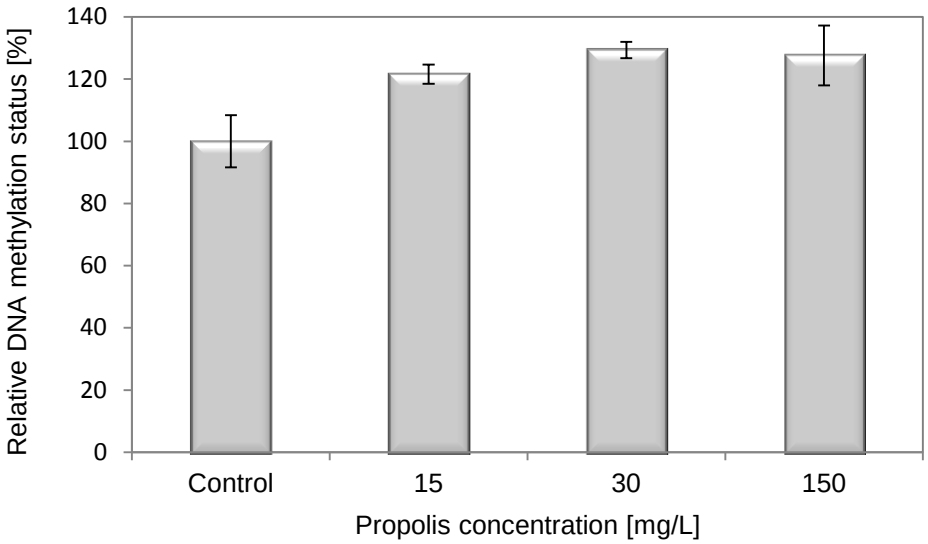

Figure 59: Relative DNA methylation status [%] in exon 3 of *CDKN2A* in MCF-7 cells incubated with propolis*;* Incubation experiment P1; Mean and standard deviation of n = 2 measurements

MCF-7 cells were also treated with the tomato extract. The relative DNA methylation status in exon 3 of *CDKN2A* was determined in the MCF-7 cells of incubation experiment TE1 (first incubation experiment with tomato extract). The MCF-7 cells were incubated five times with fresh culture medium and tomato extract (dissolved in DMSO) every 24 hours. The tomato extract concentration range was from 2.5-10 mg/L. The relative DNA methylation levels obtained in the individual measurements are listed in *Appendix C, Table C3*.

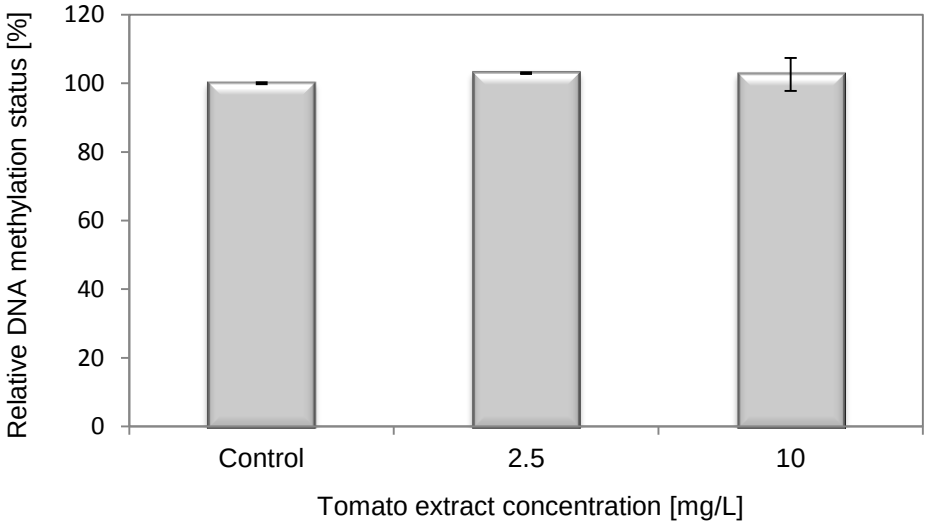

Figure 60: Relative DNA methylation status [%] in exon 3 of *CDKN2A* in MCF-7 cells incubated with tomato extract*;* Incubation experiment TE1; Mean and standard deviation of n = 2 measurements

Figure 60 summarizes the results of incubation experiment TE1. It can be seen that the tomato extract did not change the DNA methylation status of MCF-7 cells in exon 3 of *CDKN2A*.

4.4.3 *CCND2*

The MS-HRM method had already been used to determine the DNA methylation status of the biopsy samples (see *Chapter 4.3.6*). Details on the method can be found in the *Appendix A, Table A1*. PCR and HRM conditions are described in *Chapter 5.8*.

The DNA methylation status of the MCF-7 cells of incubation experiment P1 was determined. In *Appendix C, Table C4,* the DNA methylation levels obtained in the individual measurements are listed. *Figure 61* summarizes the results of the incubation experiment P1. No drastic change in the DNA methylation of the *CCND2* promoter could be observed.

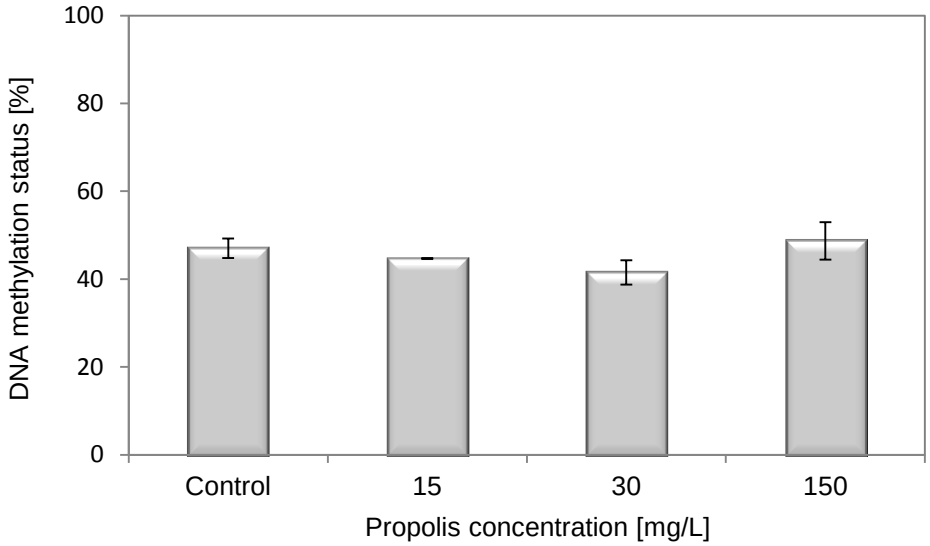

Figure 61: DNA methylation status [%] of *CCND2* in MCF-7 cells incubated with propolis*;* Incubation experiment P1; Mean and standard deviation of n = 2 measurements

4.4.4 *RASSF1A, APC* and *BRCA1*

The MS-HRM methods had already been used to determine the DNA methylation status of the biopsy samples (see *Chapters 4.3.5, 4.3.1 and 4.3.2*). Details on the methods can be found in *Appendix A, Table A1*. PCR and HRM conditions are described in *Chapter 5.8*.

The DNA methylation status of untreated MCF-7 cells was determined to be:

- *RASSF1A* 81 ± 3%
- *APC* 51 ± 3%
- *BRCA1* below LOQ

In *Appendix C, Table C5,* the DNA methylation levels in the individual measurements are listed. Further investigations on incubated MCF-7 cells should be done for *RASSF1A* and *APC* since the DNA methylation status of MCF-7 cells is quite high in the promoter region of these genes. Untreated MCF-7 cells show no DNA methylation in the *BRCA1* promoter, however, incubated MCF-7 cells could be investigated to determine possible methylating effects of propolis or tomato extract.

4.4.5 *GSTP1* and *MGMT*

The MS-HRM method for *GSTP1* had already been used to determine the DNA methylation status of the biopsy samples (see *Chapter 4.3.7*). Details on the methods can be found in *Appendix A, Table A1*. PCR and HRM conditions are described in *Chapter 5.8*.

The amplicons of MCF-7 DNA show different melting behavior compared to the human control standards in the genes *GSTP1* and *MGMT*. According to the melting profiles shown in *Figure 62*, MCF-7 cells seem to be partially methylated in the *GSTP1* promoter. In my opinion determination of the DNA methylation status in the *GSTP1* promoter in MCF-7 cells would be possible, however, care must be taken to avoid wrong conclusions. It must be monitored if alleles with different methylation patterns occur and thereof heterogeneous dsDNA is formed.

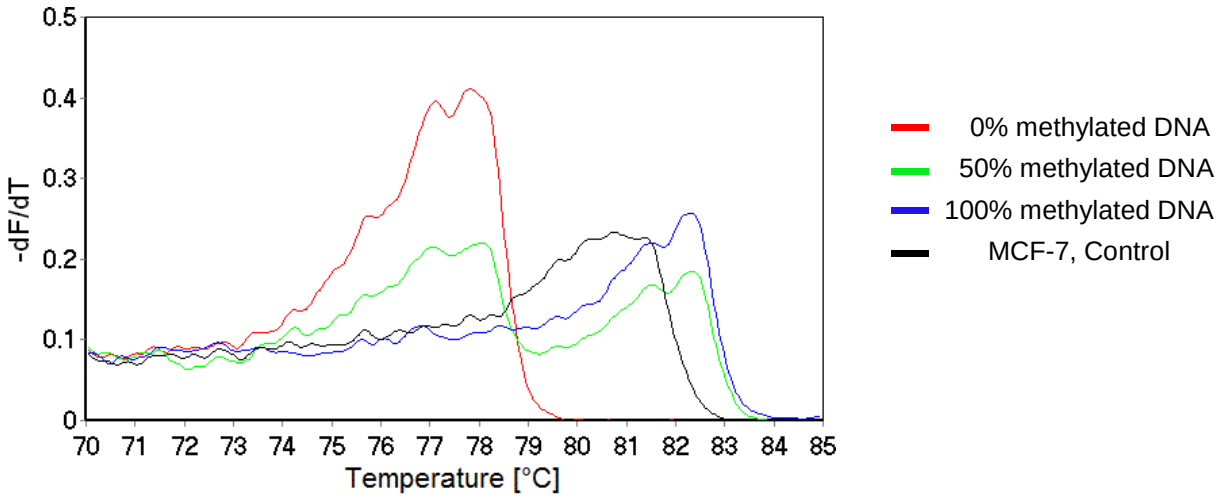

Figure 62: Melting profiles of the amplicons *for GSTP1*; Replicate view
(Human control DNA standards and MCF-7 DNA)

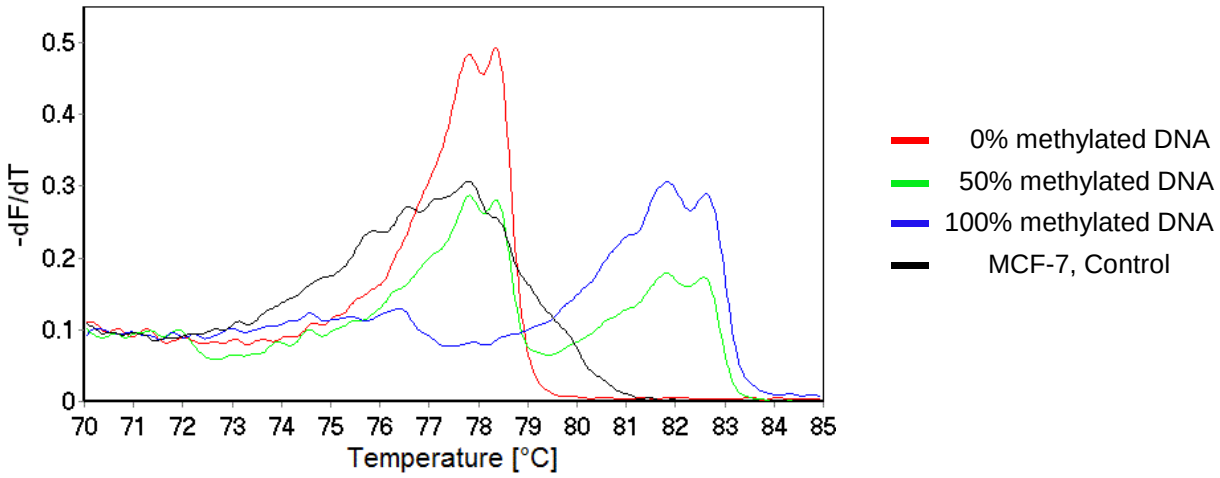

Figure 63: Melting profiles of the amplicons *for MGMT*; Replicate view
(Human control DNA standards and MCF-7 DNA)

Figure 63 shows the melting profile of the amplicons for *MGMT* of human control DNA standards and MCF-7 DNA. The melting profile of the amplicons of MCF-7 DNA indicates heterogeneous methylation. It may be tried to add a hybridization step with slow temperature decrease to reduce the formation of heterogeneous dsDNA before HRM analysis is performed (see *Chapter 4.2*).

5 Experimental Part

5.1 Sample Preparation for Incubation Experiments

5.1.1 Propolis

The raw propolis was received from the apiculture Josef Holzweber, Zwettl, Austria. The raw substance was powdered and dissolved in DMSO so that a solution with a propolis concentration of 100 mg/mL was obtained. In a preliminary test it was noted that by mixing the propolis solution and culture medium a yellow precipitate was formed, which most probably was beeswax. Therefore, the propolis solution was mixed with water 1:3 and the precipitate was removed. A stock solution with 25 mg/mL propolis in DMSO/water (1:3) was obtained. The stock solution was stored in the refrigerator.

Figure 64: Raw propolis

Since the exact composition of the utilized propolis sample was not known it could not be excluded that superoxide radicals ($\bullet O_2^-$) would be formed during the incubation experiment. The radicals can cause a chain reaction of free radical formation and cancer cells would be exposed to oxidative stress. Addition of the enzyme superoxide dismutase (SOD) enables the conversion of $\bullet O_2^-$ to hydrogen peroxides (H_2O_2) and thus inhibits the progression of a chain reaction. H_2O_2 is cytotoxic and responsible for the induction of apoptosis. By addition of the enzyme catalase H_2O_2 is reacted to water and oxygen. [78]

5.1.2 Tomato Extract

For MCF-7 incubation experiments a tomato extract containing about 5% lycopene was used. *Lycopin Kapseln 20 mg* were produced by ZeinPharma and purchased from Vitalabo, Feldbach, Austria. The tomato powder was dissolved in DMSO so that a stock solution of 8.6 mg/mL was obtained. The stock solution was stored in the refrigerator.

Figure 65: Tomato extract (*Lycopin Kapseln 20 mg*)

5.2 Cultivation and Incubation of MCF-7 Cells

The human cancer cell line MCF-7 (Michigan Cancer Foundation-7) was established by Soule and co-workers in 1973 and is today one of the most widely used breast cancer cell lines. The MCF-7 cells were cultivated from an amputated breast tissue of a 69-year old white woman. [79, 80]

Cultivation of MCF-7 cells was carried out in collaboration with the Institute of Food Chemistry and Toxicology, University of Vienna, Austria. The required facilities such as incubators and laminar flow were provided by Univ. Prof. Dr. Doris Marko.

Cell culturing requires a sterile environment and a sterile way of working. Therefore, the MCF-7 cells were cultivated exclusively in a suitable cell culturing space and the work on the cell cultures was performed within the laminar flow. In addition, before starting any work all materials and utensils were sterilized with 70% ethanol. While working with cell culture, a clean lab coat and latex gloves were worn.

5.2.1 Working within the Laminar Flow Cabinet

To ensure a germ-free laminar flow cabinet, it had to be cleaned regularly. First, all parts were cleaned with water and detergent and disinfected with ethanol. The filter was purified or replaced and after the laminar flow was reassembled, it was again sprayed with 70% ethanol and then sterilized by using a UV lamp.

First of all the instrument was switched on. After reaching a constant airflow, the surface of the laminar flow was sprayed with 70% ethanol to kill any germs by dehydration. Disinfection with ethanol (absolute) does not act, as bacterial spores are conserved. All utensils that were placed in the laminar flow were previously disinfected with 70% ethanol. All consumables were autoclaved. Before opening chemicals and diverse other containers, they were flamed

with a Bunsen burner. In addition, glass pipettes were flamed for sterilizing before being used.

Contamination by cancer cells had to be avoided too. Therefore, all contaminated consumables were collected separately and then autoclaved. All fluids, such as culture medium or buffer were aspirated with a vacuum pump and collected in a separate container. This had to be sterilized in an autoclave too before proper disposal. Bottle necks should not have been wetted with liquid, especially not with culture medium, since they would be a preferred habitat for microorganisms. Generally, it had to be ensured that no liquid has been spilled. In such a case, the liquid had to be wiped off immediately and the work area had to be disinfected. After work, the laminar flow was cleaned again, closed and turned off.

5.2.2 Cell Cultivation and Splitting

MCF-7 cells were cultivated in 75 cm^2 cell culture flasks with a contamination-proof ventilation cap. *Roswell Park Memorial Institute (RPMI) 1640* medium was used as culture medium. The cells were incubated at 37°C and 5% CO_2 in an incubator. To the medium 10% fetal calf serum (FCS) and 1% penicillin/streptomycin (P/S) were added before using. FCS is necessary for the cell growth and P/S is an antibiotic to protect the cells against contamination by foreign cultures. In addition, the medium contains the dye phenol red. The production of metabolites and the loss of nutrients lead to a decrease in the pH value, which is indicated by a color change from red to orange-yellow. In this case the cell medium had to be changed.

The cell culture was assessed microscopically with respect to the cell number and the morphology. MCF-7 cells need about 50 hours to double themselves, so they need to be split about every fourth day to avoid too high confluence. The term splitting means the separation and implementing of the cells. To perform this process, the following solutions are required:

- *RPMI 1640* medium
- Phosphate buffered saline (PBS)
- Trypsin solution (500 mg/L trypsin and 250 mg/L EDTA)

The solutions were stored in the refrigerator and heated to 37°C in a water bath before using. First, the culture medium was aspirated with a pipette. Afterwards the cells were washed with 5 mL PBS to remove medium residues. To replace the adherent cells from the flask bottom the cells were overlaid with 1 mL trypsin solution and after a short incubation phase (about 2 min) the cell layer was completely removed from the flask bottom by gently tapping. The enzyme was inactivated by addition of 5 mL fresh culture medium. Depending on the desired cell number approximately 1 mL of cell suspension was left in the culture flask and the rest

was aspirated. After adding 20 mL of culture medium, the cell culture was replaced into the incubator. After three splitting processes a new culture flask was used.

5.2.3 Vitality Test and Cell Quantification

In order to obtain reproducible results the same number of cells should be spread out for all incubation experiments. Therefore, the cell number was determined using a hemocytometer. The hemocytometer consists of a thick glass microscope slide with a laser-etched grid and a thin cover glass. The two glass plates were cleaned with 70% ethanol. For assembling, the cover glass was damped, placed on the microscope slide and moved slightly until the Newton's rings were visible. Newton's rings indicate that the counting chamber has reached the specified volume. [81]

The cells were detached by trypsinization and disconnected. 20 µL of cell suspension were mixed with 180 µL of trypan blue solution. Approximately 10 µL of the suspension were pipetted into the counting chamber. In this work, a Neubauer counting chamber was used. Thereafter, the hemocytometer was regarded under the microscope. As shown in *Figure 66,* there are four squares in the corners with 4 x 4 subunits.

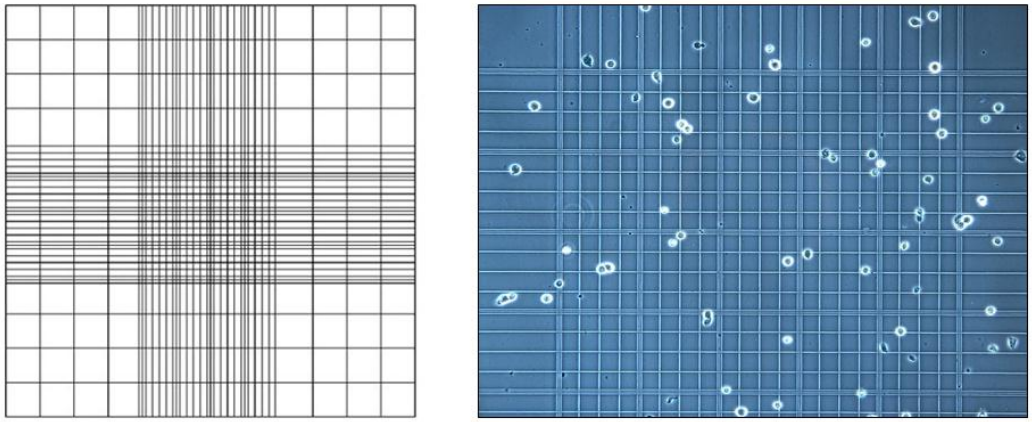

Figure 66: Schematic view of a Neubauer counting chamber; from [82] (left) and cells colored with trypan blue; from [83] (right)

Each square has a volume of 0.1 µL. Viable cells (seen as white spots) and dead cells (seen as blue spots) were counted in all four squares and the mean was calculated. The total number of cells in 1 mL of cell suspension was calculated as follows [81]:

$$n = x_m * f_1 * f_2$$ *Equation 1:* Calculation of the cell number per mL suspension

n Number of cells per mL
x_m Mean number of viable cells
f_1 Conversion factor of 0.1 µL to 1 mL (f_1 = 10 000)
f_2 Dilution factor (f_2 = 10)

5.2.4 Incubation Experiments

After the cell number was determined, 50 000 cells were suspended in 5 mL culture medium and pipetted into a Petri dish with a diameter of 6 cm. The Petri dish was gently swirled for uniform distribution of the cells and the cells were left in an incubator to grow for 72 hours.

For the propolis incubation experiments, the propolis stock solution (25 mg/mL) (see *Chapter 5.1.1*) was diluted with DMSO/water (1:3) to obtain working solutions with concentrations between 0.375 mg/mL and 3.75 mg/mL. Incubation experiments were carried out by adding the working solution (see *Table 5*) to 5 mL of culture medium to obtain a final DMSO amount of 1%. In addition, catalase (1500 units/mL) and SOD (4500 units/mL) were added to avoid effects caused by reactive metabolites. In *Table 5* the propolis incubation experiments are listed including substances, propolis concentration and incubation period.

Table 5: Incubation experiments with propolis (P1 and P2)

Experiment	Propolis [mg/L]	Substances
P1	--	50 µL of DMSO, 100 µL of catalase, 5.5 µL of SOD
	150	200 µL of 3.75 mg/mL propolis in DMSO/water (1:3), 100 µL of catalase, 5.5 µL of SOD
	30	200 µL of 0.75 mg/mL propolis in DMSO/water (1:3), 100 µL of catalase, 5.5 µL of SOD
	15	200 µL of 0.375 mg/mL propolis in DMSO/water (1:3), 100 µL of catalase, 5.5 µL SOD
Incubation period: 2 days, changing the incubation solution every 48 hours		
P2	--	50 µL of DMSO, 100 µL of catalase
	20	200 µL of 0.5 mg/mL propolis in DMSO/water (1:3), 100 µL of catalase
	--	50 µL of DMSO, 100 µL of catalase, 5.5 µL of SOD
	20	200 µL of 0.5 mg/ml propolis in DMSO/water (1:3), 100 µL of catalase, 5.5 µL of SOD
Incubation period: 5 days, changing the incubation solution every 24 hours		

For the tomato extract incubation experiments the stock solution (8.6 mg/mL) (see *Chapter 5.1.2*) was diluted with DMSO to obtain working solutions with concentrations between 0.01 mg/mL and 1 mg/mL. The working solution (see *Table 6*) was added to 5 mL culture medium.

Table 6: Incubation experiments with tomato extract (TE1 andTE2)

Experiment	Tomato extract [mg/L]	Substances
TE1	--	50 µL of DMSO
	10	50 µL of 1 mg/mL tomato extract in DMSO
	2.5	50 µL of 0.25 mg/mL tomato extract in DMSO
Incubation period: 5 days, changing the incubation solution every 24 hours		
TE2	--	50 µL of DMSO
	10	50 µL of 1 mg/mL tomato extract in DMSO
	2.5	50 µL of 0.25 mg/mL tomato extract in DMSO
	0.1	50 µL of 0.01 mg/mL tomato extract in DMSO
Incubation period: 5 days, changing the incubation solution every 24 hours		

The components were mixed before adding them to the cells to avoid local overconcentration and thus damaging of the cells. The incubation solution was replaced regularly (every 24 or 48 hours) by carefully aspiring the old incubation solution and adding fresh solution. Afterward the Petri dish was gently swirled and replaced in the incubator. After the incubation period, the cells were harvested. The culture medium was aspired, the cells were washed with 2 mL PBS and detached by trypsinization (first 0.5 mL of trypsin solution are added and after 2 min 2 mL of culture medium are added). The cell suspension was completely transferred into a 15 mL centrifuge tube and the DNA was isolated as described in *Chapter 5.4*.

5.3 Sulforhodamine B (SRB) Assay

The SRB assay is used for cytotoxicity screening in incubation experiments by cell density determination. SRB is a red dye that binds to basic amino acid residues of protein components of cells under mild acidic conditions and dissociates under alkaline conditions. [84]

5.3.1 Experimental Procedure of the SRB Assay

First incubation experiments were carried out in a small batch using a 24 well plate. 8 400 cells in 1 mL of culture medium were spread per well. After 24 hours the incubation experiments were started with propolis or tomato extract using different concentrations.

For the propolis SRB assays, the propolis stock solution (25 mg/mL) (see *Chapter 5.1.1*) was diluted with DMSO/water (1:3) to obtain working solutions with propolis concentrations in the

range from 0.025-12.5 mg/mL. 40 µL of working solution were mixed with 1 mL culture medium to a final DMSO amount of 1%. Furthermore, 20 µL of catalase (1500 units/mL) and 1.1 µL of SOD (4500 units/mL) were added. Information on why SOD and catalase were added can be found in *Chapter 5.1.11.8.1*. The final propolis concentration ranged from 1-500 mg/L. In addition, a control sample with 1 mL of culture medium, 10 µL of DMSO, 20 µL of catalase (1500 units/mL) and 1.1 µL of SOD (4500 units/mL) was prepared. MCF-7 cells were incubated for either one, three or five days changing the incubation solution every 24 hours. Incubation experiments are described in detail in *Chapter 5.2.4*.

For the tomato extract SRB assay, the tomato extract stock solution (8.6 mg/mL) (see *Chapter 5.1.2*) was diluted with DMSO to obtain working solutions with tomato extract concentrations in the range from 0.016-8 mg/mL. 10 µL of working solution were mixed with 1 mL of culture medium to a final DMSO amount of 1%. The final tomato extract concentration ranged from 0.16-80 mg/L. In addition, a control sample with 1% DMSO was prepared. MCF-7 cells were incubated for five days changing the incubation solution every 24 hours. Incubation experiments are described in detail in *Chapter 5.2.4*.

Then, the old medium was removed. 200 µL of medium and 40 µL of 30% trichloroacetic acid (TCA) were added to fix the cells. The mixture was allowed to stand for one hour at 4°C and afterwards it was washed three times with distilled water. The well plate was dried overnight. 200 µL of 0.057 (w/v) SRB in 1% (v/v) acetic acid were added to each well and was allowed to stand at room temperature for one hour in the dark. Thereafter the plates were washed three times with 1% TCA solution and dried overnight. [84]

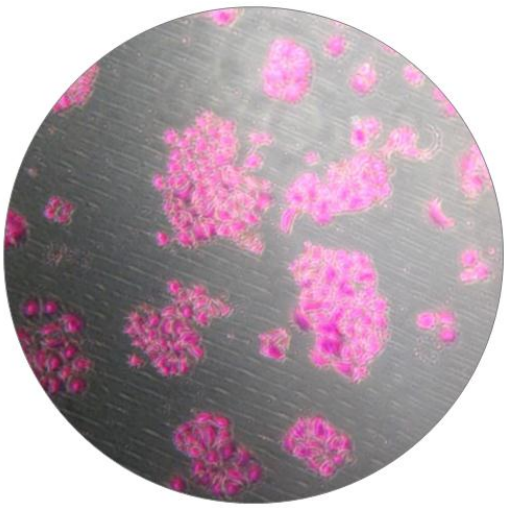

Figure 67: MCF-7 cells stained with SRB reagent

5.3.2 Measurement and Evaluation

The SRB dye was dissolved in 500 µL of 10 mM Tris/HCl (pH 10). The absorbance was measured at 570 nm using the multilabel counter *Victor3 V 1420* and the software *Wallac 1420 Manager*. The absorbance signal was standardized with respect to the control sample without incubation substance. [84]

5.4 DNA Extraction and Purification

For both DNA extraction from MCF-7 cells and tissue samples the *QIAamp DNA Mini Kit* (Qiagen) was used. The working steps were performed following the manufacturer's directions. [85]

5.4.1 DNA Isolation from MCF-7 Cells

The harvested cells were centrifuged for 5 min at 300 x g using the *Centrifuge 4K10* (Sigma). The culture medium was removed and the pellet resuspended in 2 mL of PBS. Next, the suspension was centrifuged again for 5 min at 300 x g. The liquid was discarded and the pellet resuspended in 200 µL of PBS and then transferred into a 1.5 mL Eppendorf tube. 20 µL of *Proteinase K solution* and 200 µL of lysis buffer (*Buffer AL)* were added, mixed for 15 sec and incubated at 56°C for 10 min. After the incubation step 200 µL of ethanol (absolute) were added and mixed by vortexing for 15 sec. Then the solution was briefly centrifuged with the *Centrifuge 5424* (Eppendorf) to remove any drops from the inside of the lid. Afterwards the solution was carefully transferred to the *QIAamp Mini spin column* (equipped with a 2 mL collection tube) and centrifuged at 8 000 rpm for 1 min. The spin column was placed in a new 2 mL collection tube and the filtrate was discarded. 500 µl of wash buffer (*Buffer AW1*) were added and the mixture centrifuged at 8 000 rpm for 1 min. The spin column was again placed in a new collection tube and 500 µl of wash buffer (*Buffer AW2*) were added and the mixture centrifuged for 3 min at 14 000 rpm. After discarding the filtrate the spin column was placed into a new 1.5 mL Eppendorf tube and centrifuged for 1 min at 14 000 rpm to remove any buffer residues. Thereafter, the spin column was placed in a new 1.5 mL Eppendorf tube, 200 µl of elution buffer (*Buffer AE*) were added and incubated for 5 min at room temperature. The DNA was eluted by centrifugation for 1 min at 8 000 rpm. In order to increase the yield this step was repeated with a further aliquot (200 µL) of *Buffer AE* and a new 1.5 mL Eppendorf tube. DNA extracts were stored at -80°C.

5.4.2 DNA Isolation from Biopsy Samples

Biopsy samples were taken from breast cancer patients by Ass. Prof. Dr. Georg Pfeiler, Department of Obstetrics and Gynecology, Medical University of Vienna, Vienna. From each patient three different tissue samples (tumor, adjacent and surrounding normal tissue) were taken. The tumor tissue was biopsied directly from the carcinoma. The adjacent tissue was taken in a 1 cm distance from the tumor margin. The normal tissue was located at least 3 cm away from the tumor margin. Both diagnosis of the tumors and determination of the hormone receptor status were carried out at the Medical University of Vienna. This information can be found in *Appendix A, Table A2*. The tissue samples were stored in PBS at -20°C until sample preparation.

Figure 68: Biopsy samples from patient 14
(T = tumor, A = adjacent tissue, N = normal tissue)

For DNA extraction not more than 25 mg of tissue could be used. Hence, the samples were weighed in using a microbalance. The tissue was placed in a 1.5 mL Eppendorf tube. Next, 180 µL of tissue lysis buffer (*Buffer ATL*) and 20 µL of *Proteinase K solution* were added and incubated at 56°C in the incubator until the tissue was totally lysed. That took about 2 hours and in between the mixture was vortexed frequently. The solution was briefly centrifuged to remove any drops from the lid. Thereafter, 14 µL of Ribonuclease A (RNase A) solution (30 mg/mL) were added and the solution was vortexed and incubated for 2 min at room temperature. Next, the solution was mixed with 200 µL of lysis buffer (*Buffer AL*) and incubated at 70°C for 10 min. The solution was briefly centrifuged, 200 µL of ethanol (absolute) were added and the solution was vortexed for 15 sec. After short centrifugation the mixture was transferred to the *QIAamp Mini spin column.* Further steps were performed equally to DNA isolation from MCF-7 cells as described in *Chapter 5.4.1*. DNA extracts were stored at -80°C.

5.5 Determination of DNA Concentration and Purity

To determine the yield after DNA extraction *NanoDrop 2000c Spectrophotometer* and *NanoDrop 2000/2000c Software* were used. Working steps were performed according to the manufacturer's protocol [86]. Before starting, a zero adjustment was performed with the elution solution (*Buffer AE*) of the samples. For the measurement 1.5 µL of the DNA sample were pipetted onto the pedestal. A spectrum was taken in the range from 220-350 nm. The program calculated the DNA concentration via Lambert-Beer law considering the absorbance at 260 nm. Furthermore the purity of the sample was determined. The ratio of A_{260}/A_{280} indicated contamination with proteins. A value between 1.7 and 1.9 indicates high purity. [85]

5.6 Bisulfite Conversion of DNA

Bisulfite treatment was carried out with the *EpiTect Fast DNA Bisulfite Kit* (Qiagen). The working steps were performed according to the manufacturer's protocol [87]. Both human control DNA and sample DNA were bisulfite treated before PCR.

5.6.1 Procedure of Bisulfite Conversion

Before starting, the samples were prepared as described in the protocol. The bisulfite reaction components were pipetted into a 200 µL PCR reaction tube according to *Table 7*. For samples with high DNA concentration reaction batch 1 was prepared and for samples with low DNA concentration reaction batch 2 was used.

Table 7: Pipetting scheme for the two bisulfite reaction batches [87]

	Reaction batch 1 (1 ng – 2 µg DNA)	**Reaction batch 2** (1 – 500 ng DNA)
Component	**Volume [µL]**	**Volume [µL]**
DNA	Variable x (0 – 20)	Variable x (0 – 40)
RNase-free water	Variable (20 minus x)	Variable (40 minus x)
Bisulfite Solution	85	85
DNA Protect Buffer	35	15
Total volume	140	140

The reaction mixtures were vortexed and placed in the thermal cycler *Rotor-Gene® Q* (Qiagen). The thermal cycler conditions for bisulfite conversion are listed in *Table 8*.

Table 8: Thermal cycler conditions for bisulfite conversion

Step	Time [min]	Temperature [°C]
Denaturation	5	95
Incubation	10	60
Denaturation	5	95
Incubation	10	60
Hold	1	25

5.6.2 Cleanup of Converted DNA

The reaction mixtures were transferred into 1.5 mL Eppendorf tubes, mixed with 310 µL of loading buffer (*Buffer BL*) and centrifuged briefly. In some reaction batches the DNA content was very low (about 100 ng) so that 3.1 µL of carrier RNA solution (1 µg/µL) were added to *Buffer BL*. After the addition of 250 µL of ethanol (absolute) the solutions were mixed for 15 sec by pulse vortexing and briefly centrifuged afterwards to remove any drops from the lid.

The entire content of each tube was transferred to a *MinElute DNA spin column* equipped with 2 mL collection tube and centrifuged at 12 000 rpm for 1 min with the *Centrifuge 5424* (Eppendorf). The filtrates were discarded and 500 µL of wash buffer (*Buffer BW*) were added. The spin columns were centrifuged at 14 000 rpm for 1 min. After discarding the filtrate 500 µL of desulfonation buffer (*Buffer BD*) were pipetted onto the spin columns and incubated for 15 min at room temperature. The columns were centrifuged at 14 000 rpm again and the filtrates were discarded. Next two washing steps with 500 µL of *Buffer BW* were carried out including centrifugation at 14 000 rpm for 1 min. Afterward 250 µL of ethanol (absolute) were added and the spin columns were centrifuged at 14 000 rpm for 1 min. Then the spin columns were placed into a new 2 mL collection tube and centrifuged at 14 000 rpm for 1 min to remove any ethanol. Furthermore, the spin columns were incubated at 56°C for 5 min to remove ethanol residues. Thereafter, the spin columns were placed into new 1.5 mL Eppendorf tubes.

For DNA elution, 15 µL of *Buffer BE* were pipetted onto the center of each membrane, incubated for 1 min and centrifuged at 12 000 rpm for 1 min. The converted DNA was diluted with RNase-free water to a concentration of 5 ng/µL and stored at -20°C for further use.

5.7 Design and Optimization of MS-HRM Methods

5.7.1 Search for Appropriate Target Sequence

For the development of new HRM methods, the gene sequence of interest was searched in the *NCBI* database [71]. With the help of the *Eukaryotic Promoter Database* (*EPD*) [88] and *Transcriptional Regulatory Element Database* (*TRED*) [89] the transcription initiation sites of the genes were located. By matching the CpG islands with the exons and the transcription initiation sites, an appropriate sequence segment was chosen for primer design.

5.7.2 Primer Design

The design of the primers was performed with the *Methyl Primer Express® Software v 1.0*. First, CpG islands with a length of 300 to 2 000 bases were searched. Starting with the first target sequence several primer sets for bisulfite treated DNA were searched with the settings listed in *Table 9*. In case of the occurrence of several CpG islands, this procedure was repeated.

Table 9: Settings for primer research in *Methyl Primer Express® Software v 1.0*

Parameters	
Amplicon length [bases]	90 – 150
Primer length [bases]	18 – 27
T_m reaction [°C]	56 – 68
Δ T_m forward and reverse primer [°C]	7
Maximum numbers of designed primer sets	10
Numbers of CpG (forward and reverse)	3
Numbers of Cs not in CpG (forward and reverse)	1 – 10
Minimum numbers of Cs not in CpG per primer	3

Afterwards, a pre-selection was made for the suggested primer sets. The selected primers were individually checked if they fit to the requirements with respect to their sequence. The guidelines for primer design are listed in *Chapter 3.4.1*. If a primer did not fulfill all the criteria, either the position of the primer was changed slightly or single bases were attached or removed. Afterwards, the primers were tested for the probability of forming primer dimers or secondary structures by using the two web servers *Oligo Analyzer 3.1* [90] and *RNAfold* [72].

Finally, the melting temperature of the primers was assessed by using different approaches:

- Wallace rule

$$T_m = 2 * (N_A + N_T) + 4 * (N_G + N_C)$$ *Equation 2:* Wallace rule

N_A Number of adenosines N_G Number of guanines

N_C Number of cytosines N_T Number of thymines

- Web server *Oligo Calc* [73]

Having defined the primer sequence, the melting profiles of the unmethylated and methylated amplicons were simulated by *uMelt Batch v2.1* [91].

5.7.3 Primer Ordering

The primers were synthesized by Sigma-Aldrich, Vienna, Austria. In compliance with the manufacturer's instructions, the lyophilized primers were dissolved in RNase-free water.

5.7.4 Development and Optimization of MS-HRM Methods

First of all, a preliminary experiment with the new primer set was carried out under standard conditions. The workflow of PCR is described in detail in *Chapter 5.8* . *Table 10* shows the parameters under in-house standard conditions.

Table 10: In-house standard conditions for preliminary experiments

Parameters	**Standard conditions**
Annealing temperature	5°C under T_m of the primers
Primer concentration	250 nM
Additional $MgCl_2$ concentration	2 mM

The methods were optimized in order to obtain low C_T values, amplification curves reaching the plateau and high fluorescence signals. Furthermore, no by-products, in particular primer dimers should be formed. The melting point of primer dimers was determined using a "no template control" sample (see *Chapter 5.8.1*). In *Table 11*, the conditions of the individual optimization experiments are summarized.

Table 11: Conditions of the individual optimization experiments

Method	**PCR run**	**Ta [°C]**	**Primers [nM]**	**MgCl2 [mM]**
BRCA1 Primer set 1	Run 1	55 → 49*	250	2
BRCA1 Primer set 2	Run 1	55 → 49*	250	2
CCND2 Primer set 1	Run 1	56 → 50*	250	0 and 1
	Run 2	56 → 50*	250	0
CCND2 Primer set 2	Run 1	56 → 50*	250	2

*Touchdown: 1°C for the first seven cycles

5.8 PCR and HRM Analysis

PCR and HRM analysis were carried out using the *EpiTect HRM PCR Kit* (Qiagen). The working steps were performed according to the manufacturer's protocol. [56]

5.8.1 Preparation of Reaction Mixtures

For the implementation of a PCR run following reagents were used:

- Primer (forward and reverse) solutions (10 µM)
- $MgCl_2$ solution (40 mM)
- DNA solutions of the samples (5 ng/µL)
- DNA solutions of human control DNA (methylated and unmethylated) (5 ng/µL)
- RNase-free water

Before starting, the working place was cleaned with *DNA-Exitus Plus™ IF* to remove DNA residues in order to avoid contamination.

First 100% methylated und 0% methylated bisulfite treated human control DNA were mixed together in different amounts to obtain standards for calibration. The methylated human control DNA (*CpGenome™ Universal Methylated DNA*) was supplied by Millipore. The unmethylated human control DNA (*EpiTect Control DNA, Human, Unmethylated*) was supplied by Qiagen. A master mix was prepared for all samples containing both primers, optionally $MgCl_2$ and RNase-free water. To ensure that the master mix was sufficient for the desired number of samples, the master mix was prepared at least for two more samples (18+2). *Table 12* shows the pipetting scheme for a standard master mix for 18 samples. Concentrations of primers and $MgCl_2$ are summarized for all methods used in this master thesis in *Appendix A, Table A1*.

Table 12: Pipetting scheme for a standard master mix

Substance	Volume per sample [µL]	Volume for 18+2 samples [µL]
Primer solution (forward)	0.5	10
Primer solution (reverse)	0.5	10
$MgCl_2$ solution	1	20
RNase-free water	6	120
	8	160

The reaction solutions were mixed in 0.1 mL strip tubes, which were inserted into a cooled aluminum loading block. First, 10 µL of 2x *EpiTect HRM PCR Master Mix* were pipetted into each tube. Then, 8 µL of master mix were added. And finally, 2 µl of DNA solution (5 ng/µL)

were added to the reaction mixture. “No template control” samples were prepared similar, however, 2 µL of RNase-free water were added instead of the DNA solution.

5.8.2 Temperature Program and Settings

The experiments were performed with the use of a thermal cycler *Rotor-Gene® Q* (Qiagen) and the software *Rotor-Gene® Q Series Software 2.1.0*.

Table 13 shows the temperature program and settings for the method of *CCND2*. Temperature program and settings were equal for all methods, only the annealing temperature was different. The annealing temperatures of all methods are summarized in *Appendix A, Table A1*.

Table 13: Temperature program for the method of *CCND2*

Initialization		10 min	95°C
3-step cycling (50 cycles)	Denaturation	10 sec	95°C
	Annealing	30 sec	56 → 50°C*
	Extension**	10 sec	72°C
Denaturation		1 min	95°C
Hybridization		1 min	40°C
HRM step A**		0.1°C per 2 sec	73 – 83°C
HRM step B**		0.1°C per 2 sec	83 – 73°C
HRM step C**		0.1°C per 2 sec	73 – 83°C

*Touchdown: 1°C for the first seven cycles

**Fluorescence measurement

In order to achieve a specific amplification of the required templates the annealing temperature was set 6°C higher than the actual annealing temperature, adding a touchdown of 1°C for the first seven cycles.

Fluorescence measurement was carried out at the end of each extension step to monitor the increase of the PCR products. Moreover the fluorescence signal was detected during the HRM analysis steps to determine the melting profile of the PCR products.

The HRM step C was performed after a slow hybridization step (HRM step B). The slow hybridization step was included to increase specific hybridization of the different alleles by avoiding incorrect base pairing.

5.9 Data Analysis

5.9.1 Evaluation of Raw Data

The raw data were edited using *Rotor-Gene® Q Series Software 2.1.0* (Qiagen). First the amplification curves were examined to check if the standards and samples were amplified with similar efficiency. The fluorescence signals of the HRM curves were normalized in order to compensate initial variations (see Chapter 3.3.2). Two normalization regions exist: the region before and after the decrease of the fluorescence signal.

5.9.2 Calibration and Calculation of DNA Methylation Status

The data of the normalized HRM curves were exported to *Microsoft Excel 2010*. The mean value of the normalized fluorescence (NF) signal was calculated over the course of the normalized HRM curve for each sample. The obtained value was standardized between 0-100%, using following equation:

$$Standardized\ NF\ of\ a\ sample\ [\%] = \frac{NF_{sample} - NF_{0\%\ methylated\ DNA}}{NF_{100\%\ methylated\ DNA} - NF_{0\%\ methylated\ DNA}} * 100$$

Equation 3: Equation for data standardization

The calibration function for each method was established by using the program *SigmaPlot 11.0*. The DNA methylation status of the samples was calculated in *Microsoft Excel 2010* by using the calibration function from the calibration equation. By repeated measurements of the samples (most commonly four measurements were carried out) the mean value and the standard deviation were calculated.

5.9.3 Nalimov Test for Outlier

Outliers were detected with the Nalimov test. The data were arranged in ascending order and both the smallest and the largest value were considered as potential outlier. The t-value was calculated according to *Equation 4* using *Excel 2010* and compared with the critical value (P = 0.95). Data values higher than the critical value were identified as outliers and therefore removed from the data set. Calculation was repeated with the new data set until no outlier was determined. [92]

$$t = \frac{|x_i - x_m|}{s_x} * \sqrt{\frac{N}{N-1}}$$

Equation 4: Nalimov test for outlier

t	Test value	s_x	Standard deviation
x_i	Suspected outlier value	N	Number of measurements
x_m	Mean value		

5.9.4 Determination of Limit of Detection (LOD) and Limit of Quantification (LOQ)

Limit of detection (LOD) and limit of quantification (LOQ) of each MS-HRM method were determined by repeatedly measuring the 0% methylated DNA standard. First, the mean of the normalized fluorescence signal was calculated and standardized for each measurement (see *Chapter 5.9.2*). Next, the mean value and standard deviation of the repeated measurements was calculated. Finally, LOD and LOQ were calculated according to *Equation 5* and *6*. [93]

$$LOD = x_m + 3 * s_x$$ *Equation 5:* Limit of detection (LOD)

x_m Mean value of 0% methylated DNA standard

s_x Standard deviation

$$LOQ = x_m + 10 * s_x$$ *Equation 6:* Limit of quantification (LOQ)

x_m Mean value of 0% methylated DNA standard

s_x Standard deviation

5.9.5 Significance Test

Differences in the DNA methylation status between tumor and adjacent tissue and tumor and normal tissue were tested for significance using analysis of variance (ANOVA). The test was carried out using the software *SPSS 15.0*. The null hypothesis is that there are no differences. And the first hypothesis was that there are differences.

The results were clustered in three groups:

P ≤ 0.05	significant	*
P ≤ 0.01	very significant	**
P ≤ 0.001	highly significant	***

The significance test could only be carried out for samples with DNA methylation above the LOQ. In some cases it was obviously that there is a significant difference between the tissue types, however the value of the adjacent/normal tissue was below the LOQ. These samples were marked as: $^{+}$significant (no test possible).

5.10 List of Utensils

5.10.1 Chemicals and Kits

Catalase from bovine liver	Sigma-Aldrich	USA
CpGenome™ Universal Methylated DNA	Millipore	USA
Dimethylsulfoxide (DMSO)	Roth	Germany
DNA-Exitus Plus™ IF	AppliChem	Germany
EpiTect Control DNA (human), Unmethylated	Qiagen	Germany
EpiTect Fast DNA Bisulfite Kit	Qiagen	Germany
EpiTect HRM PCR Kit	Qiagen	Germany
Ethanol (EtOH)	VWR	Germany
Fetal Calf Serum (FCS)	Gibco-Invitrogen	Germany
Magnesiumchloride-Hexahydrate ($MgCl_2$ * 6 H_2O)	Sigma-Aldrich	Germany
Penicillin/Streptomycin (PS)	Gibco-Invitrogen	Germany
Phosphate buffered saline (PBS)	Sigma-Aldrich	Germany
Primer	Sigma-Aldrich	Germany
Proteinase K solution from *Engyodontium album*	Sigma-Aldrich	USA
QIAamp DNA Mini Kit	Qiagen	Germany
Ribonuclease A solution from bovine pancreas	Sigma-Aldrich	USA
RNase-free water (ultra-filtered and autoclaved)	Sigma-Aldrich	Germany
Roswell Park Memorial Institute (RPMI) 1640 Medium	Gibco-Invitrogen	Germany
Sulforhodamine B (SRB)	Sigma-Aldrich	Germany
Superoxide dismutase from bovine erythrocytes	Sigma-Aldrich	USA
Trichloroacetic acid (TCA)	Sigma-Aldrich	Germany
Tris/HCl	Sigma-Aldrich	Germany
Trypan blue solution (0.4%)	Sigma-Aldrich	Germany
Trypsin solution (500 mg/L)	Serva	Germany

5.10.2 Sample Material

Biopsy samples	Taken from breast cancer patients by Ass. Prof. Dr. Georg Pfeiler, Department of Obstetrics and Gynecology, Medical University of Vienna, Vienna
MCF-7 cells	Leibniz Institute DSMZ – German Collection of Microorganisms and Cell Cultures

5.10.3 Dietary Supplements

Propolis	Apiculture Josef Holzweber	Austria
Tomato extract (Lycopin Kapseln 20 mg)	ZeinPharma	Germany

5.10.4 Consumables

Plate 24 well	VWR	Germany
Petri dishes, 60 mm	VWR	Germany
Centrifuge tubes, 50 mL	VWR	Germany
Centrifuge tubes, 15 mL, sterile	VWR	Germany
Reaction tubes, 1.5 mL, sterile	VWR	Germany
PCR tubes, 0.2 mL, sterile	Qiagen	Germany
Pipette tips racked, PE-filter, sterile BIO-CERT®	VWR	Germany
Strip Tubes and caps, 0.1 mL	Qiagen	Germany
Flask cell culture, 75 cm²	VWR	Germany
Pasteur pipettes, glass	VWR	Germany

5.10.5 Equipment

Analytical balance	TE2144S	Sartorius
Bunsen burner	Fuego basic	WLD-Tec
Centrifuge	Centrifuge 5424 Rotor FA-45-24-11	Eppendorf
Centrifuge	4K10	Sigma
Draw-off pump	Vacusafe comfort	IBS Integra Biosciences
Drying oven	Memmert Modell 500	Memmert
Hemocytometer	Neubauer	Marienfeld
Incubator	Heracell 240i	Thermo Scientific
Laminar flow cabinet	Herasafe KS	Thermo Scientific
Loading block	(72 x 0.1 mL Strip tubes)	Corbett Life Science
Microscope	Axiovert 40 C	Zeiss
Multilabel counter	Victor3 V 1420	Perkin Elmer
Pipettes		Eppendorf, Biorad
Pipetting aids	Pipetus®	Hirschman Laborgeräte
Spectrophotometer	NanoDrop 2000c	Thermo Scientific
Thermo cycler	Rotor-Gene® Q	Qiagen
Vortex mixer	VF2	Janke & Kunkel
Vortex mixer	VV3	VWR
Water bath	GD 100	Grant

5.10.6 Web Servers

uMelt Batch v2.1	https://www.dna.utah.edu/umelt/umb.php
Oligo Analyzer 3.1	http://eu.idtdna.com/analyzer/Applications/OligoAnalyzer/
Oligo Calc	http://www.basic.northwestern.edu/biotools/OligoCalc.html
RNAfold	http://rna.tbi.univie.ac.at/cgi-bin/RNAfold.cgi

5.10.7 Databases

Eukaryotic Promoter Database (EPD)	http://epd.vital-it.ch/
National Center for Biotechnology Information (NCBI)	http://www.ncbi.nlm.nih.gov/nucleotide/
Transcriptional Regulatory Element Database (TRED)	http://rulai.cshl.edu/cgibin/TRED/tred.cgi?process=home

5.10.8 Software Programs

Methyl Primer Express® Software v 1.0
Microsoft Excel 2010
NanoDrop 2000/2000c Software
Rotor-Gene® Q Series Software 2.1.0
SigmaPlot 11.0
SPSS 15.0
Wallac 1420 Manager

List of Tables

List of Figures

I have tried to obtain the consent of the owner of the image rights to use the images in this work. Should a copyright infringement be known, I request to contact me.

List of Equations

Literature

1. Jemal, A., Bray, F., Center, M.M., Ferlay, J., Ward, E., and Forman, D., *Global cancer statistics.* CA Cancer Journal for Clinicians, 2011. **61**(2): p. 69-90.
2. Lozano, R., Naghavi, M., Foreman, K., Lim, S., Shibuya, K., Aboyans, V., *et al.*, *Global and regional mortality from 235 causes of death for 20 age groups in 1990 and 2010: a systematic analysis for the Global Burden of Disease Study 2010.* Lancet, 2013. **380**(9859): p. 2095-2128.
3. Das, P.M. and Singal, R., *DNA methylation and cancer.* Journal of Clinical Oncology, 2004. **22**(22): p. 4632-4642.
4. Ruddon, R.W., ed. *Cancer Biology*. 5th ed. 2007, Oxford University Press, Inc.
5. Hanahan, D. and Weinberg, R.A., *The hallmarks of cancer.* Cell, 2000. **100**(1): p. 57-70.
6. Pecorino, L., ed. *Molecular Biology of Cancer: Mechanisms, Targets, and Therapeutics*. 2nd ed. 2008, Oxford University Press Inc.: New York.
7. Baldaszti, E., *Jahrbuch der Gesundheitsstatistik*, AUSTRIA, S., Editor. 2012, Verlag Österreich GmbH: Vienna.
8. Tost, J., *DNA methylation: An introduction to the biology and the disease-associated changes of a promising biomarker.* Molecular Biotechnology, 2010. **44**(1): p. 71-81.
9. Egger, G., Liang, G., Aparicio, A., and Jones, P.A., *Epigenetics in human disease and prospects for epigenetic therapy.* Nature, 2004. **429**(6990): p. 457-463.
10. Robertson, K.D., *DNA methylation, methyltransferases, and cancer.* Oncogene, 2001. **20**(24 REV. ISS. 3): p. 3139-3155.
11. Fraga, M.F., Ballestar, E., Paz, M.F., Ropero, S., Setien, F., Ballestar, M.L., *et al.*, *Epigenetic differences arise during the lifetime of monozygotic twins.* Proceedings of the National Academy of Sciences of the United States of America, 2005. **102**(30): p. 10604-10609.
12. *Basic priciples of genetic*. Available from: http://cnx.org/content/m26565/latest/. 5th September 2013.
13. Goll, M.G. and Bestor, T.H., *Eukaryotic cytosine methyltransferases*. 2005. p. 481-514.
14. Gonzalez-Zulueta, M., Bender, C.M., Yang, A.S., Nguyen, T., Beart, R.W., Van Tornout, J.M., and Jones, P.A., *Methylation of the 5' CpG island of the p16/CDKN2 tumor suppressor gene in normal and transformed human tissues correlates with gene silencing.* Cancer Research, 1995. **55**(20): p. 4531-4535.
15. Herman, J.G., Merlo, A., Mao, L., Lapidus, R.G., Issa, J.P.J., Davidson, N.E., *et al.*, *Inactivation of the CDKN2/p16/MTS1 gene is frequently associated with aberrant DNA methylation in all common human cancers.* Cancer Research, 1995. **55**(20): p. 4525-4530.
16. Merlo, A., Herman, J.G., Mao, L., Lee, D.J., Gabrielson, E., Burger, P.C., *et al.*, *5' CpG island methylation is associated with transcriptional silencing of the tumour suppressor p16/CDKN2/MTS1 in human cancers.* Nature Medicine, 1995. **1**(7): p. 686-692.
17. Fearnhead, N.S., Britton, M.P., and Bodmer, W.F., *The ABC of APC.* Human Molecular Genetics, 2001. **10**(7): p. 721-733.
18. Klarmann, G.J., Decker, A., and Farrar, W.L., *Epigenetic gene silencing in the Wnt pathway in breast cancer.* Epigenetics, 2008. **3**(2): p. 59-63.
19. Virmani, A.K., Rathi, A., Sathyanarayana, U.G., Padar, A., Huang, C.X., Cunnigham, H.T., *et al.*, *Aberrant methylation of the Adenomatous Polyposis Coli (APC) gene promoter 1A in breast and lung carcinomas.* Clinical Cancer Research, 2001. **7**(7): p. 1998-2004.
20. Dulaimi, E., Hillinck, J., De Caceres, I.I., Al-Saleem, T., and Cairns, P., *Tumor suppressor gene promoter hypermethylation in serum of breast cancer patients.* Clinical Cancer Research, 2004. **10**(18 I): p. 6189-6193.

21. Tserga, A., Michalopoulos, N.V., Levidou, G., Korkolopoulou, P., Zografos, G., Patsouris, E., and Saetta, A.A., *Association of aberrant DNA methylation with clinicopathological features in breast cancer.* Oncology Reports, 2012. **27**(5): p. 1630-1638.
22. Jin, Z., Tamura, G., Tsuchiya, T., Sakata, K., Kashiwaba, M., Osakabe, M., and Motoyama, T., *Adenomatous polyposis coli (APC) gene promoter hypermethylation in primary breast cancers.* British Journal of Cancer, 2001. **85**(1): p. 69-73.
23. Sarrió, D., Moreno-Bueno, G., Hardisson, D., Sánchez-Estévez, C., Guo, M., Herman, J.G., *et al.*, *Epigenetic and genetic alterations of APC and CDH1 genes in lobular breast cancer: Relationships with abnormal E-cadherin and catenin expression and microsatellite instability.* International Journal of Cancer, 2003. **106**(2): p. 208-215.
24. Boulton, S.J., *Cellular functions of the BRCA tumour-suppressor proteins.* Biochemical Society Transactions, 2006. **34**(5): p. 633-645.
25. Miki, Y., Swensen, J., Shattuck-Eidens, D., Futreal, P.A., Harshman, K., Tavtigian, S., *et al.*, *A strong candidate for the breast and ovarian cancer susceptibility gene BRCA1.* Science, 1994. **266**(5182): p. 66-71.
26. Wong, E.M., Southey, M.C., Fox, S.B., Brown, M.A., Dowty, J.G., Jenkins, M.A., . . . Dobrovic, A., *Constitutional methylation of the BRCA1 promoter is specifically associated with BRCA1 mutation-associated pathology in early-onset breast cancer.* Cancer Prevention Research, 2011. **4**(1): p. 23-33.
27. Rice, J.C., Ozcelik, H., Maxeiner, P., Andrulis, I., and Futscher, B.W., *Methylation of the BRCA1 promoter is associated with decreased BRCA1 mRNA levels in clinical breast cancer specimens.* Carcinogenesis, 2000. **21**(9): p. 1761-1765.
28. Evron, E., Umbricht, C.B., Korz, D., Raman, V., Loeb, D.M., Niranjan, B., *et al.*, *Loss of cyclin D2 expression in the majority of breast cancers is associated with promoter hypermethylation.* Cancer Research, 2001. **61**(6): p. 2782-2787.
29. Fackler, M.J., McVeigh, M., Evron, E., Garrett, E., Mehrotra, J., Polyak, K., *et al.*, *DNA methylation of RASSF1A, HIN-1, RAR-β, cyclin D2 and twist in in situ and invasive lobular breast carcinoma.* International Journal of Cancer, 2003. **107**(6): p. 970-975.
30. Lewis, C.M., Cler, L.R., Bu, D.W., Zöchbauer-Müller, S., Milchgrub, S., Naftalis, E.Z., *et al.*, *Promoter hypermethylation in benign breast epithelium in relation to predicted breast cancer risk.* Clinical Cancer Research, 2005. **11**(1): p. 166-172.
31. Sinha, S., Chunder, N., Mukherjee, N., Alam, N., Roy, A., Roychoudhury, S., and Kumar Panda, C., *Frequent deletion and methylation in SH3GL2 and CDKN2A loci are associated with early- and late-onset breast carcinoma.* Annals of Surgical Oncology, 2008. **15**(4): p. 1070-1080.
32. Hara, E., Smith, R., Parry, D., Tahara, H., Stone, S., and Peters, G., *Regulation of p16CDKN2 expression and its implications for cell immortalization and senescence.* Molecular and Cellular Biology, 1996. **16**(3): p. 859-867.
33. Woodcock, D.M., Linsenmeyer, M.E., Doherty, J.P., and Warren, W.D., *DNA methylation in the promoter region of the p16 (CDKN2/MTS-1/INK4A) gene in human breast tumours.* British Journal of Cancer, 1999. **79**(2): p. 251-256.
34. Curran, J.E., Weinstein, S.R., and Griffiths, L.R., *Polymorphisms of glutathione S-transferase genes (GSTM1, GSTP1 and GSTT1) and breast cancer susceptibility.* Cancer Letters, 2000. **153**(1-2): p. 113-120.
35. Shargh, S.A., Mohaddes, S.M., Sakizli, M., Gharesouran, J., and Karami, F., *Evaluation of methylation status in glutation Stransferase P1(GSTP1) gene promoter in human breast cancer and it relation to tumor grade and stage.* Research Journal of Chemistry and Environment, 2011. **15**(2): p. 492-497.
36. Van der Weyden, L. and Adams, D.J., *The Ras-association domain family (RASSF) members and their role in human tumourigenesis.* Biochimica et Biophysica Acta - Reviews on Cancer, 2007. **1776**(1): p. 58-85.
37. *National Cancer Institue (NCI)*. Available from: http://www.cancer.gov/dictionary?CdrID=45618. 11th September 2013.

38. Mulero-Navarro, S. and Esteller, M., *Epigenetic biomarkers for human cancer: The time is now.* Critical Reviews in Oncology/Hematology, 2008. **68**(1): p. 1-11.
39. Levenson, V.V., *DNA methylation as a universal biomarker.* Expert Review of Molecular Diagnostics, 2010. **10**(4): p. 481-488.
40. Levenson, V.V. and Melnikov, A.A., *DNA methylation as clinically useful biomarkers - Light at the end of the tunnel.* Pharmaceuticals, 2012. **5**(1): p. 94-113.
41. Giovannucci, E. and Ogino, S., *DNA methylation, field effects, and colorectal cancer.* Journal of the National Cancer Institute, 2005. **97**(18): p. 1317-1319.
42. Chai, H. and Brown, R.E., *Review: Field effect in cancer-an update.* Annals of Clinical and Laboratory Science, 2009. **39**(4): p. 331-338.
43. Shen, L., Kondo, Y., Rosner, G.L., Xiao, L., Hernandez, N.S., Vilaythong, J., *et al.*, *MGMT promoter methylation and field defect in sporadic colorectal cancer.* Journal of the National Cancer Institute, 2005. **97**(18): p. 1330-1338.
44. Yan, P.S., Venkataramu, C., Ibrahim, A., Liu, J.C., Shen, R.Z., Diaz, N.M., *et al.*, *Mapping geographic zones of cancer risk with epigenetic biomarkers in normal breast tissue.* Clinical Cancer Research, 2006. **12**(22): p. 6626-6636.
45. Choi, S., Corricher, R., and Friso, S., eds. *Nutrients and DNA Methylation*. Nutrients and Epigenetics, ed. Choi, S. and Friso, S. 2009: CRC Press. 105-125.
46. Lee, W.J., Shim, J.Y., and Zhu, B.T., *Mechanisms for the inhibition of DNA methyltransferases by tea catechins and bioflavonoids.* Molecular Pharmacology, 2005. **68**(4): p. 1018-1030.
47. King-Batoon, A., Leszczynska, J.M., and Klein, C.B., *Modulation of gene methylation by genistein or lycopene in breast cancer cells.* Environmental and Molecular Mutagenesis, 2008. **49**(1): p. 36-45.
48. Davis, C.D. and Uthus, E.O., *DNA methylation, cancer susceptibility, and nutrient interactions.* Experimental Biology and Medicine, 2004. **229**(10): p. 988-995.
49. Sawicka, D., Car, H., Borawska, M.H., and Nikliński, J., *The anticancer activity of propolis.* Folia Histochemica et Cytobiologica, 2012. **50**(1): p. 25-37.
50. Barbarić, M., Mišković, K., Bojić, M., Lončar, M.B., Smolčić-Bubalo, A., Debeljak, Z., and Medić-Šarić, M., *Chemical composition of the ethanolic propolis extracts and its effect on HeLa cells.* Journal of Ethnopharmacology, 2011. **135**(3): p. 772-778.
51. Aggarwal, B.B. and Shishodia, S., *Molecular targets of dietary agents for prevention and therapy of cancer.* Biochemical Pharmacology, 2006. **71**(10): p. 1397-1421.
52. McPherson, M.J. and Moller, S.G., *PCR*. 2006, Taylor & Francis Group: New York.
53. Saiki, R.K., Gelfand, D.H., Stoffel, S., Scharf, S.J., Higuchi, R., Horn, G.T., *et al.*, *Primer-directed enzymatic amplification of DNA with a thermostable DNA polymerase.* Science, 1988. **239**(4839): p. 487-491.
54. Müller, H.J., *PCR - Polymerase-Kettenreaktion*. 2001, Berlin: Spektrum Akademischer Verlag.
55. *HotStarTaq Plus DNA Polymerase*. Available from: http://www.qiagen.com/Products/Catalog/Assay-Technologies/End-Point-PCR-and-RT-PCR-Reagents/HotStarTaq-Plus-DNA-Polymerase?cmpid=QVen6GAHotStartTaq#productdetails. 11th July 2013.
56. Qiagen, *EpiTect® HRM™ PCR Handbook.* 2009.
57. Shipley, G.L., *An introduction to real-time PCR*, in *Real-time PCR*, Tevfik Dorak, M., Editor. 2006, Taylor & Francis Group: New York. p. 1-37.
58. *EvaGreen*. Available from: http://www.biotium.com/product/product_info/newproduct/evagreen.asp. 2nd September 2013.
59. Wojdacz, T.K., Dobrovic, A., and Hansen, L.L., *Methylation-sensitive high-resolution melting.* Nature Protocols, 2008. **3**(12): p. 1903-1908.
60. Frommer, M., McDonald, L.E., Millar, D.S., Collis, C.M., Watt, F., Grigg, G.W., *et al.*, *A genomic sequencing protocol that yields a positive display of 5- methylcytosine residues in individual DNA strands.* Proceedings of the National Academy of Sciences of the United States of America, 1992. **89**(5): p. 1827-1831.
61. Clark, S.J., Harrison, J., Paul, C.L., and Frommer, M., *High sensitivity mapping of methylated cytosines.* Nucleic Acids Research, 1994. **22**(15): p. 2990-2997.

62. Reed, G.H., Kent, J.O., and Wittwer, C.T., *High-resolution DNA melting analysis for simple and efficient molecular diagnostics.* Pharmacogenomics, 2007. **8**(6): p. 597-608.
63. Vossen, R.H.A.M., Aten, E., Roos, A., and Den Dunnen, J.T., *High-resolution melting analysis (HRMA) - More than just sequence variant screening.* Human Mutation, 2009. **30**(6): p. 860-866.
64. Wojdacz, T.K. and Dobrovic, A., *Melting curve assays for DNA methylation analysis.* Methods in molecular biology (Clifton, N.J.), 2009. **507**: p. 229-240.
65. Erali, M., Voelkerding, K.V., and Wittwer, C.T., *High resolution melting applications for clinical laboratory medicine.* Experimental and Molecular Pathology, 2008. **85**(1): p. 50-58.
66. Manz, A., Pamme, N., and Iossifidis, D., *Bioanalytical chemistry.* Imperial College Press, 2004: p. 19.
67. Migheli, F., Stoccoro, A., Coppedè, F., Wan Omar, W.A., Failli, A., Consolini, R., *et al.*, *Comparison Study of MS-HRM and Pyrosequencing Techniques for Quantification of APC and CDKN2A Gene Methylation.* PLoS ONE, 2013. **8**(1).
68. Kristensen, L.S., Wojdacz, T.K., Thestrup, B.B., Wiuf, C., Hager, H., and Hansen, L.L., *Quality assessment of DNA derived from up to 30 years old formalin fixed paraffin embedded (FFPE) tissue for PCR-based methylation analysis using SMART-MSP and MS-HRM.* BMC Cancer, 2009. **9**.
69. Wojdacz, T.K., Hansen, L.L., and Dobrovic, A., *A new approach to primer design for the control of PCR bias in methylation studies.* BMC Research Notes, 2008. **1**.
70. Wojdacz, T.K. and Hansen, L.L., *Reversal of PCR bias for improved sensitivity of the DNA methylation melting curve assay.* BioTechniques, 2006. **41**(3): p. 274-278.
71. *National Center for Biotechnology Information (NCBI)*. Available from: http://www.ncbi.nlm.nih.gov/nucleotide/.
72. *RNAfold web server*. Available from: http://rna.tbi.univie.ac.at/cgi-bin/RNAfold.cgi.
73. *Oligonucleotide Properties Calculator (Oligo Calc)*. Available from: http://www.basic.northwestern.edu/biotools/OligoCalc.html.
74. Balic, M., Pichler, M., Strutz, J., Heitzer, E., Ausch, C., Samonigg, H., *et al., High quality assessment of DNA methylation in archival tissues from colorectal cancer patients using quantitative high-resolution melting analysis.* Journal of Molecular Diagnostics, 2009. **11**(2): p. 102-108.
75. Pettigrew, C.A., French, J.D., Saunus, J.M., Edwards, S.L., Sauer, A.V., Smart, C.E., *et al.*, *Identification and functional analysis of novel BRCA1 transcripts, including mouse Brca1-Iris and human pseudo-BRCA1.* Breast Cancer Research and Treatment, 2010. **119**(1): p. 239-247.
76. Werner, B.K. *Analyse der Auswirkung lebensmittelrelevanter Substanzen auf die DNA-Methylierung mittels hochauflösender Schmelzkurvenanalyse*. 2012. Master thesis, University of Vienna, Vienna.
77. Raab, A. *Bestimmung des Promoter-Methylierungsgrades Brustkrebs-relevanter Tumorsuppressorgene in vitro und in vivo mittels hochauflösender Schmelzkurvenanalyse*. 2013. Diploma thesis, University of Vienna, Vienna.
78. Hou, Z., Sang, S., You, H., Lee, M.J., Hong, J., Chin, K.V., and Yang, C.S., *Mechanism of action of (-)-epigallocatechin-3-gallate: Auto-oxidation- dependent inactivation of epidermal growth factor receptor and direct effects on growth inhibition in human esophageal cancer KYSE 150 cells.* Cancer Research, 2005. **65**(17): p. 8049-8056.
79. Soule, H.D., Vazguez, J., Long, A., Albert, S., and Brennan, M., *A human cell line from a pleural effusion derived from a breast carcinoma.* Journal of the National Cancer Institute, 1973. **51**(5): p. 1409-1416.
80. *MCF-7 Cells (human breast adenocarcinoma cell line)*. Available from: http://www.mcf7.com/mcf7_cell_culture.html. 6th September 2013.
81. Lindl, T., *Zell- und Gewebekultur*. 5. Auflage ed. 2002, Berlin: Spektrum Akademischer Verlag.
82. *Neubauer counting chamber*. Available from: http://www.zaehlkammer.de/deutsch/neubauer.html. 18th September 2013.

83. *Zählkammer - Wikipedia*. Available from: http://de.wikipedia.org/wiki/Z%C3%A4hlkammer. 18th September 2013.
84. Vichai, V. and Kirtikara, K., *Sulforhodamine B colorimetric assay for cytotoxicity screening.* Nature Protocols, 2006. **1**(3): p. 1112-1116.
85. Qiagen, *QIAamp® DNA Mini and Blood Mini Handbook.* 2010.
86. Mullis, K., Faloona, F., Scharf, S., Saiki, R., Horn, G., and Erlich, H., *Specific enzymatic amplification of DNA in vitro: The polymerase chain reaction.* Cold Spring Harbor Symposia on Quantitative Biology, 1986. **51**(1): p. 263-273.
87. Qiagen, *EpiTect® Fast Bisulfite Conversion Handbook.* 2012.
88. *Eukaryotic Promoter Database (EPD)*. Available from: http://epd.vital-it.ch/.
89. *Transcriptional Regulatory Element Database (TRED)*. Available from: http://rulai.cshl.edu/cgi-bin/TRED/tred.cgi?process=home.
90. *Oligo Analyzer 3.1*. Available from: http://eu.idtdna.com/analyzer/Applications/OligoAnalyzer/.
91. *uMelt Batch v2.1*. Available from: https://www.dna.utah.edu/umelt/umb.php.
92. Gottwald, W., *Statistik für Anwender*. 1st ed. 1999, Weinheim: Wiley-VCH.
93. Keith, L.H., Crummett, W., Deegan Jr, J., Libby, R.A., Taylor, J.K., and Wentler, G., *Principles of environmental analysis.* Analytical Chemistry, 1983. **55**(14): p. 2210-2218.
94. Bayer, N. *Untersuchung des DNA-Methylierungsgrades im Serum von Brustkrebspatientinnen mittels hochauflösender Schmelzkurvenanalyse*. 2013. Bachelor thesis, FH Campus Wien, Vienna.

APPENDIX A

Table A1: Overview of MS-HRM methods used in this master thesis

Gene	Primer sequences 5' → 3'	c_{Primer} [nM]	c_{MgCl2} [mM]	T_a [°C]	HRM [°C]	Lit.
APC	f: AAGTAGTTGTGTAATT**CG**TTGGAT r: CACCTCCATTCTATCTCCAATA	500	0	53	73-84	[74]
BRCA1	f: TTGTTGTTTAG**CG**GTAGTTTTTTGGTT r. AACCTATCCCC**CG**TCCAAAAA	250	2	61	70-85	[26]
CCND2	f: GTTTTAGAG**CG**GAGAAGAG r: AACAAAACCT**CG**AAACTACC	250	0	50	73-83	--
CDKN2A	f: **CG**GAGGAAGAAAGAGGAGGGGT r: **CG**CTACCTACTCTCCCCCTCT	400	0	62	75-87	[67]
	f: GG**CG**GAGTTGTTGTTGTTTTA**TG** r: ACAACACCACCAA**CG**TATCCAA	250	1.5	52	70-85	[76]
GSTP1	f: GTGAAG**CG**GGTGTGTAAGTTT r: TAAACAAACAACAAAAAAAAAACC	250	1	56	70-85	[21]
RASSF1A	f: GT**CG**GGGTTTGTTTTGTGGTT r: CAACTCC**CA**CAACTCAATAAACT	250	2	56	70-85	[77]
MGMT	f: TTGATTAGGGGAG**CG**GTATTAG r: C**CA**CATACC**CG**AATAATCCTAAAA	250	0	52	70-85	[94]

CpGs are shown in bold.

Ts that correspond to Cs in the gDNA at the 3' end of the forward primer are highlighted in gray.

As that correspond to Gs in the gDNA at the 3' end of the reverse primer are highlighted in gray.

Table A2: Clinicopathological data of the breast cancer patients

Patient	Age [y]	Diagnosis	Position		Hormone receptor status		
			Right	Left	ER	PR	HER2
1	75	IDC		X	+++	++	-
2	65	IDC	X		+++	++	-
3	54	IDC	X		n.s.	n.s.	n.s.
4	39	IDC		X	+++	++	+++
5	66	IDC	X		+++	++	-
6	50	IDC		X	+++	+++	+++
7	73	IDC		X	+	+	-
8	76	IDC		X	+++	+++	-
9	63	IDC		X	++	+++	-
10	48	IDC	X		+++	+++	+
11	58	IDC		X	+++	+++	+
12	61	IDC	X		-	-	-
13	52	ILC		X	+++	++	-
14	42	IDC		X	++	-	-
15	67	IDC	X		+++	++	-

ER Estrogen receptor
PR Progesterone receptor
HER2 Human epidermal growth factor receptor 2
IDC Invasive ductal carcinoma
ILC Invasive lobular carcinoma

- negative, + weakly positive, ++ moderately positive, +++ strongly positive, n.s. not specified

APPENDIX B

Calculated DNA Methylation Status of the Biopsy Samples

T … Tumor tissue

A … Adjacent tissue

N … Normal tissue

n.v. = no value

Measurements performed by Anna Raab are shown with a gray background

Outliers are in brackets and highlighted in gray

* Heterogeneous methylation, calculated value is most probably slightly lower than the actual value

Table B1: Methylations status [%] in the *APC* promoter of the biopsy samples

APC		**Methylation status [%]**									
		Run 1		**Run 2**		**Run 3**		**Run 4**		**Mean**	**SD**
Biopsy sample 1	T	0.7-3.0	0.7-3.0	< 0.7	< 0.7					**< 0.7**	
	A	0.7-3.0	0.7-3.0	< 0.7	< 0.7					**< 0.7**	
	N	< 0.7	< 0.7	< 0.7	< 0.7					**< 0.7**	
Biopsy sample 2	T	0.7-3.0	0.7-3.0	< 0.7	< 0.7					**< 0.7**	
	A	6	0.7-3.0	0.7-3.0	0.7-3.0					**0.7-3.0**	
	N	4	4	0.7-3.0	< 0.7					**0.7-3.0**	
Biopsy sample 3	T	51	48	61	63	67	68	55	59	**59**	7
	A	23	24	(27)	(40)	24	22	21	20	**22**	2
	N	15	15	29	28	8	(46)	7	11	**16**	9
Biopsy sample 4	T	0.7-3.0	0.7-3.0	0.7-3.0	< 0.7					**0.7-3.0**	
	A	0.7-3.0	< 0.7	< 0.7	< 0.7					**< 0.7**	
	N	< 0.7	< 0.7	< 0.7	< 0.7	0.7-3.0	0.7-3.0			**< 0.7**	
Biopsy sample 5	T	8	9	7	6	< 0.7	0.7-3.0			**7**	1
	A	8	10	6	5	0.7-3.0	0.7-3.0			**7**	2
	N	9	10	7	6	0.7-3.0	3			**8**	2
Biopsy sample 6	T	6	8	5	5					**6**	2
	A	3	4	3	0.7-3.0					**3**	0.3
	N	6	6	4	4					**5**	2
Biopsy sample 7	T	0.7-3.0	0.7-3.0	5	0.7-3.0					**0.7-3.0**	
	A	4	6	4	0.7-3.0					**5**	1
	N	3	4	0.7-3.0	0.7-3.0					**0.7-3.0**	
Biopsy sample 8	T	11	12	4	8					**9***	3
	A	7	7	0.7-3.0	0.7-3.0					**0.7-3.0***	
	N	0.7-3.0	0.7-3.0	< 0.7	< 0.7					**< 0.7**	
Biopsy sample 9	T	0.7-3.0	< 0.7	< 0.7	< 0.7					**< 0.7**	
	A	0.7-3.0	0.7-3.0	0.7-3.0	0.7-3.0					**0.7-3.0**	
	N	0.7-3.0	0.7-3.0	< 0.7	0.7-3.0					**0.7-3.0**	
Biopsy sample 10	T	88	89	85	88					**88**	0.5
	A	12	26	24	15					**19**	7
	N	5	4	5	4					**4**	0.5
Biopsy sample 11	T	61	57	58	60	53	53			**57**	3
	A	(14)	8	8	9	9	8			**8**	0.7
	N	(18)	12	11	(8)	11	13			**12**	1
Biopsy sample 12	T	78	84	73	79					**79**	4
	A	10	11	8	8					**9**	1
	N	32	29	21	20					**25**	6
Biopsy sample 13	T	76	74	72	75					**74**	2
	A	5	(9)	5	4					**5**	0.5
	N	(14)	9	8	9					**9**	0.9
Biopsy sample 14	T	75	74	73	75					**74**	1
	A	14	16	13	13					**14**	1
	N	4	3	0.7-3.0	0.7-3.0					**0.7-3.0**	
Biopsy sample 15	T	90	87	85	88					**87**	2
	A	23	22	(4)	21					**22**	0.9
	N	10	6	6	12					**8**	3

Table B2: Methylations status [%] in the *BRCA1* promoter of the biopsy samples

BRCA1		**Methylation status [%]**							
		Run 1		**Run 2**		**Run 3**		**Mean**	**SD**
	T	< 0.4	< 0.4	< 0.4	< 0.4	< 0.4	< 0.4	**< 0.4**	
Biopsy sample 1	A	< 0.4	< 0.4			< 0.4	< 0.4	**< 0.4**	
	N	< 0.4	< 0.4			< 0.4	< 0.4	**< 0.4**	
	T	< 0.4	< 0.4	< 0.4	< 0.4	< 0.4	< 0.4	**< 0.4**	
Biopsy sample 2	A	< 0.4	< 0.4			n.v.	n.v.	**< 0.4**	
	N	< 0.4	< 0.4			< 0.4	n.v.	**< 0.4**	
	T	< 0.4	< 0.4	0.4-1.6	< 0.4	< 0.4	n.v.	**< 0.4**	
Biopsy sample 3	A	< 0.4	< 0.4			< 0.4	< 0.4	**< 0.4**	
	N	< 0.4	n.v.			< 0.4	< 0.4	**< 0.4**	
	T	< 0.4	< 0.4	< 0.4	< 0.4			**< 0.4**	
Biopsy sample 4	A	0.4-1.6	0.4-1.6	< 0.4	< 0.4			**< 0.4**	
	N	< 0.4	< 0.4	< 0.4	< 0.4			**< 0.4**	
	T	0.4-1.6	< 0.4	< 0.4	< 0.4			**< 0.4**	
Biopsy sample 5	A	0.4-1.6	< 0.4	< 0.4	< 0.4			**< 0.4**	
	N	< 0.4	< 0.4	< 0.4	< 0.4			**< 0.4**	
	T	2.2	0.4-1.6	2.0	0.4-1.6			**0.4-1.6**	
Biopsy sample 6	A	< 0.4	< 0.4	< 0.4	< 0.4			**< 0.4**	
	N	1.8	< 0.4	0.4-1.6	< 0.4			**0.4-1.6**	
	T	< 0.4	< 0.4	< 0.4	< 0.4			**< 0.4**	
Biopsy sample 7	A	< 0.4	< 0.4	< 0.4	< 0.4			**< 0.4**	
	N	< 0.4	< 0.4	< 0.4	< 0.4			**< 0.4**	
	T	0.4-1.6	0.4-1.6	0.4-1.6	0.4-1.6			**0.4-1.6**	
Biopsy sample 8	A	0.4-1.6	< 0.4	< 0.4	< 0.4			**< 0.4**	
	N	< 0.4	0.4-1.6	0.4-1.6	0.4-1.6			**0.4-1.6**	
	T	< 0.4	< 0.4	< 0.4	< 0.4			**< 0.4**	
Biopsy sample 9	A	< 0.4	< 0.4	0.4-1.6	< 0.4			**< 0.4**	
	N	0.4-1.6	0.4-1.6	< 0.4	< 0.4			**< 0.4**	
	T	0.4-1.6	0.4-1.6	< 0.4	< 0.4	< 0.4	< 0.4	**< 0.4**	
Biopsy sample 10	A	n.v.	n.v.	< 0.4	< 0.4	n.v.	n.v.	**< 0.4**	
	N	< 0.4	< 0.4	< 0.4	< 0.4	< 0.4	< 0.4	**< 0.4**	
	T	< 0.4	< 0.4	< 0.4	0.4-1.6			**< 0.4**	
Biopsy sample 11	A	< 0.4	0.4-1.6	0.4-1.6	0.4-1.6			**0.4-1.6**	
	N	0.4-1.6	0.4-1.6	0.4-1.6	0.4-1.6			**0.4-1.6**	
	T	41	35	53	50			**45**	9
Biopsy sample 12	A	16	12	16	20			**16**	3
	N	22	21	25	22			**22**	2
	T	< 0.4	< 0.4	< 0.4	< 0.4			**< 0.4**	
Biopsy sample 13	A	< 0.4	< 0.4	< 0.4	< 0.4			**< 0.4**	
	N	0.4-1.6	< 0.4	0.4-1.6	< 0.4			**< 0.4**	
	T	55	43	47	51			**49**	5
Biopsy sample 14	A	6	6	7	6			**6**	0.4
	N	6	6	6	7			**6**	0.5
	T	< 0.4	< 0.4	< 0.4	0.4-1.6	0.4-1.6	< 0.4	**< 0.4**	
Biopsy sample 15	A	n.v.	n.v.	n.v.	n.v.	n.v.	n.v.	**n.v.**	
	N	n.v.	n.v.	< 0.4	< 0.4	n.v.	n.v.	**< 0.4**	

Table B3: Methylations status [%] in the *CCND2* promoter of the biopsy samples

CCND2		**Methylation status [%]**					
		Run 1		**Run 2**		**Mean**	**SD**
Biopsy sample 1	T	< 0.3	< 0.3	< 0.3	< 0.3	**< 0.3**	
	A	n.v.	n.v.	< 0.3	< 0.3	**< 0.3**	
	N	n.v.	< 0.3	0.3-1.1	< 0.3	**< 0.3**	
Biopsy sample 2	T	4	6	6	5	**5**	0.8
	A	< 0.3	< 0.3	< 0.3	0.3-1.1	**< 0.3**	
	N	< 0.3	< 0.3	< 0.3	< 0.3	**< 0.3**	
Biopsy sample 3	T	< 0.3	< 0.3	< 0.3	< 0.3	**< 0.3**	
	A	< 0.3	< 0.3	< 0.3	< 0.3	**< 0.3**	
	N	< 0.3	n.v.	< 0.3	< 0.3	**< 0.3**	
Biopsy sample 4	T	< 0.3	< 0.3	< 0.3	< 0.3	**< 0.3**	
	A	< 0.3	< 0.3	< 0.3	< 0.3	**< 0.3**	
	N	< 0.3	< 0.3	< 0.3	< 0.3	**< 0.3**	
Biopsy sample 5	T	17	16	17	16	**17**	0.6
	A	< 0.3	< 0.3	< 0.3	< 0.3	**< 0.3**	
	N	< 0.3	< 0.3	< 0.3	< 0.3	**< 0.3**	
Biopsy sample 6	T	< 0.3	< 0.3	< 0.3	< 0.3	**< 0.3**	
	A	< 0.3	< 0.3	< 0.3	< 0.3	**< 0.3**	
	N	< 0.3	< 0.3	< 0.3	< 0.3	**< 0.3**	
Biopsy sample 7	T	< 0.3	< 0.3	< 0.3	< 0.3	**< 0.3**	
	A	< 0.3	< 0.3	< 0.3	< 0.3	**< 0.3**	
	N	< 0.3	< 0.3	< 0.3	< 0.3	**< 0.3**	
Biopsy sample 8	T	1	1	2	1	**1**	0.3
	A	< 0.3	< 0.3	< 0.3	< 0.3	**< 0.3**	
	N	< 0.3	< 0.3	< 0.3	< 0.3	**< 0.3**	
Biopsy sample 9	T	< 0.3	< 0.3	< 0.3	< 0.3	**< 0.3**	
	A	< 0.3	< 0.3	< 0.3	< 0.3	**< 0.3**	
	N	< 0.3	< 0.3	< 0.3	< 0.3	**< 0.3**	
Biopsy sample 10	T	6	8	7	8	**7**	1
	A	0.3-1.1	0.3-1.1	< 0.3	0.3-1.1	**0.3-1.1**	
	N	< 0.3	< 0.3	< 0.3	< 0.3	**< 0.3**	
Biopsy sample 11	T	< 0.3	< 0.3	< 0.3	< 0.3	**< 0.3**	
	A	< 0.3	< 0.3	< 0.3	< 0.3	**< 0.3**	
	N	< 0.3	< 0.3	< 0.3	< 0.3	**< 0.3**	
Biopsy sample 12	T	< 0.3	< 0.3	< 0.3	< 0.3	**< 0.3**	
	A	< 0.3	< 0.3	< 0.3	< 0.3	**< 0.3**	
	N	< 0.3	< 0.3	< 0.3	< 0.3	**< 0.3**	
Biopsy sample 13	T	< 0.3	< 0.3	< 0.3	< 0.3	**< 0.3**	
	A	< 0.3	< 0.3	< 0.3	< 0.3	**< 0.3**	
	N	< 0.3	< 0.3	< 0.3	< 0.3	**< 0.3**	
Biopsy sample 14	T	< 0.3	< 0.3	< 0.3	< 0.3	**< 0.3**	
	A	< 0.3	< 0.3	< 0.3	< 0.3	**< 0.3**	
	N	< 0.3	< 0.3	< 0.3	< 0.3	**< 0.3**	
Biopsy sample 15	T	6	6	5	5	**6**	0.6
	A	< 0.3	< 0.3	0.3-1.1	n.v.	**< 0.3**	
	N	< 0.3	< 0.3	< 0.3	< 0.3	**< 0.3**	

Table B4: Methylations status [%] in the *CDKN2A* promoter of the biopsy samples

CDKN2A		**Methylation status [%]**					
		Run 1		**Run 2**		**Mean**	**SD**
Biopsy sample 1	T	< 1.0	< 1.0	< 1.0	< 1.0	**< 1.0**	
	A	< 1.0	< 1.0	< 1.0	< 1.0	**< 1.0**	
	N	< 1.0	< 1.0	< 1.0	1.0-3.3	**< 1.0**	
Biopsy sample 2	T	< 1.0	< 1.0	1.0-3.3	< 1.0	**< 1.0**	
	A	< 1.0	< 1.0	< 1.0	< 1.0	**< 1.0**	
	N	< 1.0	< 1.0	1.0-3.3	< 1.0	**< 1.0**	
Biopsy sample 3	T	< 1.0	< 1.0	< 1.0	< 1.0	**< 1.0**	
	A	< 1.0	< 1.0	< 1.0	< 1.0	**< 1.0**	
	N	< 1.0	< 1.0	< 1.0	< 1.0	**< 1.0**	
Biopsy sample 4	T	< 1.0	< 1.0	1.0-3.3	1.0-3.3	**< 1.0**	
	A	< 1.0	< 1.0	< 1.0	1.0-3.3	**< 1.0**	
	N	< 1.0	< 1.0	1.0-3.3	< 1.0	**< 1.0**	
Biopsy sample 5	T	< 1.0	< 1.0	< 1.0	1.0-3.3	**< 1.0**	
	A	< 1.0	< 1.0	1.0-3.3	1.0-3.3	**< 1.0**	
	N	< 1.0	< 1.0	1.0-3.3	1.0-3.3	**< 1.0**	
Biopsy sample 6	T	< 1.0	< 1.0	1.0-3.3	1.0-3.3	**< 1.0**	
	A	< 1.0	< 1.0	< 1.0	< 1.0	**< 1.0**	
	N	1.0-3.3	1.0-3.3	1.0-3.3	1.0-3.3	**1.0-3.3**	
Biopsy sample 7	T	< 1.0	< 1.0	< 1.0	< 1.0	**< 1.0**	
	A	1.0-3.3	n.v.	< 1.0	< 1.0	**< 1.0**	
	N	1.0-3.3	< 1.0	< 1.0	1.0-3.3	**< 1.0**	
Biopsy sample 8	T	< 1.0	< 1.0	< 1.0	< 1.0	**< 1.0**	
	A	< 1.0	< 1.0	< 1.0	< 1.0	**< 1.0**	
	N	1.0-3.3	< 1.0	< 1.0	< 1.0	**< 1.0**	
Biopsy sample 9	T	< 1.0	1.0-3.3	n.v.	< 1.0	**< 1.0**	
	A	1.0-3.3	< 1.0	1.0-3.3	1.0-3.3	**1.0-3.3**	
	N	1.0-3.3	1.0-3.3	< 1.0	1.0-3.3	**1.0-3.3**	
Biopsy sample 10	T	< 1.0	< 1.0	< 1.0	< 1.0	**< 1.0**	
	A	1.0-3.3	1.0-3.3	< 1.0	1.0-3.3	**1.0-3.3**	
	N	1.0-3.3	1.0-3.3	< 1.0	< 1.0	**< 1.0**	
Biopsy sample 11	T	< 1.0	1.0-3.3	< 1.0	< 1.0	**< 1.0**	
	A	1.0-3.3	1.0-3.3	1.0-3.3	1.0-3.3	**1.0-3.3**	
	N	1.0-3.3	< 1.0	1.0-3.3	1.0-3.3	**1.0-3.3**	
Biopsy sample 12	T	58	55	65	69	**62**	6
	A	6	6	7	6	**6**	0.1
	N	15	15	17	16	**16**	0.8
Biopsy sample 13	T	1.0-3.3	1.0-3.3	< 1.0	< 1.0	**< 1.0**	
	A	1.0-3.3	1.0-3.3	1.0-3.3	1.0-3.3	**1.0-3.3**	
	N	1.0-3.3	1.0-3.3	1.0-3.3	1.0-3.3	**1.0-3.3**	
Biopsy sample 14	T	51	49	57	52	**52**	4
	A	5	4	4	4	**4**	0.6
	N	6	1.0-3.3	1.0-3.3	1.0-3.3	**1.0-3.3**	
Biopsy sample 15	T	1.0-3.3	< 1.0	1.0-3.3	1.0-3.3	**1.0-3.3**	
	A	1.0-3.3	1.0-3.3	< 1.0	1.0-3.3	**1.0-3.3**	
	N	1.0-3.3	1.0-3.3	1.0-3.3	1.0-3.3	**1.0-3.3**	

Table B5: Methylations status [%] in exon 3 of *CDKN2A* of the biopsy samples

CDKN2A_Exon3		**Methylation status [%]**					
		Run 1		**Run 2**		**Mean**	**SD**
	T	41	47	34	32	**39**	7
Biopsy sample 1	A	28	31	25	31	**29**	3
	N	32	30	36	(47)	**33**	3
	T	49	44	42	40	**44**	4
Biopsy sample 2	A	23	22	23	22	**23**	0.6
	N	45	36	41	36	**40**	4
	T	48	48	44	43	**46**	3
Biopsy sample 3	A	23	19	18	16	**19**	3
	N	21	24	13	14	**18**	5
	T	25	n.v.	18	15	**19**	6
Biopsy sample 4	A	28	23	20	15	**22**	5
	N	25	20	14	15	**18**	5
	T	n.v.	61	68	66	**65**	4
Biopsy sample 5	A	25	23	18	17	**21**	4
	N	17	17	17	18	**17**	0.5
	T	14	21	13	11	**15**	4
Biopsy sample 6	A	11	12	2.0-8.2	2.0-8.2	**2.0-8.2**	
	N	21	21	16	18	**19**	3
	T	49	50	43	39	**45**	5
Biopsy sample 7	A	2.0-8.2	2.0-8.2	2.0-8.2	< 2.0	**2.0-8.2**	
	N	2.0-8.2	2.0-8.2	< 2.0	2.0-8.2	**2.0-8.2**	
	T	60	56	59	60	**59**	2
Biopsy sample 8	A	27	22	27	23	**25**	3
	N	21	16	17	14	**17**	3
	T	33	32	33	32	**33**	0.7
Biopsy sample 9	A	9	2.0-8.2	12	2.0-8.2	**2.0-8.2**	
	N	12	13	14	11	**13**	1
	T	82	82	81	79	**81**	1
Biopsy sample 10	A	22	21	18	21	**20**	2
	N	2.0-8.2	2.0-8.2	2.0-8.2	2.0-8.2	**2.0-8.2**	
	T	56	56	55	57	**56**	0.8
Biopsy sample 11	A	13	12	10	13	**12**	1
	N	15	12	13	13	**13**	1
	T	2.0-8.2	2.0-8.2	< 2.0	< 2.0	**< 2.0**	
Biopsy sample 12	A	2.0-8.2	2.0-8.2	2.0-8.2	< 2.0	**2.0-8.2**	
	N	2.0-8.2	< 2.0	2.0-8.2	2.0-8.2	**2.0-8.2**	
	T	53	51	48	53	**51**	2
Biopsy sample 13	A	2.0-8.2	2.0-8.2	2.0-8.2	2.0-8.2	**2.0-8.2**	
	N	12	15	17	15	**15**	2
	T	31	31	24	24	**28**	4
Biopsy sample 14	A	2.0-8.2	2.0-8.2	< 2.0	2.0-8.2	**2.0-8.2**	
	N	< 2.0	< 2.0	< 2.0	< 2.0	**< 2.0**	
	T	59	57	56	54	**56**	2
Biopsy sample 15	A	13	11	< 2.0	2.0-8.2	**2.0-8.2**	
	N	2.0-8.2	2.0-8.2	2.0-8.2	< 2.0	**2.0-8.2**	

Table B6: Methylations status [%] in the *GSTP1* promoter of the biopsy samples

GSTP1		**Methylation status [%]**				
		Run 1		**Run 2**		**Mean**
	T	1.3-4.2	1.3-4.2	< 1.3	< 1.3	**< 1.3**
Biopsy sample 1	A	1.3-4.2	1.3-4.2	1.3-4.2	1.3-4.2	**1.3-4.2**
	N	< 1.3	< 1.3	1.3-4.2	4	**1.3-4.2**
	T	1.3-4.2	1.3-4.2	4	1.3-4.2	**1.3-4.2**
Biopsy sample 2	A	1.3-4.2	< 1.3	4	1.3-4.2	**1.3-4.2**
	N	1.3-4.2	< 1.3	1.3-4.2	1.3-4.2	**1.3-4.2**
	T	< 1.3	< 1.3	< 1.3	< 1.3	**< 1.3**
Biopsy sample 3	A	< 1.3	< 1.3	1.3-4.2	1.3-4.2	**< 1.3**
	N	< 1.3	< 1.3	1.3-4.2	1.3-4.2	**< 1.3**
	T	1.3-4.2	1.3-4.2	1.3-4.2	1.3-4.2	**1.3-4.2**
Biopsy sample 4	A	4	1.3-4.2	1.3-4.2	1.3-4.2	**1.3-4.2**
	N	1.3-4.2	1.3-4.2	4	1.3-4.2	**1.3-4.2**
	T	< 1.3	< 1.3	n.v.	< 1.3	**< 1.3**
Biopsy sample 5	A	< 1.3	< 1.3	< 1.3	1.3-4.2	**< 1.3**
	N	< 1.3	< 1.3	n.v.	1.3-4.2	**< 1.3**
	T	1.3-4.2	1.3-4.2	1.3-4.2	1.3-4.2	**1.3-4.2**
Biopsy sample 6	A	< 1.3	< 1.3	< 1.3	< 1.3	**< 1.3**
	N	< 1.3	< 1.3	< 1.3	1.3-4.2	**< 1.3**
	T	< 1.3	< 1.3	< 1.3	< 1.3	**< 1.3**
Biopsy sample 7	A	< 1.3	< 1.3	< 1.3	< 1.3	**< 1.3**
	N	< 1.3	A	< 1.3	< 1.3	**< 1.3**
	T	< 1.3	< 1.3	< 1.3	< 1.3	**< 1.3**
Biopsy sample 8	A	1.3-4.2	1.3-4.2	1.3-4.2	1.3-4.2	**1.3-4.2**
	N	1.3-4.2	1.3-4.2	< 1.3	< 1.3	**< 1.3**
	T	< 1.3	< 1.3	< 1.3	< 1.3	**< 1.3**
Biopsy sample 9	A	< 1.3	< 1.3	< 1.3	< 1.3	**< 1.3**
	N	< 1.3	< 1.3	< 1.3	< 1.3	**< 1.3**
	T	1.3-4.2	1.3-4.2	< 1.3	< 1.3	**< 1.3**
Biopsy sample 10	A	1.3-4.2	1.3-4.2	1.3-4.2	1.3-4.2	**1.3-4.2**
	N	1.3-4.2	1.3-4.2	1.3-4.2	1.3-4.2	**1.3-4.2**
	T	1.3-4.2	1.3-4.2	1.3-4.2	< 1.3	**1.3-4.2**
Biopsy sample 11	A	1.3-4.2	1.3-4.2	1.3-4.2	1.3-4.2	**1.3-4.2**
	N	1.3-4.2	1.3-4.2	1.3-4.2	1.3-4.2	**1.3-4.2**
	T	1.3-4.2	1.3-4.2	< 1.3	1.3-4.2	**1.3-4.2**
Biopsy sample 12	A	1.3-4.2	1.3-4.2	1.3-4.2	1.3-4.2	**1.3-4.2**
	N	1.3-4.2	1.3-4.2	1.3-4.2	1.3-4.2	**1.3-4.2**
	T	< 1.3	< 1.3	< 1.3	< 1.3	**< 1.3**
Biopsy sample 13	A	< 1.3	< 1.3	< 1.3	< 1.3	**< 1.3**
	N	< 1.3	< 1.3	< 1.3	< 1.3	**< 1.3**
	T	< 1.3	< 1.3	< 1.3	< 1.3	**< 1.3**
Biopsy sample 14	A	1.3-4.2	1.3-4.2	1.3-4.2	1.3-4.2	**1.3-4.2**
	N	< 1.3	< 1.3	1.3-4.2	< 1.3	**< 1.3**
	T	< 1.3	< 1.3	< 1.3	< 1.3	**< 1.3**
Biopsy sample 15	A	< 1.3	< 1.3	< 1.3	1.3-4.2	**< 1.3**
	N	< 1.3	< 1.3	< 1.3	< 1.3	**< 1.3**

Table B7: Methylations status [%] in the *RASSF1A* promoter of the biopsy samples

RASSF1A		**Methylation status [%]**							
		Run 1		**Run 2**		**Run 3**		**Mean**	**SD**
	T	1.2-4.3	< 1.2	1.2-4.3	< 1.2			**< 1.2**	
Biopsy sample 1	A	< 1.2	1.2-4.3	< 1.2	< 1.2			**< 1.2**	
	N	1.2-4.3	< 1.2	< 1.2	< 1.2			**< 1.2**	
	T	8	6	9	8			**8**	0.4
Biopsy sample 2	A	1.2-4.3	< 1.2	1.2-4.3	1.2-4.3			**1.2-4.3**	
	N	n.v.	5	6	1.2-4.3	1.2-4.3	1.2-4.3	**1.2-4.3**	
	T	13	13	15	16	22	20	**15**	1
Biopsy sample 3	A	5	5	9	9	11	12	**9**	3
	N	1.2-4.3	5	7	6	5	10	**6**	2
	T	1.2-4.3	1.2-4.3	1.2-4.3	1.2-4.3			**1.2-4.3**	
Biopsy sample 4	A	5	6	6	5			**6**	0.6
	N	1.2-4.3	1.2-4.3	1.2-4.3	1.2-4.3			**1.2-4.3**	
	T	20	18	17	16			**18**	2
Biopsy sample 5	A	7	7	6	5			**6**	1
	N	6	1.2-4.3	5	5			**5**	0.4
	T	< 1.2	< 1.2	1.2-4.3	1.2-4.3			**< 1.2**	
Biopsy sample 6	A	< 1.2	1.2-4.3	1.2-4.3	1.2-4.3			**1.2-4.3**	
	N	1.2-4.3	< 1.2	1.2-4.3	1.2-4.3			**1.2-4.3**	
	T	16	17	10	13	12	15	**14**	3
Biopsy sample 7	A	1.2-4.3	5	1.2-4.3	< 1.2			**1.2-4.3**	
	N	7	6	< 1.2	1.2-4.3			**1.2-4.3**	
	T	21	23	17	18			**20**	2
Biopsy sample 8	A	8	10	1.2-4.3	1.2-4.3			**1.2-4.3**	
	N	6	6	1.2-4.3	1.2-4.3			**1.2-4.3**	
	T	1.2-4.3	1.2-4.3	< 1.2	< 1.2			**< 1.2**	
Biopsy sample 9	A	1.2-4.3	1.2-4.3	< 1.2	< 1.2			**< 1.2**	
	N	1.2-4.3	1.2-4.3	< 1.2	< 1.2			**< 1.2**	
	T	18	19	23	22			**20**	2
Biopsy sample 10	A	1.2-4.3	1.2-4.3	1.2-4.3	1.2-4.3			**1.2-4.3**	
	N	1.2-4.3	1.2-4.3	1.2-4.3	1.2-4.3			**1.2-4.3**	
	T	9	8	6	11			**9**	2
Biopsy sample 11	A	1.2-4.3	1.2-4.3	5	1.2-4.3			**1.2-4.3**	
	N	1.2-4.3	1.2-4.3	6	5			**1.2-4.3**	
	T	1.2-4.3	< 1.2	1.2-4.3	1.2-4.3			**1.2-4.3**	
Biopsy sample 12	A	1.2-4.3	1.2-4.3	1.2-4.3	1.2-4.3			**1.2-4.3**	
	N	1.2-4.3	1.2-4.3	1.2-4.3	1.2-4.3			**1.2-4.3**	
	T	13	11	15	14			**13**	2
Biopsy sample 13	A	< 1.2	1.2-4.3	1.2-4.3	1.2-4.3			**1.2-4.3**	
	N	5	1.2-4.3	1.2-4.3	1.2-4.3			**1.2-4.3**	
	T	1.2-4.3	1.2-4.3	1.2-4.3	1.2-4.3			**1.2-4.3**	
Biopsy sample 14	A	6	4	7	7			**7**	0.9
	N	1.2-4.3	1.2-4.3	5	5			**1.2-4.3**	
	T	25	22	23	22			**23**	1
Biopsy sample 15	A	1.2-4.3	1.2-4.3	1.2-4.3	1.2-4.3			**1.2-4.3**	
	N	1.2-4.3	1.2-4.3	6	1.2-4.3			**1.2-4.3**	

APPENDIX C

Table C1: Results of the SRB assays for propolis

	Standardized absorbance [%]					
	1 day of incubation		3 days of incubation		5 days of incubation	
	Mean	SD	Mean	SD	Mean	SD
Control	100	29	100	7	100	3
1 mg/L	92	18	87	6	95	3
2 mg/L	100	12	79	11	99	10
4 mg/L	105	9	83	1	96	4
8 mg/L	107	2	73	5	100	12
16 mg/L	105	5	108	6	110	2
32 mg/L	102	13	115	5	99	16
64 mg/L	93	0	103	4	89	6
125 mg/L	89	4	90	11	72	1
250 mg/L	94	9	77	1	57	1
500 mg/L	95	7	70	12	41	4

Values are standardized with respect to the control sample

Table C2: Results of the SRB assay for tomato extract

Standardized absorbance [%]		
	5 days of incubation	
	Mean	SD
Control	100	13
0.16 mg/L	75	15
0.31 mg/L	69	9
0.63 mg/L	86	6
1.25 mg/L	66	9
2.5 mg/L	62	11
5 mg/L	74	23
10 mg/L	75	4
20 mg/L	81	12
40 mg/L	80	11
80 mg/L	85	10

Values are standardized with respect to the control sample

Table C3: Relative methylations status [%] in the exon3 of *CDKN2A* in MCF-7 cells

***CDKN2A*_Exon3**		**Relative Methylation status [%]**	
		Mean	**SD**
P1	Control	100	8
	15 mg/L	122	3
	30 mg/L	129	3
	150 mg/L	128	10
TE1	Control	100	0
	2.5 mg/L	103	0
	10 mg/L	103	5

Table C4: Methylations status [%] of the *CCND2* promoter in MCF-7 cells

CCND2		**Methylation status [%]**			
		Run 1		**Mean**	**SD**
P1	Control	45	49	47	2
	15 mg/L	45	45	45	0
	30 mg/L	40	43	42	3
	150 mg/L	46	52	49	4

Table C5: Methylations status [%] of the promoter of *RASSF1A, APC* and *BRCA1* in MCF-7 cells

			Methylation status [%]			
			Run 1		**Mean**	**SD**
RASSF1A	TE1	Control	83	79	81	3
APC	P2	Control	49	53	51	3
BRCA1	P2	Control	< 0.4	< 0.4	< 0.4	

Abstract

Breast cancer is the most commonly diagnosed cancer in women and therefore there is a great interest in developing biomarkers for its early detection. In addition to genetic changes also epigenetic modifications, particularly DNA methylation, have been identified in association with the development of breast cancer. DNA methylation is found in humans and other mammals almost exclusively at the C5 position of cytosines in CpG dinucleotides and is an early event in carcinogenesis. Several studies have shown that hypermethylation of the promoter region of genes can lead to a reduced expression and in the case of tumor suppressor genes may contribute to increased risk of cancer.

Within the framework of this master thesis, the DNA methylation status was determined *in vivo* and *in vitro* using methylation sensitive high resolution melting analysis (MS-HRM). Therefore, an MS-HRM method for the breast cancer-related gene *CCND2* was designed and optimized. Practical laboratory work consisted of DNA extraction, bisulfite conversion of sample DNA and human control standards, amplification of target sequence by polymerase chain reaction (PCR) and HRM analysis.

The focus of the present work was the investigation of the DNA methylation status in the promoter region of various tumor suppressor genes (*APC*, *BRCA1*, *CCND2*, *CDKN2A*, *GSTP1* and *RASSF1A*) of breast cancer patients. Breast samples (tumor, adjacent and normal tissue) from fifteen breast cancer patients were biopsied by Ass. Prof. Dr. Georg Pfeiler, Medical University of Vienna, and the DNA methylation status was determined using MS-HRM analysis. Significant differences in the DNA methylation status between the tissue types could be found, in which *APC* and *RASSF1A* showed the highest differences between tumor and adjacent/normal breast tissues. Furthermore, in the tumor tissues great differences between patients related to the same genes were observed. For example, two breast cancer patients showed hypermethylation of about 50% in the promoter region of BRCA1 and CDKN2A, whereas the other patients had no methylation. In addition, the DNA methylation status of the tumor tissues was very different between the genes. While *APC* was methylated over 50% in half of the tumor samples, the highest value in *CCND2* was only 17%. In none of the tissue samples, *GSTP1* was methylated above the LOQ.

Another task was the incubation of MCF-7 breast cancer cells with supplements (propolis and tomato extract). Preliminary experiments did not show any changes in DNA methylation in the promoter region of *CCND2* by incubation with propolis. In exon 3 of *CDKN2A* a low increase in the DNA methylation status was found by incubation with propolis, whereas first analyses indicate that the tomato extract does not influence the methylation status.

Zusammenfassung

Brustkrebs ist die häufigste Krebserkrankung bei Frauen und daher ist es von großem Interesse, Biomarker für die Früherkennung zu entwickeln. Neben genetischen Veränderungen wurden auch epigenetische Modifikationen, insbesondere die DNA-Methylierung, als wichtige Faktoren bei der Entstehung von Brustkrebs identifiziert. Eine DNA-Methylierung ist bei Menschen und anderen Säugetieren fast ausschließlich an der 5-Position von Cytosinen in CpG-Dinukleotiden zu finden und ist ein frühes Ereignis in der Karzinogenese. Diverse Studien haben gezeigt, dass eine Hypermethylierung in der Promotorregion von Genen zu einer verminderten Genexpression führen kann – im Falle von Tumorsuppressorgenen kann dies zu erhöhtem Krebsrisiko beitragen.

Im Rahmen der Masterarbeit wurde der DNA-Methylierungsgrad *in vivo* und in *vitro* mittels Methylierungs-sensitiver hochauflösender Schmelzkurvenanalyse (MS-HRM) bestimmt. Dafür wurde im Vorfeld eine MS-HRM Methode für das Brustkrebs-relevante Gen *CCND2* entwickelt und optimiert. Die praktische Laborarbeit bestand aus DNA-Extraktion, Bisulfit-Konvertierung von Proben-DNA und menschlicher Kontroll-DNA, Amplifikation der Zielsequenz mittels Polymerase Kettenreaktion (PCR) und HRM Analyse.

Der Schwerpunkt lag auf der Untersuchung des DNA-Methylierungsgrades in der Promotorregion verschiedener Tumorsuppressorgene (*APC*, *BRCA1*, *CCND2*, *CDKN2A*, *GSTP1* und *RASSF1A*) von Brustkrebspatientinnen. Für diesen Zweck wurden je drei Biopsieproben von fünfzehn Patientinnen mit Mammakarzinom (Tumor, tumornahes und tumorfernes Gewebe) von Ass. Prof. Dr. Georg Pfeiler, Medizinische Universität Wien, entnommen und mittels MS-HRM Analyse wurde der Methylierungsgrad bestimmt. Es konnten beträchtliche Unterschiede im DNA-Methylierungsstatus zwischen den verschiedenen Gewebearten gefunden werden, wobei in den Genen *RASSF1A* und *APC* bei etwa 60% der Patientinnen ein signifikanter Unterschied zwischen Tumorgewebe und tumornahem bzw. tumorfernem Gewebe beobachtet wurde. Weiters wurden bei den Tumorgeweben zwischen den Patientinnen große Unterschiede im DNA-Methylierungsgrad bei den einzelnen Genen festgestellt. Beispielsweise zeigten zwei Brustkrebspatientinnen in der Promotorregion der Gene *BRCA1* und *CDKN2A* eine Hypermethylierung von über 50%, wohingegen die übrigen Patientinnen keine quantifizierbare Methylierung aufwiesen. Außerdem war der DNA-Methylierungsstatus der Tumorgewebe zwischen den Genen sehr unterschiedlich. Während bei *APC* bei der Hälfte der Tumorproben eine Hypermethylierung von über 50% beobachtet wurde, war der höchste Wert bei *CCND2* lediglich 17%. Bei *GSTP1* wurde bei den Tumorproben keine Hypermethylierung festgestellt.

Eine weitere Aufgabenstellung umfasste Inkubationsexperimente an der Brustkrebs-Zelllinie MCF-7 mit Nahrungsergänzungsmitteln (Propolis und Tomatenextrakt), wobei die Präparate in unterschiedlichen Konzentrationen getestet wurden. Erste Analysen zeigten keine Änderungen im DNA-Methylierungsgrad in der Promotorregion von *CCND2* als Folge der Inkubation mit Propolis. Im 3. Exon von *CDKN2A* wurde eine geringe Erhöhung des Methylierungsgrades als Folge der Inkubation mit Propolis festgestellt. Erste Analysen lassen darauf schließen, dass der Tomatenextrakt keinen Einfluss auf den Methylierungsgrad hat.

CURRICULUM VITAE

Personal Data

Name	Elisabeth Holzweber
Address	Oberrosenauerwald 38
	3920 Groß Gerungs
Phone	0664/6392057
E-mail	elisabeth_holzweber@gmx.at
Date and Place of Birth	June 23rd 1986 in Zwettl, Austria

Education

Since 2011	Master Program in Chemistry, University of Vienna, Austria
2007 – 2011	Bachelor Program in Chemistry, University of Vienna, Austria Degree: Bachelor of Science
2000 – 2005	Higher Vocational School (HLW), Zwettl, Austria
1996 – 2000	Secondary School, Groß Gerungs, Austria
1992 – 1996	Elementary School, Groß Gerungs, Austria

Work Experience

2013	Tutor at the Institute of Food Chemistry in the Practical of Food Chemistry for Nutritionist, University of Vienna, Austria
2013	Tutor at the Institute of Analytical Chemistry in the Practical of Food Analytical for Nutritionist, University of Vienna, Austria
2012	Tutor at the Institute of Food Chemistry in the Practical of Food Chemistry for Chemists, University of Vienna, Austria
2005 – 2007	Waitress Gerlos, Austria; St. Moritz, Switzerland; Newcastle, Northern Ireland

Scientific Work

2013	13th International Symposium and Summer School on Bioanalysis, Debrecen, Hungary Poster Presentation: “Determination of the DNA Methylation Status of Tumor Suppressor Genes of Biopsy Samples taken from Breast Cancer Patients”
2011	Bachelor thesis: “Charakterisierung der β-Phase im System Al−Co−Si”

Personal Skills

Native Language	German
Other Languages	Good English Skills (Written and Spoken) Basic French Skills
Other Skills	Computer Skills, Driver's License (Class B), First Aid Course (August, 2012)